# UNIVERSITÀ DEGLI STUDI DI TRIESTE

**XXVIII CICLO DEL DOTTORATO DI RICERCA IN**

**NANOTECNOLOGIE**

# Design of Biopolymer Nanoparticles for Encapsulation and Delivery of Nutraceuticals

Settore scientifico-disciplinare: CHIM/04


DOTTORANDA

**ILENIA D'AGOSTINO**

COORDINATORE

**PROF. LUCIA PASQUATO**

SUPERVISORE DI TESI

**PROF. PAOLO TECILLA**

TUTORE

**DR. AMELIA GAMINI**


**ANNO ACCADEMICO 2014 / 2015**

## Table of Contents:

# Abstract

Nutraceuticals provide protection against several diseases included cardiovascular diseases, cancer and neurodegenerative disorders. The use of phytochemicals in daily dietary products determines several beneficial effects on human health. Curcumin, quercetin, carotenoids, resveratrol are only few examples of molecules with beneficial action on our body. However, these benefits are often limited by a low solubility in water, a poor absorption in the gastro-intestinal tract, a low stability and an easy oxidation of these molecules. In order to overcome these problems several efforts are addressed in the formulation of successful delivery systems able to protect and efficiently deliver nutraceuticals and, in particular, nanotechnology holds great promises in this field. The possibility of an efficient delivery of nutraceuticals incrementing their biological activity represents a current relevant challenge for researchers. In this Thesis biopolymers are explored as potential materials to obtain nanostructured delivery systems capable to improve water solubility of hydrophobic molecules. In particular, within the class of biopolymers, the interest has been focused on alginate and chitosan. These polymers show characteristics of non toxicity, biocompatibility, mucoadhesion that make them very attracting for the formulation of new carriers for oral administration of nutraceuticals. Despite literature reports are usually addressed in the development of new delivery systems based on a ionic attraction between the two polymers, in this Thesis the possibility to form a covalent linkage between the carboxyl functions of alginate and the amine groups of chitosan using EDC/NHS as zero-length cross-linking agents was investigated in order to obtain stable nanocarriers. Covalent interactions are indeed stronger than ionic ones and can improve stability and resistance of the nanoparticles. Moreover they should confer rigidity to the polymeric network limiting the leakage of the entrapped molecules. In literature this type of covalently crosslinked network is not widely studied, and only few articles describe a covalent alginate-chitosan linkage. Different methodologies of crosslinked alginate-chitosan nanoparticles preparation have been explored in the Thesis: from reaction in water to reaction in macroemulsion with food grade

components, to nanoemulsion using pure chemical solvents. In our approach, the W/O emulsions represent an instrument to confine the reaction between the two polymers in a small environment in order to avoid aggregation and the uncontrolled formation of large insoluble networks of polymers. In this context the inner water droplets of the W/O emulsion represent a nanoreactor in which the reaction between the two polymers takes place. Stability of the emulsion and sizes of the water droplets have a great influence on the final dimensions and stability of the polymer nanoparticles. According to that, better results in term of sizes and stability of the nanoparticles have been reached when polymers are included in W/O nanoemulsion rather than macroemulsion. Specifically, two different types of nanoemulsions have been optimized in this Thesis, using cyclohexane as oil phase and hexanol/Triton X-100 as cosurfactant/surfactant or a mixture of Tween80-Span80 as surfactants. Once nanoemulsions have been optimized, a reproducible methodology to isolate and purify the polymer nanoparticles from toxic residues has been defined. The obtained nanoparticles have been characterized with different techniques (FT-IR, NTA, DLS, TEM, SEM, UV-Vis, etc.). In particular they have been analyzed in term of polymer composition, sizes and size stability during time, shape and morphology, biocompatibility, entrapping ability of nutraceuticals and antioxidant properties of nutraceuticals after the encapsulation in the carriers. The average diameter of the nanoparticles is 180 nm with a monodisperse and homogenous particle population despite the presence of few larger aggregates. Analysis of the evolution of particle size during time confirms the presence of aggregates that precipitate during time. The precipitation of these aggregates can be accelerated by centrifugation of the fresh samples. A characterization of pure polymers and nanoparticles by spectroscopic methods has been performed using FT-IR spectroscopy. Results show the presence of both alginate and chitosan in the final composition, although a direct evidence of the formation of the covalent amide bond between alginate and chitosan was not obtained. However, relevant indirect information about the differences between covalent and ionic nanoparticles has been obtained from a comparison of nanoparticles synthesized with and without covalent crosslinkers. An *in vitro* assay (MTT) confirmed the safety of the nanoparticles revealing a good biocompatibility. The morphological investigation using transmission and scanning microscopy (TEM/SEM)

shows well defined and spherical nanoparticles. Entrapping abilities of the nanoparticles were explored using molecules of interest in nutraceuticals such as resveratrol and quercetin. Nanoparticles show good loading capacity and the bioactive compounds are stably retained in the network after the optimization of the system. The nutraceuticals tested, preserve their scavenging ability after the entrapment in the carriers. Therefore, the goals achieved in the Thesis represent an important result in the development of nanodelivery systems for uses both in food and pharmaceutical field.

# Sommario

I nutraceutici rappresentano un valido aiuto nella prevenzione di diverse patologie, malattie cardiovascolari, cancro e malattie neurodegenerative in primis. L'uso di molecole bioattive di origine vegetale nella dieta quotidiana, infatti determina effetti benefici sulla salute umana. La curcumina, la quercetina, i carotenoidi e il resveratrolo sono solo alcuni esempi di una classe di composti con attività benefica sul nostro organismo. Spesso i benefici di queste molecole sono limitati dalla scarsa solubilità in acqua, dallo scarso assorbimento nel tratto gastro-intestinale unitamente a una certa instabilità e tendenza ad ossidarsi facilmente. Nel tentativo di superare tali criticità, sono stati destinati diversi sforzi nella formulazione di sistemi di rilascio capaci di proteggere in modo efficace i nutraceutici e in particolare è nel campo della nanotecnologia che si riversano grandi promesse. La formulazione di un sistema di rilascio efficiente capace di aumentare l'attività biologica dei nutraceutici rappresenta una sfida attuale nella ricerca scientifica. In questa Tesi, sono stati utilizzati biopolimeri come potenziali materiali di partenza per ottenere sistemi di rilascio nano strutturati capaci di aumentare la solubilità in acqua di molecole idrofobiche. L'interesse si è focalizzato soprattutto sull'impiego di alginato e chitosano come potenziali carriers. Tali polimeri mostrano caratteristiche di non tossicità, biocompatibilità, e muco adesione che li rendono attraenti nella formulazione di nuovi carriers per la somministrazione orale di nutraceutici. Mentre in letteratura abbondano esempi di interazioni ioniche tra i due polimeri, in questa Tesi è stata studiata la possibilità di formare un legame covalente tra le funzioni carbossiliche dell'alginato e i gruppi amminici del chitosano grazie all'impiego di EDC/NHS, crosslinker di zero ordine, con lo scopo di ottenere nanoparticelle stabili. Le interazioni covalenti infatti sono più forti rispetto a quelle ioniche e possono aumentare la stabilità e la resistenza delle nanoparticelle. In più potrebbero determinare una maggiore rigidità del network polimerico finale limitando la perdita delle molecole incapsulate. In letteratura questo tipo di legame covalente tra alginato e chitosano è stato poco studiato e solo qualche

articolo descrive studi in questo senso. In questa Tesi sono state impiegate diverse metodologie di preparazione di nanoparticelle di alginato e chitosano nel tentativo di legare i due polimeri: da reazioni in acqua, a reazioni in macroemulsione con l'utilizzo di componenti di grado alimentare, fino a nanoemulsioni in cui sono stati impiegati solventi chimici. In quest'ottica l'uso di emulsioni A/O è un valido strumento per confinare la reazione tra i due polimeri in un ambiente ridotto così da impedire l'aggregazione e la formazione incontrollata di un network insolubile tra i due polimeri. Le gocce interne dell'emulsione A/O rappresentano infatti dei nano reattori in cui far reagire alginato e chitosano. La stabilità dell'emulsione e le dimensioni delle gocce hanno una grande influenza sulle dimensioni finali e sulla stabilità delle nanoparticelle. Di conseguenza i risultati migliori in termini di dimensioni e stabilità sono stati ottenuti nel caso in cui i polimeri sono stati inclusi in nanoemulsioni A/O piuttosto che in macroemulsioni. Nello specifico, sono state ottimizzate due tipologie di nanoemulsioni, una impiegando cicloesano come fase continua ed esanolo/Triton X-100 come cosurfattante/emulsionante, l'altra in presenza di Tween 80 e Span 80 come miscela di emulsionanti. Dopo aver ottimizzato l'emulsione si è messa a punto una metodologia riproducibile per isolare e purificare le nano particelle polimeriche dai residui tossici. Le nanoparticelle sono state poi caratterizzate con l'ausilio di diverse tecniche (FT-IR, NTA, DLS, TEM, SEM, UV-Vis, ecc.). In particolare si sono determinate la composizione, le dimensioni e la stabilità nel tempo, la forma e la morfologia, la biocompatibilità, la potenziale capacità di incapsulare nutraceutici e l'eventuale azione antiossidante dei nutraceutici una volta incapsulati. Il diametro medio delle nanoparticelle risulta essere di 180 nm con una popolazione di particelle monodispersa nonostante la presenza di qualche aggregato. L'evoluzione del diametro medio nel tempo di tali nanoparticelle conferma la presenza di questi aggregati che precipitano e può essere accelerata dalla centrifugazione del campione appena preparato. I risultati della caratterizzazione spettroscopica ottenuta tramite spettroscopia FT-IR mostrano la chiara presenza di alginato e chitosano nella composizione finale nonostante non sia stato possibile convalidare la formazione del legame covalente. Si è perciò ricorso a prove indirette basate sull'analisi di alcune importanti differenze derivanti da un confronto diretto tra nanoparticelle covalenti sintetizzate in presenza dei crosslinker e nanoparticelle ioniche sintetizzate senza i crosslinker covalenti. La valutazione della

biocompatibilità misurata con un saggio in vitro (MTT) ha dato ottimi risultati nel profilo della sicurezza delle nanoparticelle. L'analisi morfologica eseguita con microscopia elettronica a trasmissione e scansione (TEM/SEM) mostra particelle sferiche e ben definite. La capacità delle nanoparticelle di incapsulare molecole di interesse in nutraceutica come resveratrolo e quercetina è stata altresì valutata. Le nanoparticelle mostrano una buona capacità di loading e i composti sono stabilmente trattenuti nella matrice polimerica. I nutraceutici testati, inoltre, preservano la loro attività di scavenger anche dopo l'incapsulamento nei carrier. Gli obiettivi raggiunti nella Tesi pertanto rappresentano un importante risultato nel campo dei sistemi di rilascio per uso farmaceutico ed alimentare.

# Introduction

# 1

# 1.1 Food, health, diet

Rapid modifications in diet and lifestyle as a consequence of industrialization, urbanization and market globalization have had a considerable impact on health and nutrition of population. All these changes have determined an improvement in living standard , food bioavailability and access to services but with negative effects on the diffusion of improper dietary models.[1] For example, the revolution in mobility and technologies has favored a sedentary lifestyle that combined with an increased intake of food rich in saturated fats and poor in unrefined carbohydrates, has dangerous repercussions on public health. Epidemiological studies evidenced the role of diet in preventing and controlling mortality. Some nutrients in fact may retard or avoid the onset of illness, while others increase the probability to develop diseases. Although it is known that healthy food is vital for our wellbeing, many people do not follow a balanced diet, increasing the incidence of serious metabolic imbalances, responsible of the increment of disease risk factors as obesity, hypertension, food intolerance, allergy, etc.. Being universally recognized that dietary adjustments represent a valid help in fighting several diseases it is important to spread a correct pattern of nutrition to follow in daily life.

The Mediterranean diet represents a model of the correlation between food and wellbeing. Several studies underline the improvements in life quality of populations bordering the Mediterranean sea due to contributions of diet in promoting health benefits. In particular, Mediterranean dietary model is related to a defense from cardiovascular mortality and reduction in incidence of cancer and cardiovascular diseases.[2] This became evident when several data were published regarding the low or very low rate of heart diseases among the inhabitants of the Mediterranean basin despite a normal high consumption of fats (although with regional differences). The lower incidence in hearth diseases produced a longer life expectation respect to other populations. The fundamental sources of food, in Mediterranean diet, are plants foods i.e. vegetables, fresh and dried fruits, nuts, legumes, and grain cereals. The principal source of fats is represented by olive oil followed by fish, egg, cheese, yoghurt and

white meat, while fats of red meat, saturated fats and trans fatty acids are present in limited amounts.[3] Also a moderate consumption of wine represents part of daily diet.

### 1.1.1 Polyphenols: an example of dietary source of wellbeing

All the typical foods of Mediterranean diet contain significant amounts of healthy nutrients as *polyphenols.* These compounds and their derivatives represent a class of food constituents with the ability to regulate metabolic processes and to determine a positive impact on health and wellbeing.[4] They abound in different food sources, generally fruits, vegetables, cereals, beverages. For example fresh fruits as apples are rich in polyphenols: a variable fraction between 60-120 mg/100 g is made of polyphenols. Also red wine, tea, coffee, chocolate, cereals and dry legumes are rich in polyphenols. In the plants, polyphenols are produced as secondary metabolites acting in the defense from UV radiations and pathogen injury.[5]

During the time several articles and epidemiological studies confirmed the important role of a daily dose consumption of polyphenols in the protection of human healthiness. The action of polyphenols is basically due to a strong antioxidant activity in human body against the reactive oxygen/nitrogen species (ROS, RNS) formed as byproducts in the normal metabolic processes. In particular, in case of stress or alteration, ROS and RNS are produced in excessive amounts and the body is not able to detoxify them. Figure 1.1 illustrates all the injuries in which polyphenols are involved with a protective rule.


**Fig.1.1** Health effects of polyphenols in human body (adapted from reference [5]).

Several hundreds of different compounds have been recognized to belong to the class of polyphenols. The most useful classification is based on the number of phenol rings and on the structural elements connecting phenols between them. Figure 1.2 illustrates a schematic classification of polyphenols.

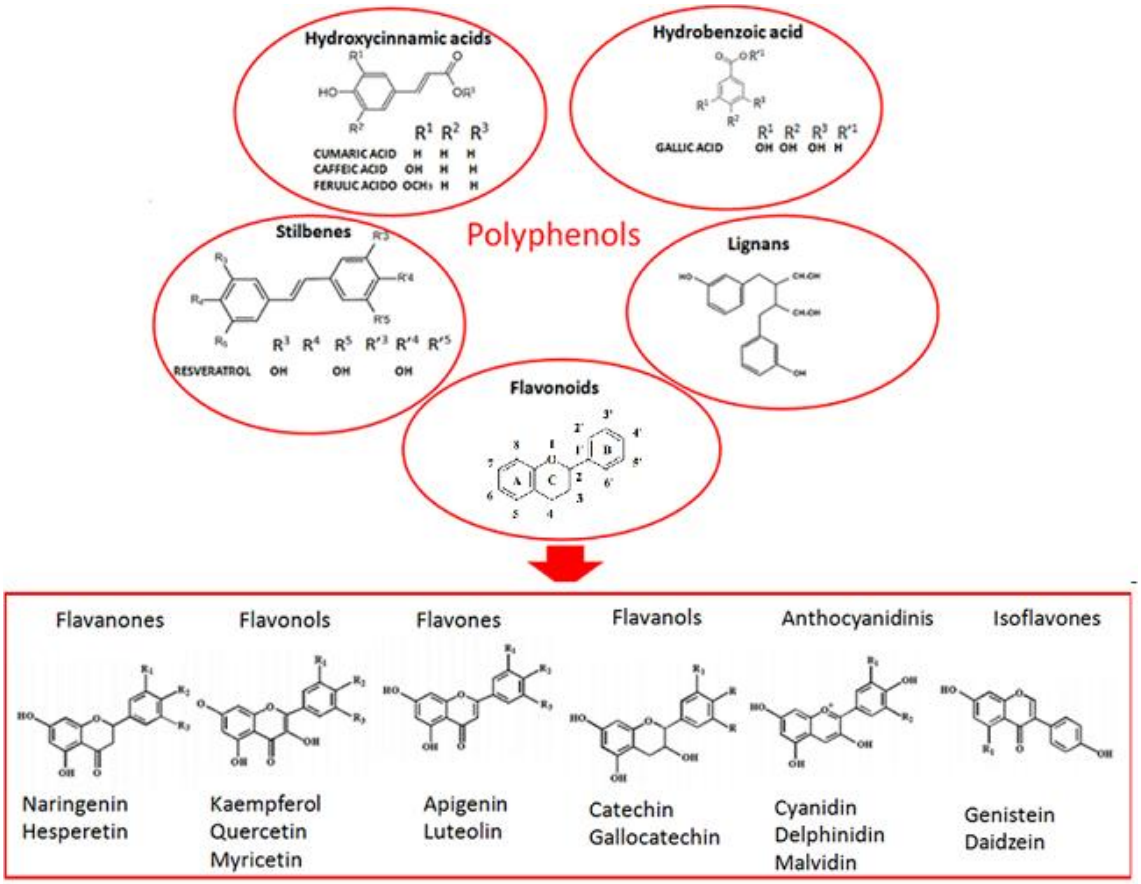


**Fig.1.2** Schematic classification of polyphenols present in nature.

Bioavailability of polyphenols varies depending on the class considered and is not related to the amounts present in food. The aglycone form is usually absorbed in the small intestine, but most polyphenols are taken up in complexes with esters, glycosides or polymers. Intestinal enzymes and colonic microflora provide to the hydrolysis of the conjugated form before the absorption. During absorption, the molecules undergo processes of modification and they finally enter in the blood stream in a modified form making complicated to identify all metabolites originating from a class of molecules and to monitor their biological activity.[5] For this purpose, a *Phenol-Explorer web database* has been created that counts 383 different polyphenol metabolites identified up to date.[6] These data represent the starting point to characterize the metabolome, the set of all components originating from a class of compounds, in this case polyphenols. Following the schematic resume in figure 1.2, polyphenols are divided in five principal classes: stilbenes, lignans, hydroxycinnamic acids, hydrobenzoic acids and flavonoids.

Among these classes, stilbenes are present only in little amounts in the human diet. Within the group of stilbenes, resveratrol, was extensively investigated for its anticarcinogenic effects.[7] Resveratrol is found mostly in grape and in derived products such as wine. However, being present in a very low quantity in the diet, the protective role of this compound is improbable in a normal diet dose.[8]

In nature, resveratrol exists in two structural isomers, but only the *trans* form is active in scavenging free radicals.[9] Its active role in preventing diseases such as neurodegenerative injuries, cardiovascular diseases, cancers and viral infections, has been sustained by *in vitro* and *in vivo* studies.[10]

Another important class of polyphenols is the class of flavonoids. Flavonoid derivatives represent the most ubiquitous polyphenols in nature and are divided in seven sub-classes. The basic structure of flavonoids presents a carbon skeleton formed by two benzene rings (A and B) bonded via a heterocyclic pyrane ring (C), as shown in figure 1.2. The most common sub classes are: isoflavones, flavonols, flavanones, flavanols, anthocyanidinis and flavones.

Studies in absorption spectroscopy showed that flavones and flavonols display two absorption bands in different wavelength ranges. Band I in the interval between 320-385 nm due to B ring absorption and Band II in the range from 250 to 285 nm

corresponding to A ring absorption, with the position of the maxima influenced by the substituents on the two aromatic rings. The presence of different functional groups gives to every class of flavonoids exclusive physicochemical properties and biological activities. For example, the antioxidant activity depends on the number and position of the hydroxyl groups in the structure. Systems in which the B-ring contains two hydroxyl moieties and the C ring has a double bond and a 4-oxo function seem to have improved antioxidant ability.[11] Aglycone form or glycoside derivatives are the common forms in which flavonoids are present in nature.[12] The aglycone form is easily absorbed in the small intestine, while glycoside flavonoids must be first hydrolyzed to the aglycones before to be absorbed. The hydrolysis may occur by action of digestive enzymes and, in this case, once the aglycones are formed, they are absorbed in the small intestine, too. Glycosides that are not substrates of enzymes are transported in the colon, whose capacity of absorption is lower than that of small intestine and where bacteria provide to the hydrolysis. After the absorption step, different enzymes promote the conjugation of flavonoids in the liver producing glucuronidated, sulphated and methylated derivatives or small metabolized molecules. These modifications make difficult to control pharmacokinetic parameters. The solubility of flavonoids has a significant action in the therapeutic efficacy of these molecules. Indeed, the relative low residence time and low absorption exclude toxic effects derived from ingestion of flavonoids. However low solubility represents a limit for medicinal applications.[13]

Among the class of flavonols, quercetin represents the most intensively bioactive molecule studied. It has a formidable antioxidant activity, and in the flavonoids family quercetin is the most effective scavenger of ROS and RNS as reported from Hanasaki et al..[14] Quercetin structure is responsible of its strong antioxidant activity: the presence of two antioxidant pharmacophores (catechol group in B ring and hydroxyl group in position 3 of AC ring) in the molecule offers an ideal configuration for the scavenger activity. Quercetin exhibits different biological actions from antiatherogenic to antiproliferative or anticoagulative ones. This molecule is also able to regulate expression of enzymes and to inhibit cell proliferation. On the other hand, the consequence of the antioxidative activity of quercetin is the formation of its oxidized quinoid form, named QQ which exists in many tautomeric isomers. These oxidized

derivatives display a toxic action for their capacity of arylation of protein thiols present in the body. Moreover, the strong reactivity of QQ leads to the formation of an adduct with GSH, the most abundant endogenous thiol.[15]

## 1.1.2 Functional food and nutraceuticals

An increasing number of consumers is becoming aware of the role of food in health. The attention toward diet and food correlated diseases has modified the perception of food which is now often intended not only to satisfy hunger and to provide the necessary nutrients, but also to prevent chronic diseases and to increase longevity. The rapid diffusion of healthy products obtained from natural sources has determined a growing interest in modified food, enriched in bioactive molecules. The modified food is generally defined as *functional food*. As was expressed by Shibamoto and al.[16] in accordance with the International Food Information Council, a functional food is a food that "provides health benefits beyond basic nutrition". A report on functional food published by the European Commission defines which are the main requirements for a food to be considered as functional:

- the basic constituent has to be a food, which contains or is enriched with an ingredient, a micronutrient or a naturally bioactive molecule with a beneficial role in health, well-being or disease prevention,
- the beneficial activity has to go beyond normal nutrition,
- the functional action has to be "illustrated" or declared and communicated to consumers,
- the effect is expected to occur when the food is ingested in normal amounts.

In the functional food market, dairy products are the most widespread, followed by drinks, cereals, and snack food. In the dairy market, company advertisings offering "daily dosage" bottle to consumers, seem to be an appreciated strategy to increase the diffusion of functional dairy products. In the beverages class it is complicated to distinguish between energy drinks, tonic drinks and functional beverages, but the good results in term of sale of these products indicate that drinks are well perceived by

consumers in promotion of functional products. Regarding ingredients, probiotic bacteria cultures seem to be the principal bioactive nutrients, followed by dietary fibres, plant extracts based on polyphenols with anti-oxidative action or anti-age function.[17] Functional food belongs to the large category of nutraceuticals that includes also food supplements, usually presented in form of pills and tablets.

All kinds of nutraceuticals are considered as dietary products linking nutrition with health and having a key role in promoting wellness. Some researchers have defined also nutraceuticals as potent adjuvants in clinical therapy.[18] It is not possible to identify a specific mechanism of action of nutraceuticals but it can be understood that their addition to food matrixes decreases disease risk. This experimental evidence represents a starting point to develop functional food potentially able to produce physiological benefits or to reduce the risk to develop disorder and prevent chronic diseases.[19] In fact, apart from the actual medical treatments based on fast reduction of symptoms, dietary regulation promotes a moderate long term process for illness prevention or treatment.[20] Summarizing cancer, diabetes, cardiovascular diseases and other correlated diseases are the main pathologies affecting patients, and several investigations have demonstrated that nutraceuticals maintain or control physiological functions correlated to the pathologies mentioned above. Therefore, the current tendency is to regard nutraceuticals as a valid instrument for prevention and a complementary tool for the treatment of diseases. Their beneficial action in preventing diseases is associated in part to the production of secondary phytochemical metabolites that was demonstrated to have several biological effects. In general, drugs have a more potent action in the treatment of illness thanks to the higher concentration in bioactive components, but if natural substances become part of daily diet, they may have long term effects on health.[21] Moreover, nutraceuticals are expected to produce relative low toxicity and less side effects compared to drugs.[20]

### 1.1.2.1 Oral administration route of nutraceuticals

In order to be taken as daily dietary products, and being the oral administration the most preferred route for its non-invasive character, the actual studies are exploring new delivery mechanisms to optimize the oral intake. In fact oral administration is influenced by several factors that can enhance or reduce the absorption of the active ingredients. In particular, the hard and different conditions to which bio-molecules are exposed in the body, the presence of degradative and metabolic enzymes, the susceptibility to first pass metabolism, may determine a modification of the chemical structure of the nutraceuticals and a loss in bioavailability. The oral cavity is the first site of the body in which food mass is chopped in small pieces by enzymes present in the mouth, producing the so called bolus. The process is fast and the pH ranges from 5,6 to 7,6. The changes due to temperature and ionic strength are considered as the first step of the digestion, preparing food for the next step in the stomach. Here the pH is regulated, with the production of hydrochloric acid to values ranging from 1 to 3, depending on the characteristics of the bolus, to ensure an optimal activity of the digestive enzymes. The gastric environment is a crucial step for stability of bioactive molecules, in fact, most of them lose their activity because of important physicochemical modifications. Stomach permanence time of the various components depends on their physiological and individual characteristics, and it is a predictive factor of the consequent bioavailability of molecules. For example, an insufficient time of residence in the stomach reduces the primary absorption of many polyphenols and of other poorly soluble bioactive molecules. A short permanence in stomach reduces also oral bioavailability for molecules absorbed in the upper section of small intestine. The small intestine receives the partly digested food, chyme, from stomach. Gut is divided in three different segments: duodenum jejunum and ileum. The mucosa is protected from injury of the acidic chyme by the secretion of alkaline pancreatic juice that mixed to enzymes, phospholipids, bile salts and sodium bicarbonate continues to process food. In the intestine, food undergoes the conversion in simple nutrients ready to be absorbed. The composition of ingested food has a role in the type of nutrients absorbed, for example lipids enhance the absorption of lipophilic molecules, which

being not soluble in the water intestinal environment, tend to precipitate and to be excreted in absence of lipids. Instead, ingesting fatty molecules along with food, leads to the formation of micelles made of lipase degraded fatty acids in which the lipophilic nutrients are incorporated and made available to pass through intestinal villi. Active and passive transport are the mechanisms that allow the absorption of nutrients. In active transport cells use their own energy to internalize nutrients exploiting channels on the surface. In passive transport nutrients are internalized without spending energy following a simple diffusion mechanism. The rate of absorption and the consequence availability depend from the physicochemical characteristics of the molecules as stability to different pH, resistance to ionic strength, enzymatic transformations, hydrolysis. The last tract of GI apparatus is represented by the colon, here, the last nutrients and water are absorbed.

Moreover some nutrients undergo a first pass metabolism which causes a reduction in the amount available to be absorbed in the site of action. Liver and intestinal cells are the common responsible of first pass metabolism for molecules administered orally.[22] The fraction of bioactive molecules that undergoes first metabolism is variable in each individual, so it is difficult to forecast the effect of a standard dose of a drug.

### 1.1.2.2 Other administration routes of nutraceuticals

Being absorption of nutrients in many cases compromised in the gastro-intestinal tract, recent studies illustrate the possibility for lipophilic drugs to penetrate the dermis. Dermal administration represents an innovative solution for systemic delivery with a reduced toxicity. In some cases the concomitant use of oral and dermal products enhances the antioxidants action of nutraceuticals[18] as reported by Palombo et al.[23] in the case of consumption of some carotenoids. There is an increasing demand of products incorporating nutraceuticals with a function in retarding aging too. Bioactive compounds can also be released transdermally as coadjuvants in the treatment of dermatitis, psoriases, skin cancer and other skin pathologies.

In the case of ocular related therapies, the ophthalmic route remains the principal route of administration in the clinical practice despite oral route presents a major acceptability by consumers. In ophthalmic route, nutraceuticals rapidly reach the target explicating a fast anti-inflammatory and antioxidant action.

## 1.2 Encapsulation technology

Encapsulation is an effective way to regulate the delivery of bioactive molecules. Using encapsulation technology, bioactive drugs are included in a matrix acting as a barrier, protecting and preserving sensitive molecules from degradation during processing and digestion.[24] In the modeling of a delivery system, it is of primary importance to formulate the best system considering the type of instability of the encapsulated agent, the final application of the system and the properties (protection, degradation, etc.) that one need to improve. The following criteria are the parameters to evaluate during formulation of delivery systems:

*Loading capacity* represents the amount, expressed as percentage, of encapsulated drug/bioactive molecule per unit of carrier matrix. In the formulation of a delivery system is important to obtain a high final loading capacity. The value ranges from 0% to 100% depending on the nature of the bioactive drug, the structure of the matrix and the mutual interactions between them.

*Loading efficiency* evaluates the capacity of the matrix to retain the bioactive molecules during time. This factor is important to be controlled for instance in the case in which the carrier matrix has to resist to the acidic conditions of the stomach enabling the nutrients to cross the gastro environment. This property has also particular importance for systems that require a long period of storage. Ideally a loading efficiency of 100% corresponds to a complete preservation of the encapsulated material.

*Encapsulation efficiency* is defined as the percentage of bioactive molecules entrapped in the carrier respect to their initial concentration. The value can be calculated indirectly by subtracting the amount of non encapsulated molecules to the total mass

of bioactive molecules used, or with a direct measure of the encapsulated compound.[25]

*Delivery mechanism* is related to the release of the bioactive molecules from the carrier in a controlled rate in response to different stimuli i.e. pH variations, ionic strength, temperature, once the carrier arrives in the target site. For example, in a delivery system formed by polymers having swelling properties, swelling is the principal mechanism of delivery of bioactive compounds.

*Delivery efficiency* is the ability of the carrier to deliver the drug in the desired site of action. Drugs have affinity for certain organs or tissue exerting their action in a specific area defined as target site. In order to ensure a high delivery efficiency, the matrix has to arrive intact to the target site where the drug is delivered in response to stimuli. There is also the possibility to modify the carrier, making it able to be recognized by specific receptors of the target site cells thus facilitating cell internalization.

*Protection of the bioactive* represents the starting factor in the stabilization of a bioactive component. In fact usually molecules need to be encapsulated to resist to the action of oxygen, heat, light, contact with other substances promoting degradation,[26] and strong value of pH.

*Bioavailability* is a crucial factor in the action of a bioactive molecule. It is a pharmacokinetic property regarding the fraction of bioactive molecules that reaches in a unchanged state the systemic circulation. When the route of administration of a drug is intravenous, the bioavailability has a percentage of 100%. If other routes are used, the bioavailability decreases considerably. Orally administered drugs present a reduced absorption and a possible first pass metabolism.[27] Encapsulation of the drug may strongly affect its bioavailability.

During the production of enriched food systems, encapsulation technology is a useful method for different reasons that are listed below:

- increased release of bioactive molecules,
- protection from oxidation, light, degradation, hydrolysis,
- limited susceptibility to gastro-intestinal environment,
- protection from first pass metabolism,
- limited interaction with food matrix,
- preservation of stability during processing and storage,

- creation of a barrier toward other components,
- masking bitter taste and astringency (as for polyphenols),
- increased bioavailability,
- prevention of reactions with other components,
- providing a sufficient amount,
- uniforming dispersion of a compound,
- control of the rate of release,
- delivery in a target site.

### 1.2.1 From “micro to nano” encapsulation

Encapsulation technologies have been extensively explored for the delivery of bioactive compounds of low and high molecular weight. In this field the use of microspheres or microparticles is largely diffuse and, in general, the presence of a micrometric matrix ensures a controlled release of entrapped bioactive molecules. Food biopolymers are receiving great interest in the formulation of microsphere delivery systems, thanks to their natural origin, edible nature, stability and processability. Biopolymers include a large number of different polymers, from protein to carbohydrates. Among proteins, the widespread types are: whey protein, gluten, gelatin. Among carbohydrates, polymers as starch, maltodextrins, chitosan, celluloses, alginates are usually adopted in fabrication of micro and nano structures for pharmaceutical, food and cosmetic applications. Also poly(lactic acid) (PLA) having good biocompatibility is frequently used as material in microencapsulation technology. The requirements for a technology in the manufacturing of carriers deal with aspects such as safety, economicity, reproducibility and high controlled methodology.

Several procedures are available to encapsulate food bioactive molecules. Since the compounds to be entrapped are normally in a solution, various technologies of encapsulation include drying processes and, for example, spray drying is one of the oldest method used in food sector. Also gelling techniques enable the formation of microparticles. Other common adopted methodologies originate from modification of

the basic methods: solvent extraction/evaporation, phase separation (coacervation), ionic gelation.[28] This field has grown and diversified in few years and in the last period the principal efforts are concentrated in the exploration of nano delivery systems thus moving from micro- to nanoparticles. Nanotechnology has a growing role in agriculture, pharmaceutical and food systems. Concerning food and agriculture, the control at a nanoscale level of the material characteristics may modify features as texture, flavor, solubility, stability, processability with strong impact on final applicability. Several studies are also focused on the development of new materials for detection of pathogen, tools for protecting food, methodology to increase safety and efficacy and smart packaging.[29]

The novel interest in nutraceuticals and the consequent need of new designed delivery systems to encapsulate functional food make attractive the investigation in the area of nanotechnology too. The last trend in encapsulation and stabilization methodologies is to adopt novel strategies to ensure targeted delivery and good bioavailability of nutrients. Nanotechnology offers some advantages in the design and optimization of delivery systems to overcome drawbacks of conventional carriers. In fact, active intracellular delivery of nutrients and modification of pharmacokinetic and pharmacodynamic properties depend from the sizes and surface properties of the carriers[30] with the nano-structured systems usually more effective in promoting the uptake of nutrients. A scientific review published by Acosta [31] compares data collected by five different research groups on the influence of the particle sizes on bioavailability/uptake properties. The results show that the size of carriers affects the process, in fact nano-particles below 500 nm of sizes increase the uptake of the carriers and the absorption of encapsulated nutrients. The equation of Ostwald-Freundlich well describes the dependence of solubility of spherical nanoparticles from their sizes and represents a good way to predict solubility of small particles:

$$\ln\left(\frac{S}{S_0}\right) = \frac{2M\mathrm{w} \times \gamma}{\rho \times R \times T} \times \frac{1}{r} \qquad (1)$$

where $S$ is the solubility of the nanoparticles at a given particle size and $s_0$ is the value of solubility of the nanoparticles for big $r$ values, $\mathrm{Mw}$ is the molecular weight of

the nanoparticle, $\gamma$ is the surface tension or interfacial tension as in this case between solvent and nanoparticle, $\rho$ is the density of nanoparticle, $R$ the Universal gas constant, $T$ is temperature expressed in Kelvin, $r$ is the radius of the nanoparticle.

A simulation based on the Ostwald-Freundlich equation for a hypothetic compound shows a large influence of the size of the nanocarriers on bioavailability for carriers below 100 nm of diameter (where solubility is the limiting factor for bioavailability). Instead for nanoparticles ranging from 100 nm to 500 nm different mechanisms are hypothesized to act: the increase of solubility of active ingredients, the increment of the gastro residence time, the consequent enhancement of the absorption favoring the direct uptake.[32]

This result implies that absorption is strongly influenced by uptake of the carrier, and uptake of the carrier is influenced by its size. This observation is also confirmed by other studies describing for example how particles with a size of 100 nm generally increase the absorption by 2,5 times compared to 1 μm particles in CaCo-2 [33] cells and that nanoparticles are able to cross the submucosal layer in a rat model.[34] These scientific evidences of increased uptake of nanoparticles justify the strong interest in the potentiality of nanocarriers.[35]

## 1.2.2 Delivery systems based on nanocarriers

Nanoencapsulated systems are formed by entrapping one or more different molecules in a structured matrix. In the development of nanocarriers, the most explored matrices are lipid components and polymeric materials.

In the family of lipids, liposomes represent the major investigated nanocarriers in agro-food and pharmaceutical areas. The structure of a liposome derives from the self-aggregation of phospholipids once they are exposed to a water environment.

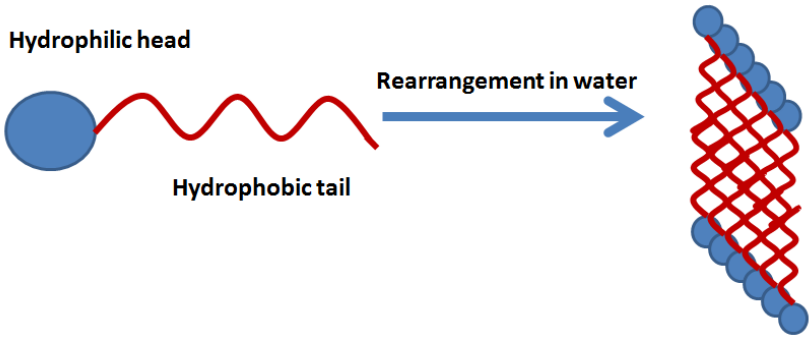


**Fig. 1.3** Schematic structure of phospholipids and rearrangement in aqueous system.

In fact to minimize the hydrophobic area exposed to water, phospholipids self-aggregate forming a bilayer in which hydrophobic tails are in the internal layer and hydrophilic heads are exposed to water (see figure 1.3) both in the internal and in the external compartment. The procedure of formation needs some necessary steps and often involves the use of toxic solvents that may remain in traces. Carriers obtained after hydration in water are multi lamellar vesicles (MLV), with several double layers of phospholipids arranged in a concentric way and an usually large size distribution. Multi lamellar vesicles are able to entrap both hydrophilic (in the internal compartment and in the compartments between different bilayers) and hydrophobic molecules (in the bilayers). A further step of extrusion of MLV through filters with a controlled pore sizes (see figure 1.4) gives a narrow distribution of unilamellar vesicles (LUV).

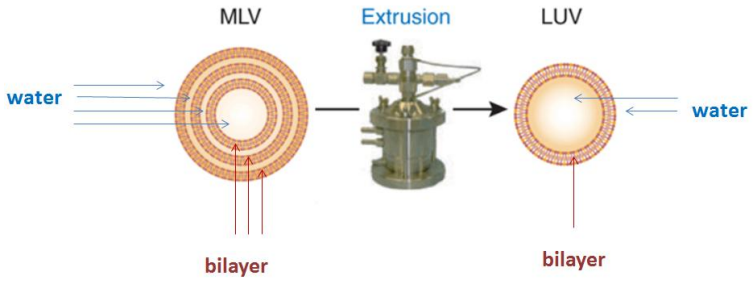


**Fig.1.4** Schematic representation of LUV obtained by extrusion process.

Liposomes are excellent carriers to increase the bioavailability and stability of polyphenols. In vitro studies of liposomes internalized polyphenols show an incremented efficacy compared to polyphenols alone. In a work of Tonnesen et al. [36] it was demonstrated an increase of 20-fold for the uptake of curcumin by red blood cells

after encapsulation in liposomes respect to curcumin in solution. Also encapsulation of resveratrol resulted in a more effective protection against UVB radiation. Liposomal formulations of trans-resveratrol determined also an increment in bioavailability due to a prolonged exposure of the cells to the molecule. Several articles show the same results on advantages of polyphenols encapsulated in liposomes. Table 1.1 shows a resume of the literature available about inclusion of polyphenols in different type of liposomes:

| Polyphenol | Formulation | % (*w/w*) | Effect of the formulation |
|---|---|---|---|
| Catechin | Epikuron 200/Chol/Tween 80/ethanol 6/1/80/13, film hydration | 0.3 | Increased bioavailability and cerebral distribution |
| Curcumin | SPC; film Hydration, extrusion, MLV | 3 | Prolonged antioxidant protective effect |
| Curcumin | DMPC or DMPC/DMPG lyophilisate | 10 to 25 | Similar efficacy *in vitro*. Antiangiogenic effect and tumor growth reduction *in vivo* |
| Curcumin/resveratrol | DMPC, lyophilisate | 20 | Improved bioavailability and reduction of prostate cancer incidence |
| Dehydro-silymarin | SPC/Chol/IPM/sodium cholate 1.5/0.3/1/1 film + freeze-drying | 25 | Increased oral bioavailability |
| EGCG Catechin | EPC/Chol/DA 4/1/0.25 film hydration + sonication or extrusion | 20 | Protection from degradation; Increased carcinoma cell death at lower concentrations |
| Fisetin | DOPC/DOPC/DODA-$PEG_{2000}$/Fis 8/1.3/0.4/0.3 film hydration + extrusion, MLV | 18 | Increased bioavailability and antitumor efficacy |
| Quercetin | PE/Chol/DPC/QC 7/1/1/1 film hydration + sonication | 10 | Antioxidative effect with the formulation (i.v.) |
| Quercetin | Lecithin/Chol/ PEG 4000 film hydration + lyophilization, SUV | 30 | Increased solubility, bioavailability and antitumor efficacy *in vivo* (i.v.) |
| Resveratrol | DPPC/DSPE PEG2000/Chol 1.85/0.15/1 film Hydration + extrusion | 0.1–5 | Improved solubility and chemical stability |
| Resveratrol | P90G/DCP/Chol sonication + extrusion | 1.5 | Prolonged efficacy and improved protection from UV B |
| Silymarin | Lecithin/Chol/stearyl amine/Tween 20 9/1/1/0.5 film hydration | | Increased stability, bioavailability and liver protection |
| Silymarin | Mannitol, phospholipids proliposomes | 20 | Improved oral bioavailability |

**Tab.1.1** Different examples of inclusion of polyphenols in liposomes (adapted from reference [37]).

Thus, liposomes have several advantages in the protection and delivery of the bioactive molecules and in the relatively easy way of preparation which ensures high control of the size and size uniformity. However they present some several limitations mainly related to problems in long-term storage and rapid excretion.

Other carriers originating from lipids are micelles which are formed by amphipathic molecules and which structure depends on the solvent they are exposed. If the surrounding medium is water, the polar portion of the surfactant is exposed to the aqueous environment and the hydrophobic tails organize in clusters in the core, avoiding the contact with water. The micelles originating from this interaction are known as regular micelles. If the surrounding medium is of hydrophobic nature, the orientation of molecules changes, and the hydrophobic tails are exposed to the solvent while the hydrophilic heads are in the core of the structure usually embedded in a small water pool. Micelles of this kind are known as reverse micelles.[38] Studies concerning encapsulation of artemisinin [39] and curcumin [40] in sodium dodecyl sulfate (SDS) micelles suggest an increment in stability against oxidation. Micelles made of SDS seem also able to protect green tea polyphenols extracts.[41]

Polymers are also able to form micelles, in particular the self assembling of amphiphilic block copolymers forms polymeric micelles. This kind of micelles show a great ability to solubilize relevant amounts of hydrophobic drugs, and enable the modification of the surface with targeting ligands. Usually such micelles present a hydrophilic blocks formed by PEG and a core including various structures.[42] For example, curcumin loaded polymeric micelles formed by monomethoxy poly(ethylene glycol)-poly(epsilon-caprolactone) (MPEG-PCL) have been investigated.[43]

Cyclodextrins (CD) represent also a model of molecular inclusion. They are formed from enzymatic modifications of starch and present a cavity in which the hydrophobic molecules are incorporated. The CD family consists of glucopyranose subunits bonded with $\alpha$ (1-4) links. Based on the number of sugars forming the ring, cyclodextrins are distinguished in $\alpha, \beta, \gamma$ cyclodextrins (see figure 1.5). In literature there are several examples of polyphenols as resveratrol,[44] olive leaf extracts,[45] flavonoid rich Hipericum,[46] quercetin,[47] rutin,[48] rosmarinic acid [49] and polyphenol extract [50] included in cyclodextrins. In general inclusion increases aqueous solubility and antioxidant capacity.

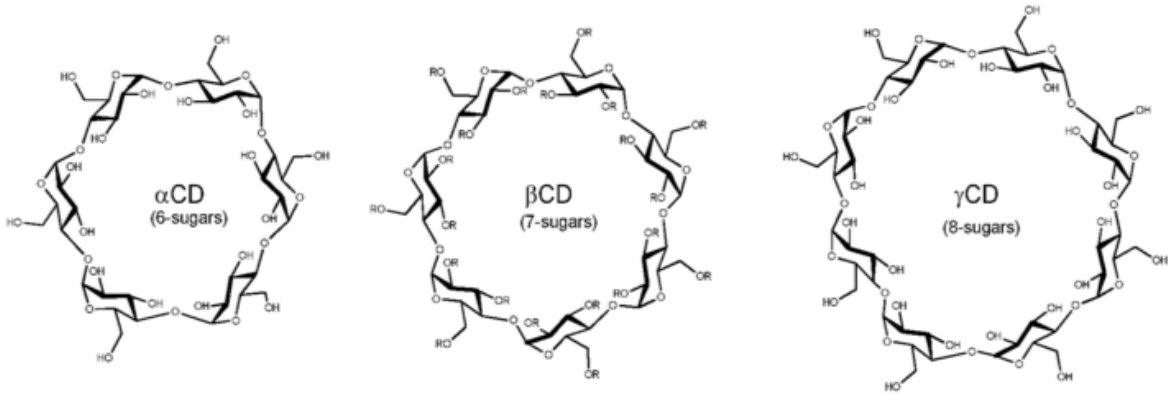


**Fig.1.5** Structures of α-, β-, γ-cyclodextrins.

## 1.3 Polymers

The term polymer designs a large molecule constituted of smaller repeating units known as *monomers* which are connected through covalent bonds.

A monomer is thus a fragment that combines with other fragments of the same or different type. A homopolymer derives from the repetition of a single monomer, instead a copolymer (in addition to the need of specifying the monomeric composition) is formed by two or more structurally different monomers. Another useful distinction is between *random copolymers i*n which monomers are randomly arranged in the chain, *alternating copolymers* in which the different monomers are arranged in an alternating sequence and *block copolymers* which are made up of blocks of different polymerized monomers. The final conformation of the chain depends from the modality in which monomers are joined to each others: in linear polymers the units are linked together end to end in a single flexible chain, in branched polymers, side or branch chains are connected to the principal ones, in crosslinked polymers several branches connect different polymer chains (see figure 1.6).

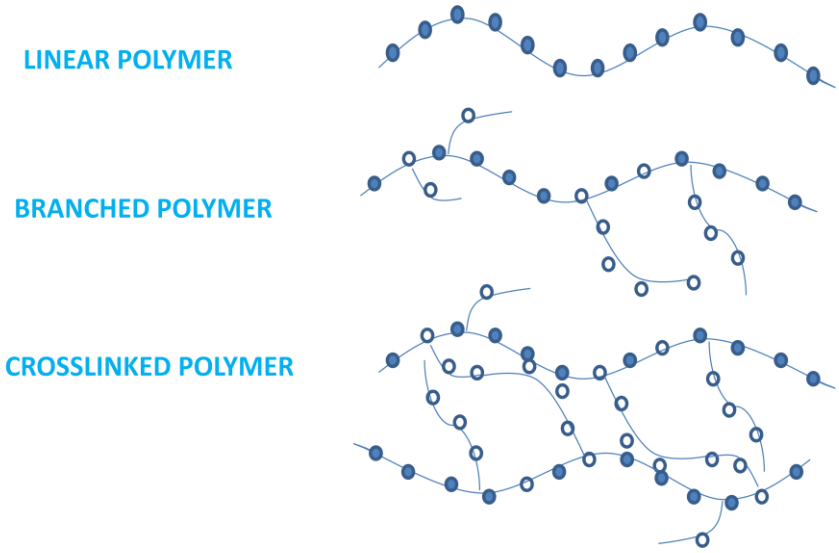


**Fig.1.6** Schematic representation of different types of polymers.

One important characteristic of polymers is that the polymeric chains may establish a large number of contact interactions between each other thus leading to the formation of higher level structures (fiber, particles, etc.) with important physicochemical and mechanical properties. The force of these intermolecular attractions is more important respect to the molecular weight of the polymer, and consequently to the number of repeating units, in determining the final properties of the system. In fact polymers with a low molecular weight but strongly interacting have better mechanical properties of high molecular weight polymers with weaker interactions.[51]

## 1.3.1 Polyelectrolytes

In the case in which the repeating units of a polymer bear a charged group, the polymer is identified as a polyelectrolyte. This class of polymers has several applications in all fields related to human uses. It is surprising, indeed, that many of biopolymers of living systems are polyelectrolytes, as nucleic acids, proteins, and glycosaminoglycans. Thanks to their hydrosolubility, the attention about possible applications is continuous. For example, in the oldest food technology the polyelectrolytes themselves are not only involved in the formation of the proper

texture but have been also used as thickening or gelling agents in juices, chocolate and other foods. Nowadays, potential applications in food industry are based on exploitation of polyelectrolytes and polyampholytes in mixed systems such as phase separated nanogels or multilayered membranes to improve stability of food emulsion.

As explained above, a polyelectrolyte is a polymer carrying ionizable groups with positive or negative charge. The fraction of dissociated ionic groups strongly affects the behavior of polyelectrolytes in solution. Solubility of the polymer in the solvent and presence of salt are other parameters influencing the final properties.

Dispersion of polyelectrolytes in polar solvents can determine a dissociation of the ionic groups leading to a charged polymer chain. The interactions between the charges confer to the polyelectrolyte characteristics strongly different from uncharged polymers. The main effects about electrostatic interactions on the chain are visible in:

- Short radius effect, due to the repulsion between sequent charges on the chain, these interactions cause a local stiffening of the chain, that can be characterized by the value of the persistence length.
- Long radius effect, in which different segments of the chain can interact and repulse. Repulsion affects both segments of the same chain (expansion) and segments of different chains, a phenomenon that generates an increase of the so-called “excluded volume”.

The addition of a salt to the solution, i.e. an increase of the ionic strength, results in a general shielding of polymer charges, with a decrease of polyelectrolyte dimensions.

Charges are organized in *clusters* on the polymer chain with elevated local electric potential. The model used to interpret properties of polyelectrolyte solution refers to the idea of a molecule as an impenetrable sphere made of low dielectric constant material. This model is similar to that expressed by Debye and Huckel in theorization of simple electrolytes. The model provides that electric charge is uniformly distributed on the surface of the sphere and that charge density can be calculated by Poisson-Boltzmann equation. In many cases this model is not sufficient and leads to serious error, as an example in the count of electrostatic free energies of polyelectrolytes. The theory was improved replacing the assumption of a uniform surface charge density with the introduction of the concept of well defined arrangement of the charged groups (clusters).[52]

The viscosity of a normal polymer solution is related to the nature of polymer and solvent, concentration of polymer, average molar mass, temperature etc.. If the solution is very diluted the viscosity can be expressed as:

$$[\eta] = \lim\left(\frac{\eta_{sp}}{c}\right)_{c\to 0} \tag{2}$$

For several polyelectrolytes the equation (2) is applicable only if the polymer is dissolved in aqueous salt solution, otherwise, the ratio $\eta_{sp}/c$ does not approach to a constant value for *c* approaching to zero.

Normally intrinsic viscosity depends from molecular weight as expressed from the Mark Houwink Sakurada (MHS) equation:

$$[\eta] = K \times M^{a} \tag{3}$$

and from radius of gyration $R_g$ and end-to-end distance *r*:

$$[\eta] \propto \left\langle R_g^2 \right\rangle^{3/2} \propto \left\langle r^2 \right\rangle^{3/2} \tag{4}$$

For polyelectrolytes, instead, intrinsic viscosity depends from charge density (calculated with the relation $Z_e/L$ in which *Z* is the number of charges (e) along the polymers and *L* is the length of the chain) and concentration of added salt. At constant concentration of salt, the more is the charge density, the more is the viscosity. At fixed charge density an increment in the amount of salt results in a decrement of viscosity.

Polyelectrolytes present some common behaviors such as, for example, the ability to form gel.

Gelling properties confer the ability to swell and retain water thanks to the presence of a cross-linked polymer network. Hydrogel can reach a swollen status in response to different stimuli based on the type of polymer used in the formulation (see figure 1.7).

The ability to absorb water depends on the characteristics of polymers and the type of crosslinking between the chains. The presence of large amounts of water confers properties of flexibility similar to the natural tissue and this represents an advantage for biomedical application also.[53]

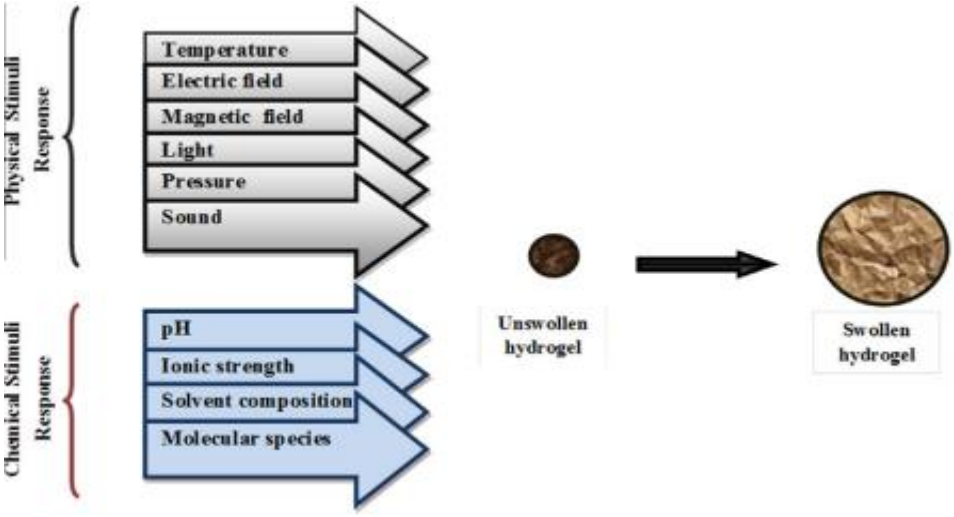


**Fig.1.7** Gelling properties in response to different stimuli (adapted from reference [53]).

Moreover the exclusive opportunity to control the swelling makes these systems advantageous to be employed in drug delivery and food field as encapsulating agents for biomacromolecules including proteins, DNA and nutrients. The formation of the gel occurs at ambient temperature, without addition of toxic solvents.

The polymers commonly used in the hydrogel formulations can have a natural or synthetic source. In food and pharmaceutical the use of natural polymers is preferred notwithstanding these materials have a poorer mechanical properties respect to synthetic ones.[54]

## 1.3.1.1 An overview on chitosan and alginate

Alginate and chitosan are biocompatible, biodegradable, safe and versatile polyelectrolytes of natural origin widely used in biotechnology and in the pharmaceutical sector. The principal application is as thickening agents in food field.

Their particular properties make them ideal matrices in cell immobilization or controlled release of proteins and other macromolecules. Chitosan derives from alkaline N-deacetylation of the chitin (see figure 1.8), the principal constituent of the outer shells of crustaceans and insects. Chitin is a structural polysaccharide, the most abundant after cellulose.

Deriving usually from a partial deacetylation, chitosan consists of a copolymer of β 1-4 linked 2-amino-2-deoxy-β-D-glucan (D-glucosamine) and N-acetyl-D-glucosamine with varying degree of deacetylation and molecular weights.

Chitosan is a basic biopolymer and its properties of solubility and biodegradability depend on the degree of deacetylation and on the number of protonated amino groups which, in turn, depend on pH. The full protonation of the amino groups occurs in acidic medium with a pKa smaller than 6.2: in this condition chitosan is water soluble.[55]

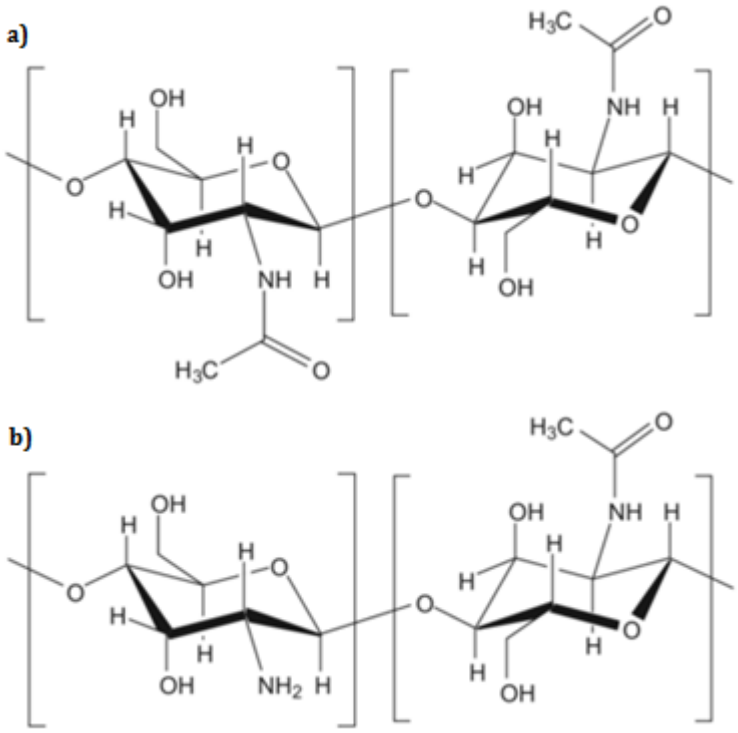


**Fig.1.8** Structure of chitin a) and chitosan b).

Alginates instead, derive from brown seaweed. The production of the polymer starts with a first step of grinding of the dried material, followed by acidic extraction to

remove residues of other polymers and to exchange alkaline cations with $H^+$. At the end of these steps, protonated alginate is converted in its sodium salt. Alginate is a linear copolymer with homopolymeric blocks of (1-4)-linked β-D-mannuronate (M) and its C-5 epimer α-L-guluronate (G) residues, respectively, covalently linked together in different sequences or blocks. The polymer belongs to the class of linear block copolymers (see figure 1.9).

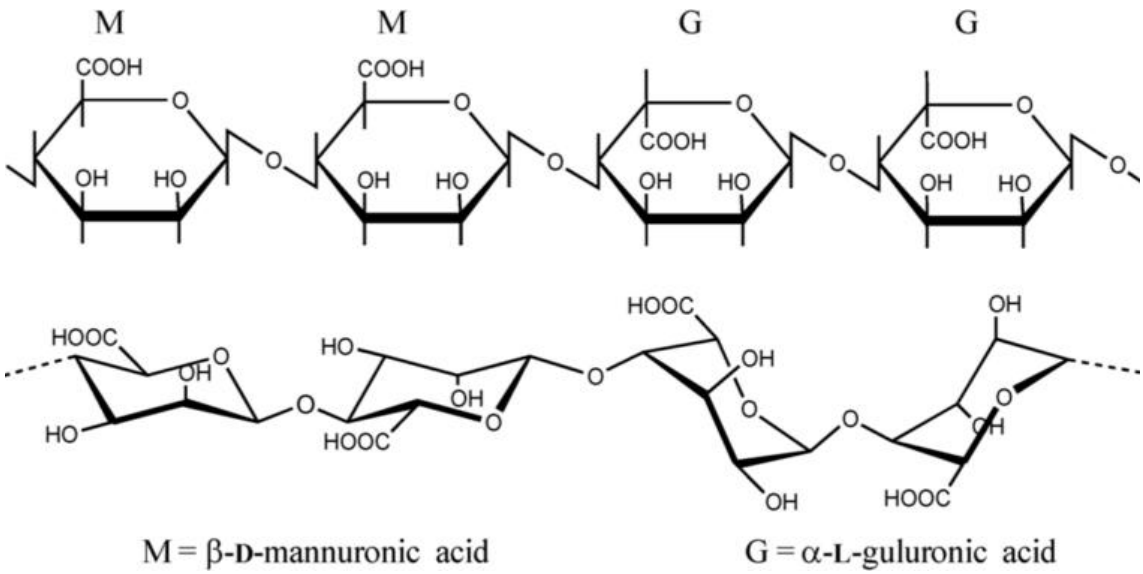


**Fig.1.9** Structure of polymeric chains of Alginate: Guluronic and Mannuronic units.

The typical arrangement of blocks copolymer chain in alginate is characterized by the alternance in homopolymeric regions and heteropolymeric regions. The former are composed by GG blocks alternated to MM blocks, the second instead are formed by sequence of mixed composition M-G blocks.[56] M units give a flat aspect to chain, while G monomers confer a characteristic buckled aspect. These provide a certain flexibility in homopolimeric tracts of MM residues and minor flexibility in GG blocks due to the steric hindrance of the carboxyl groups. As a consequence, the more is the content of M units, the more is the flexibility of chains. The diaxial linkage in G blocks results in a difficult rotation around the glycosidic bond that gives reason for the stiff and extended nature of alginate chain. Considering that alginate belongs to the class of polyelectrolytes as referred before, the repulsion between the charged groups increases the expansion of chains enhancing intrinsic viscosity. In fact considering the MHS relationship (3) *a* coefficient increases with chain extension, ionic strength and

alginate composition, having a direct role on intrinsic viscosity: low value of *a* is related to large fractions of MG region, high value of *a* is related to extended regions of G-blocks.[57]

Due to their polyelectrolyte behavior, chitosan and alginate are able to interact ionically with several charged polyelectrolytes. The type of ionic interactions can be summarized in ionic crosslinking and polyelectrolyte complexation.

The ionic crosslinking is a very appealing phenomenon: the presence of charged amino groups on chitosan in acidic conditions as an example, allows to crosslink the polymer by using negatively charged ions, such as triphosphate (usually reported in pharmaceutical literature as tripolyphosphate (TPP)), which is the most widely used. The interaction, commonly referred as ionotropic gelation, was extensively studied and described by Calvo,[58] after that Bodmeier[59] first reported the preparation of beads by dropping chitosan in a TPP solution. The ionic gelation takes place spontaneously via electrostatic interactions between chitosan chains and TPP.[60] This methodology of nano-particles preparation allows to encapsulate several types of biomolecules, from protein,[61,62,63] to small drugs[64,65] and genes[66] and because of its versatility it was extensively studied and optimized.[67,68]

An interesting study published by Stoica[69] shows encapsulation of a polyphenol complex extracted from Rosa canina with satisfactory results in term of efficiency. The article underlines the importance of Chitosan-TPP ratio in determining the characteristics of the nanoparticles. The capacity of chitosan to interact with TPP is translated in formation of inter and intra molecular crosslinking between amine groups of chitosan and phosphate groups of TPP. Operative parameters, such as stirring time and speed affect the properties of the nanoparticles and their yield[70] thus becoming important too.

TPP is not the only charged compound able to interact ionically with chitosan, and metallic ions as Mo (VI) and Pt (II) can also be used as cross-linkers. This metal ions give stronger crosslinking interaction respect to TPP. However, the use of TPP as crosslinker, has the advantage to give the possibility to check the crosslinking density by measuring the pH, because as the reaction proceeds, $OH^-$ ions are released in the reaction media. With other crosslinking agent, at the moment, there are not applicable

methods to control the crosslinking density and to predict the final properties of the gel.[71]

In alginate instead, the presence of G residues is responsible of the gelling property. Water solution of alginate may form gel in presence of bivalent cations. In fact, guluronic residues[72] may exchange $Na^+$ ions with divalent cations such as $Ca^{2+}$, $Sr^{2+}$ and $Ba^{2+}$, which act as bivalent linkers, promoting the formation of a strong network between GG blocks of different chains. The resulting network is known as *egg-box* structure (see figure 1.10).[73]

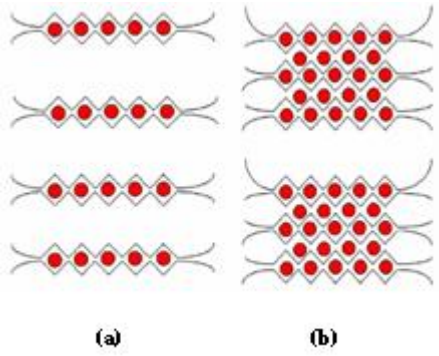


**Fig.1.10** Egg-box structure in presence of low (a) and high (b) concentration of bivalent ions. Red points represent ions between G sequences.

The formation of alginate gel using $Ca^{2+}$ is a widespread technology in the field of polyelectrolytes. A pioneering work by Rajaonarivony,[74] involves the use of alginate and $Ca^{2+}$ in such a concentration to form a pre-gel status with a lower level of crosslinking respect to a fully formed gel. In this pre-gel status the G residues not involved in the network may be saturated using a different polycation such as poly-Lysine. An example of this procedure is the encapsulation of doxorubicin in a alginate/$Ca^{2+}$ pre-gel which has been then fully jellified by interaction with poly-lysine.[75] Since the beginning, such mild conditions of gelation appeared very attractive for the encapsulation of labile drugs, characterized by poor bioavailability upon oral administration, as polyphenols. Nevertheless, articles showing encapsulation of polyphenolic antioxidants in ionic crosslinked chitosan or alginate matrices are limited but some examples are available such as the works of Liang[76] and Harris[77] regarding

encapsulation of tea polyphenols and a natural extract of Illex Paraguariensis, respectively.

Another very popular methodology for an easy formation of nanoparticles is through polyelectrolyte complexations (PECs). From this point of view, chitosan, is an attractive polymer, being the only natural polymer with a positive charge,[78] and, therefore, having the possibility to complex with a wide range of negatively charged polysaccharides by electrostatic interactions, forming PECs.

Since the early work published on PECs by Fuoss and Sadek (1949),[79] different studies and reviews have been published on this topic. PEC complexes obtained using natural biopolymers with opposite charge have been previously formulated as protein carriers[80] but represent also an ideal colloidal carrier for gene delivery[81] and for a sustained release of bioactive molecules. Hyaluronian, a biocompatible polymer negatively charged can be used to form complexes with chitosan[82,83,84], and has the ability to bind several receptors as CD44, once internalized in the body.[85] It can also be used as coating for chitosan-TPP nanoparticles.[67]

In literature there are not many reports on complex coacervation for the delivery of nutraceuticals, with some examples regarding interaction between chitosan and xanthan to deliver an oily seed rich[86]in lignans and physical interaction of alginate with polycaprolactone[87] to encapsulate white tea extract. On the other hand, scientific works dealing with nanoparticles preparation using coacervation methods to deliver polyphenols are lacking.

A sub-category of complex coacervation is represented by polyelectrolyte-colloids coacervates that have some advantages respect to polyelectrolyte-polyelectrolyte coacervation in reducing the heterogeneity of the final system. In particular protein-polymers coacervates belong to this category and represent an interesting system for preservation of bio-functionality and are particularly important in enzyme immobilization, protein purification, antigen delivery and stabilization of food.[88] An interesting article regarding polyphenol encapsulation describes the formulation of a complex coacervate made of catechin loaded chitosan-pectin.[89] Polyelectrolyte-protein coacervation can also occurs between the ammonium function of chitosan and reactive group of heparin,[90] BSA[88] and casein.[91] Also complexes between alginate and protein seem to act as potential carriers of nutraceuticals, in fact, nutraceuticals with

low solubility in water were successfully entrapped in β-lactoglobulin-sodium alginate complex. [92]

Along with the preparation methods, it is worthy to stress that the achievement of nanoparticles with tailored characteristics requires a full knowledge of the physicochemical properties of the chitosan and alginate[93] and various parameters affect the final properties.

As an example, the increase in chitosan and alginate MW, has a consequent on both encapsulation efficiency and release of protein, deacetylation degree of the chitosan instead has an effect on hydrophobic interactions that can improve the retention of a lipophilic molecule and G/M ratio of alginate affects the final stiffness of the network. Ratio and concentration between components furthermore determine the amount of available hydroxyl groups that may be engaged in hydrogen bonding, influencing the results in terms of sizes and stability of nanoparticles.[94]

Concentration and density charge of the crosslinking agent, Mw and reaction time instead influence the final crosslinking density, a determining factor in order to ensure swelling capacities, pH-dependance, acceptable mechanical properties and release of drug from gel.

The control of all the variables affecting swelling behavior and network pore sizes, becomes a limiting factor reducing the field of application of these systems.[95] Furthermore, the possible lack of mechanical properties,[96] the possibility of dissolution due to pH dependence, the strong dependence from external conditions after administration lead to weak systems. Nevertheless, improvements and modifications may promise further progresses in pharmaceutical applications.[97]

Chitosan and alginate can also interact each other's forming a polyelectrolyte complex. The exact definition of the mechanism by which these complexes are formed is difficult mainly due to the complexity in following the multi-ionic interaction which are established at the interface of the macromolecules and which are strongly influenced by pH. Simsek and al.,[98] gives a description of these interactions based on a FT-IR characterization of the complex formed at different pH in extremely dilute solution of polymers. The complex is formed mainly thanks to Coulomb forces with some participation of hydrogen and ionic bonding. As seen above the first ionic interaction studied between alginate and a polycation was with poly Lysine, but in several

subsequent research works, chitosan was used instead of poly-Lysine.[72,73,99,100,101] Alginate and chitosan are able to interact forming PECs as reported by Sarmento [102] in a comparative study on nanoparticulate systems prepared by coacervation and by ionotropic pre-gelation. The coacervation is due to interactions between the carboxyl functions of guluronic/mannuronic units of alginate and the positively charged amine groups of chitosan.[103,104,105] Chitosan-alginate systems are usually obtained in the form of beads for a controlled release of high molecular weight drugs, whose release rate is strongly influenced by chitosan concentration and pH. The properties of low toxicity, high biocompatibility, biodegradability of alginate and chitosan make them attractive candidates for the development of nutraceuticals delivery systems, exploiting their polyelectrolytes behavior. For example, alginate and chitosan coacervates can preserve a polyphenolic plant extract.[106] Other examples are microspheres formed by ionic attractions between the two polymers able to entrap tea polyphenols[107] or crocin.[108] The synergic action of alginate and chitosan improves the mechanical stability of the encapsulating systems while the presence of alginate improves impermeability and prevent rapid diffusion of bioactive molecules at acidic pH. Moreover, the two polymers were shown to cooperate in the protection of bioactive molecules from degradation and in the increment of residence time of liphophilic molecules such as *trans*-cinnamaldehyide.[101]

Apart from these and other few examples the use of systems made by alginate and chitosan interacting together for delivery of nutraceuticals to date remains largely unexplored, but potentially it should ensures the same results of delivery systems conceived for protein or antibiotics.

Another interesting reaction is the covalent modification of alginate and chitosan. For example glutaraldehyde has been used as covalent crosslinker for chitosan. The reaction occurs between the amine function of chitosan and the aldehyde group of the linker leading to an imine bond via a Schiff reaction linking the polymer to chain belonging to the same polymeric chain or to a different one.[71] In literature several articles present the crosslinking of chitosan with itself in presence of glutaraldehyde.[109] The crosslink reaction with glutaraldehyde offers also the possibility to bind different polymers to chitosan and the synthesis of macroporous chitosan-gelatin scaffold[110] is an example.

The main feature of such crosslinking is that it is irreversible and gives rise to rigid network structures.[111] Drug release occurs mainly via diffusion and depends on chain relaxation characteristics of the crosslinked network after dissolution in the medium. The main drawbacks encountered are the high toxicity of the aldehydes and insufficient biocompatibility. These problems actually limit the use of this crosslinker. Similar considerations can be done for epichlorohydrin. A new crosslinking agent, genipin, which is found in gardenia fruit extract, is becoming an interesting alternative to glutaraldehyde.[112,113,114,115]

Another suitable modification includes the use of ethyl-dimethyl-aminopropyl-carbodiimide hydrochloride (EDC), a more biocompatible agent compared to glutaraldehyde. EDC enables the formation of amide bonds between the amino groups of chitosan and the carboxyl groups of different macromolecules. EDC is also known as zero length crosslinker. EDC is used to produce a great number of chemical derivatives. The mechanism involves the reaction of EDC with a carboxyl acid to produce a reactive o-acylisourea as intermediate. Reaction of this activated acid with a nucleophile such as a primary amine leads to the formation of an amide bond. Moreover, thanks to its water solubility, EDC is readily used in aqueous environment. The final structure results in a permanent network with high mechanical properties and high resistance to dissolution also in extreme conditions of pH. The use of a crosslinker zero length is a valid instrument to modify hydrophobically an hydrophilic polymer, as chitosan or alginate. Several articles show in fact the possibility to modify chitosan with cholesterol preventively conjugated with succinyl molecule [116] or to graft chitosan with linoleic acid.[117] Alginate instead can be hydrophobically modified with octylamine using EDC as coupling agent.[118] The coupling reaction is also a strategy to improve mucoadhesive property of alginate grafting the polymer with cystein.[119] Despite coupling reaction was explored to bind macromolecules to small molecules also macromolecules can be coupled as in the case of chitosan-hyaluronian[120]and chitosan-gelatin.[121] Alginate is potentially able to interact covalently with chitosan through amide bond formation. A recent article[122] describes an amide linkage between chitosan and alginate forming nanoparticles with high stability even in acidic environment.

Nevertheless, the reaction between alginate and chitosan using EDC is still an unexplored route for production of nanoparticles but it may be a valid methodology to formulate stable nanoparticles as carriers. A central feature in the optimization of the reaction, regards the reaction conditions and in particular the medium in which the reactions is performed which can be water but also more complex systems such as emulsions. The formulation of systems in emulsion can stabilize the polymers during the reaction and the formation of the nanoparticles will take place in the nanocompartments of the internal phase separated from each other by the continuous phase.[123] The optimization of the reaction in emulsion requires an adequate knowledge of the emulsion formation.

## 1.4 Emulsions

Emulsions are thermodynamically unstable systems obtained by mixture of two immiscible liquids. Emulsions are generally classified as dispersed systems consisting of an internal phase forming droplets dispersed in a continuous, external phase. Emulsions can be distinguished in W/O if the continuous phase is water or O/W if oil is the external surrounding phase.[124] The type of emulsion (W/O, O/W) depends on water-oil ratio, temperature and other parameters such as electrolyte concentration and type of emulsifying agent. Any phase under agitation can be broken in droplets dispersed in a continuous immiscible phase but an emulsion formed in such way tends to a rapid coalescence of the droplets leading to phase separation.[125] The predominant force for phase separation is the interfacial free energy of droplets, that increases after dispersing a phase into another one. The addition of surfactants, molecules acting as "surface active" agent, can reduce the *interfacial tension*. A depth elucidation on what is intended as interfacial tension enables a full comprehension of the mechanism of action of surfactants.

## 1.4.1 Phenomenological description of theory of interfaces

The interfacial tension is the event occurring at liquid-liquid interface, the same phenomenon happens in case of liquid-air contact and it is called surface tension.
The phenomenon can be interpreted using two different models. From a mechanical point of view, in the bulk of a liquid, molecules have balanced cohesive forces acting in all directions with a resultant zero force. Instead molecules at the interface, being not surrounded from other molecules in all sides, have a resultant force that is no zero, so they tend to reduce the area of contact with the other liquid to a minimum value, limiting the mixing. Based on these considerations, the interfacial tension is considered as the contractive force for unit length operating at the interface. It is mechanically quantifiable as the force needed to extend an interface of an infinitesimal amount. Considering the phenomenon with a thermodynamic approach, the interfacial tension is considered as the increase of Helmholtz or Gibbs energy after the increasing of the interfacial area of an infinitesimal quantity.[126] The two approaches lead to equivalent dimensional units. The inclusion of a surfactant in the emulsion enables the reduction of the interfacial tension, promoting the mixing of the immiscible phases. Surfactants have an amphipathic molecular structure consisting of a hydrophilic group with a good attraction for the water phase and a lipophilic portion with affinity for the oil phase.[127] When placed in an oil-water system, they orient to consent the interaction of the polar head with water and of the apolar tail with oil. The reduction of interfacial tension takes place by concentration of the surfactants at the oil-water interface, preventing emulsion breaking due to the rapid coalescence of droplets.[128] They usually are added during the emulsion formation to increase the process of dispersion and to ensure stability during time. The type of surfactant used is a very important aspect. In fact the phase in which the emulsifier is better partitioned tends to be the external phase. This principle is summarized by Bancroft's rule according to which the external phase of an emulsion tends to be the phase in which the emulsifier is more soluble.[129] Following this theory is important to determine the contribution of hydrophilic and hydrophobic portions of the emulsifier introducing the concept of HLB. In fact, to reach a good predictability of emulsion stability, Griffin introduced in 1949 [130] the so called HLB

number (Hydrophilic-Lipophilic Balance) that is a scalar numerical value which differentiates the emulsifiers. Davies, in 1963 optimized the original concept introducing the HLB group number based only on the structure of emulsifier. This methodology enables to calculate the HLB referring to the functional groups present in the emulsifier and matching the value to the required HLB value for oil emulsification.[131] Actually the HLB number has been determined for each available emulsifier. For an easy choice of the right emulsifier is good to learn that a value of HLB lower than 9 corresponds to an emulsifier with a lipophilic character so it could be employed for W/O emulsions, on the contrary emulsifiers with HLB above 11-12 have hydrophilic characteristics and could be used to formulate an O/W emulsion. Emulsifiers with HLB value ranging from 9 to 11 have an intermediate behavior.[132] This classification is sometimes not very rigid and depends also from the ratio between the continuous and internal phases. As a consequence, it is possible to formulate a good emulsion by using a single emulsifier or a blend of emulsifiers having the same final HLB. An emulsifier has a multiplicity of roles in emulsion which are related to:

- lowering the interfacial energy between the two phases,
- producing smaller droplet sizes,
- improving stability of the dispersed phase,
- determining the type of emulsion (W/O or O/W).

## 1.4.2 Different types of surfactants

Surfactants can be classified for their physical properties and functions. In relation to the chemical structure and the consequent hydrophobic and hydrophilic character, surfactants have different chemical properties and behavior. The most useful distinction of surfactants is based on the charge of the polar head. This leads to a classification of four classes of surfactants briefly described below:

- Anionic surfactants, formed by a ionizable head, dissociated in water generally in an anionic amphiphilic portion associated to an alkaline metal cation and by a hydrophobic tail of different nature. This category includes carboxylates (-

$CO_2^-$) e.g. sodium stearate, sulfonates ($-SO_3^-$) e.g. sodium dodecyl benzene sulfonates, phosphate ($-PO_3^{-2}$) and sulfates ($OSO_3^-$) e.g. sodium dodecyl sulfates (SDS), and alkylphenols. The hydrophobic chain can be of different typology as saturated, unsaturated, aromatic, or aliphatic. Anionic surfactants are widely employed as cleaning agents.

- Cationic surfactants, of which the most common have a nitrogen atom positively charged. In the case of amines the compound is pH sensitive, acting as emulsifier only when the amine group is protonated e.g. laurylamine hydrochloride. Ethoxylated amines, instead, can be considered cationic or non ionic depending on pH conditions. The properties of surfactants carrying a quaternary ammonium group are not pH dependent. Cationic surfactants usually are used for their adsorbing capacities at anionic surfaces of plastics, minerals etc. and as antiseptic agents.
- Zwitterionic surfactants have opposite charged groups; generally the cationic function derives from the presence of a nitrogen atom and the anionic part is a carboxylic unit. Usually these surfactants are employed in shampoo and dermatological formulations for their low irritation properties.
- Non ionic surfactants include polymerized derivatives of ethylene oxide in which the polyoxyethylene chain represents the polar head. The length of oxyethylene chain usually ranges from 5 to 10 units but in some cases can be longer. The reaction of ethoxylation is normally performed in alkaline condition in the presence of different type of nucleophiles. Indeed, fatty acids, fatty alcohols, fatty amines and alkylphenols are readily ethoxylated.

  Another important group of non ionic surfactants is constituted by hydroxyl derivatives. Poly-ol based surfactants include sorbitan, sucrose, poly glycerol esters. Alkyl glucoside compounds can be ethoxylated too. Spans are examples of sorbitan esters and Tweens are examples of ethoxylated sorbitan esters. Non ionic surfactants have an important role in emulsion formation for their peculiar characteristics such as low interaction with electrolytes, compatibility with other classes of surfactants and strong dependence of their behavior from temperature. This last aspect in particular is a characteristic of polyoxyethylene

derivatives that present a reverse behavior respect to sugar based ones: increasing temperature their solubility in water decreases.

### 1.4.3 Instability of emulsions

Emulsions have a natural predisposition to macroscopically separate in two different phases. In fact once emulsion has been formed several phenomena of instability may occur leading to the breakdown of the emulsion. Some of these processes are:

*Creaming*: this phenomenon leads the dispersed globules to separate out forming a film on the top of the continuous phase. The internal phase remains in globular form so an intense agitation can restore the emulsion. The phenomenon is visible on the top of the external phase when the internal phase is less dense than the external one such as in O/W emulsion. If the droplets are monodisperse, charged and coated they tend to repel so they don't approach each other minimizing the tendency to cream.[133] Stock law well describes the rate of creaming of an emulsion at infinite dilution.

Sedimentation: when internal droplets have a density higher than external phase as in the case of W/O emulsion, particles fall, becoming visible at the bottom of the container. The process is called sedimentation, and is the same of creaming but in opposite direction. Creaming and sedimentation represent a first step towards phase separation.

*Flocculation*: is due to the aggregation of small droplets in big aggregated globules without coalescence. All droplets maintain integrity being totally separated from each other.

*Coalescence*: this type of instability occurs when droplets become gradually larger without no mechanical or physical barriers to prevent aggregation.[134] It can be considered as a continuation of the flocculation process.

*Ostwald ripening***:** in addition to these events another mechanism of instability to be mentioned is Ostwald ripening. As time evolves, emulsion changes: the number of total particles decreases and particles diameter increases,[135] in fact larger particles swallow the smaller ones with the total volume fraction remaining constant. This is

due to the fact that the larger particles having a higher volume to surface area ratio are thermodynamically more stable.

## 1.4.4 Macro/micro/nano emulsions

According to the sizes of the droplets of the internal phase it is possible to distinguish different categories of emulsions:

- macroemulsion: droplet size ranging from 0,5-100 μm
- microemulsion: droplet size from 50-500 nm
- nanoemulsion: droplet size from 50-500 nm

The main macroscopic difference between the different types of emulsions is the physical appearance of the system. In fact the aspect depends on the scattering of light by the droplets of the internal phase. The intensity of the light scattered is proportional to the sixth power of the radius of droplets. So macroemulsion scatters totally the spectrum of incident visible light owning an appearance of milky solution. As the droplets size decreases, the amount of scattered light decreases, so that the dispersion acquires the aspect of a translucent solution until to turn in transparent solution as in the case of micro and nanoemulsion. Emulsion is the term conventionally referred to macroemulsion. The relatively large droplet radius in macroemulsion leads to an increment of the droplet sizes with time that causes thermodynamic instability and phase separation. Macroemulsions are in fact kinetically stable but thermodynamically unstable. A microemulsion instead, once the right conditions of formulation are optimized, forms spontaneously so it is an example of thermodynamically stable and optically isotropic system.[136] More subtle are the differences between microemulsion and nanoemulsion, such as that in literature these two terms are often confused. Indeed, there are many structural analogies between the micro- and nanoemulsions but also several differences, the main being the thermodynamic instability of nanoemulsions.

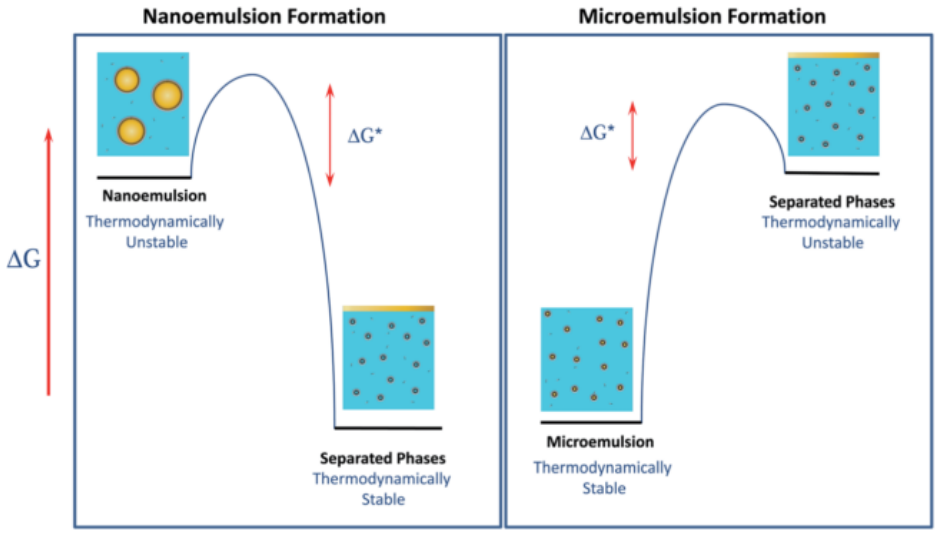


**Fig.1.12** Difference in free energy involved in nanoemulsion and microemulsion formation (adapted from [136])

To better understand the difference in thermodynamic stabilization is helpful to refer to a comparison between the free energy of the two systems (micro and nanoemulsion), considering for simplicity the case of oil in water emulsion (see figure 1.12). As a premise is essential to highlight that thermodynamic stability of a specific state is calculated as the difference in free energy between this state and another one adopted as reference state. In nanoemulsion, the free energy of the non mixed phases is lower than the free energy of the oily droplets in water. This implies that nanoemulsion is thermodynamically not favored, so instable. The formation of nanoemulsion occurs thanks to energy input as mechanical shear. This means that a nanodispersed emulsion always evolves towards the breakdown. Giving a great barrier between the two states of energy is possible to confer a kinetic stability to the dispersion that will persist until the barrier will be overcome. In microemulsion instead, the free energy of the separated phases is higher than the free energy of the stabilized colloidal droplets which indicates that the dispersed state is thermodynamically favored, the system undergoes a spontaneous emulsification process governed by self assembly. Emulsion needs to receive energy for induction of the phase separation. Preserving unchanged the conditions of formulation (as temperature or chemical composition) a microemulsion will have unlimited stability.

## 1.4.5 Construction of a phase diagram

The formulation of an emulsion requires the knowledge of the compatibility between solvents, cosolvents and amphiphilic components and of the effect of each component concentration on the final emulsion. A valid aid can be represented by the use of a phase diagram (see figure 1.13) as reference to explore stability of different regions of the mixtures.

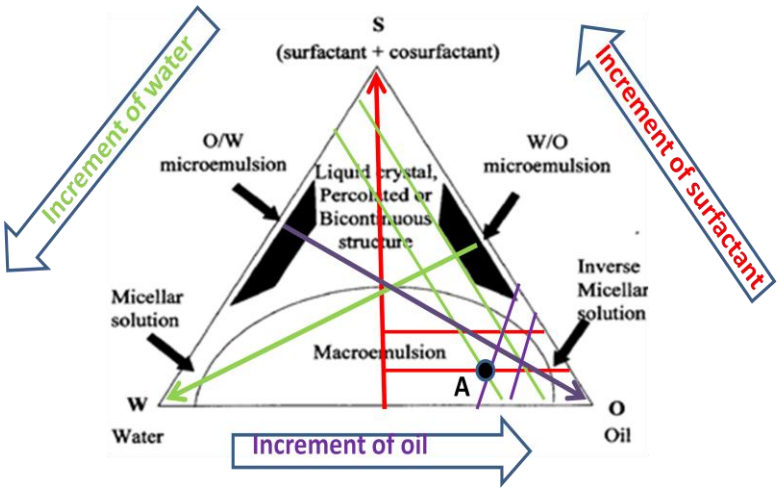


**Fig 1.13** Example of phase diagram

A phase diagram of a ternary system is represented by a triangle in which the vertexes of every angle represent one of the three components (water, oil, surfactant).

Moving inside the triangle is possible to explore different compositions and ratios between the three phases, staying within the same typology of emulsion (macro, micro or nano) or moving from one to others. For example considering the point A, three lines (red, violet, green) pass from here, so it is sufficient to move on every line, toward the side represented by the color (red for surfactant, green for water, violet for oil), to know the proportion used of that component. In this way is easy to explore near regions and to optimize the parameters.

## 1.4.6 Food grade emulsions in drug delivery and food

The colloidal delivery systems obtained from micro and nano emulsification are rapidly spreading in food and pharmaceutical to protect, stabilize and deliver lipophilic compounds. Nanosized emulsions represent a vehicles for oil soluble drugs and the presence of aqueous environment can mask eventual strong taste of oil.[134]

In the performing of a typical food-grade emulsion is of great importance to select ingredients approved in food industry. The use of corn oil olive oil, sunflower oil, castor oil [137] or other similar typologies of components founds application in several works. In particular the hydrophobicity of the oil phase and the chain extension of oil strongly affect the stability of emulsion. Also surfactants may undergo a critical evaluation of safety before to be selected. Despite possibility to select food grade ingredients is limited, usually phospholipids (lecithin overall) are the principal investigated emulsifying agents.[138] These systems present several limitation due to high viscosity and flocculation.[139]

## 1.4.7 Technologies to produce micro and nanocarriers from emulsions

The transition from food-grade emulsions to emulsions involving chemical reagents enables the formation of smaller droplets and “pure” systems thus facilitating a better analysis and a better understanding of the resulting systems. The field of nano-formulated emulsions has not been widely explored for the formation of polymer nanoparticles, although it may give the advantage respect to other methodologies of a relatively easy preparation. The final stability of the nanoparticles over time, the narrow size distribution allowed by emulsion system and a good control of all the parameters concerning reaction are other reasons for consider interesting the investigation in this field. Moreover in literature not all combinations of polymers have been explored, despite they can represent a good starting point for new delivery systems. The employed technologies for the preparation of polymer nanoparticles in

emulsion can be resumed in a few basic techniques that can undergo changes and modifications.

- Emulsification/solvent evaporation

  The drug or molecule to be encapsulated is dispersed or dissolved in an organic solvent in the presence of the encapsulating polymer matrix, then a second solvent (usually water), immiscible with the first one, is introduced to emulsify the organic phase. Finally the organic solvent is evaporated provoking the precipitation of the polymers in form of spheres in the continuous phase. Usually the use of O/W emulsions is preferred, giving the advantage of economic and safe process. The main limitation of this technology is the need to use polymers with a prevalent hydrophobic character as well as lipophilic drugs or bioactive molecules. The final sizes of spheres can be controlled acting on the viscosity of phases, stirring rate and temperature.[140] Two possible mechanisms for particles formation has been proposed. The first regards the possibility that a single nanoparticle originates from a single droplet of emulsion and this is possible in the case in which the emulsion maintains stable during the evaporation of the solvent. The stabilization of the emulsion can be reached by the addition of a surfactant. The second possible mechanism instead considers every nanoparticle as originating from the merging of many different emulsion droplets. In this case the process is determined by the instability of droplets during evaporation of the solvent.[141] Nanoparticles of poly-(lactic acid) (PLA) are usually obtained using this method of preparation. An adaptation of this methodology enables the preparation of nanocapsules of curcumin encapsulated in chitosan matrix. The technique includes a multiple emulsion O/W/O followed by the evaporation of the oil phase and the recovery of nanoparticles by centrifugation.[142] An inversion of the typology of emulsion, W/O/W, was exploited to form alginate microparticles.[143]

- Solvent displacement

  This method is a variant of the process just presented. It is known also as nanoprecipitation and is a safe, reproducible and economic wide-spread method used to produce colloidal systems. The method is based on the solubilization of a non water soluble polymer in an amphiphilic solvent totally

water miscible, normally acetone. Once polymer is solubilized, the solution is added to a water phase leading to the formation of the nanoparticles. The deposition of the polymer at the interface between the two solvents, determined by a fast diffusion of the water phase,[144] suggests that the formation of nanoparticles is based on interfacial phenomena.[145]

- Interfacial deposition

  The mechanism is based on interfacial polymerization of a monomer at the interface between two immiscible phases. If the internal phase is a liquid the monomer can be dissolved or dispersed in this phase and then the matrix can be emulsified in the external phase until to reach the required size of droplets. It is also possible to add a crosslinking agent to the external phase.[146]

- Emulsification/solvent diffusion

  This is a modified version of the emulsion/solvent evaporation, presented above. At first, a partially water soluble solvent is used to dissolve the polymer, and then the mixture is saturated with water to ensure a thermodynamic equilibrium between the phases. Then the induction of precipitation of polymers for the formation of nanoparticles is due to the dilution of the system with an excess of aqueous solution; at this point, the polymer phase added of water is emulsified with a stabilizer, leading to the diffusion of the solvent in the external water phase. At the end of the process solvent is removed by evaporation or filtration.[144]

  This method originally developed to formulate PLA nanoparticles,[147] was adapted to the formation of chitosan nanoparticles. The modified process, involves the addition of an organic phase made by methylene chloride and acetone to an aqueous solution of chitosan in presence of lecithin as emulsifying agent. After formation of O/W emulsion, methylene chloride is removed and acetone spreads in the aqueous phase causing the precipitation of chitosan.[148] Solvent diffusion enables also the formation of chitosan genipin crosslinked systems to deliver protein.[114]

- Salting out

  This is another useful technique used to produce nanoparticles. The technique is a modified form of emulsification solvent diffusion method, and involves the

formation of an oil in water emulsion. The lipophilic polymer is dissolved in an organic phase usually acetone, and an active compound is added in a water miscible solvent. Water solution instead is a gel containing a stabilizer as PVP and a salting out agent (usually electrolytes or sucrose). The presence of an appropriate salting out agent is fundamental in the evaluation of encapsulation efficiency of a bioactive compound. The diffusion of the solvent in aqueous phase is inhibited by the presence of the salting out agent. Once emulsion is diluted with water to reduce the concentration of salting out agent, organic solvent starts to spread inducing the formation of nanospheres in the aqueous phase.[149]

- Dialyses

  Dialyses is also a tool to produce nanoparticles. The method is similar to nanoprecipitation and involves solvent displacement mechanism, but unlike conventional nanoprecipitation, here, a dialysis tube with a determined cut off represents a physical barrier for polymer. The methodology involves the use of a miscible couple of solvent and non-solvent for the polymer. The polymer is dissolved in the solvent and dialyzed against the non-solvent leading to a reduction in polymer solubility and formation of nanoparticles.[150]

- Emulsification and crosslinking

  The first application of emulsion in formation of nanoparticles of chitosan regards a preparation of chitosan nanoparticles in W/O emulsion (using toluene as continuous phase and Span 80 as emulsifier). Once system was emulsified, the glutaraldehyde acting as crosslinker agent was added.[151] Different authors have then modified the continuous phase replacing toluene with liquid paraffin and petroleum ether.[152] However, the use of glutaraldehyde as written above presents some drawbacks being responsible of toxicity and possible degradation of entrapped drug. The introduction of EDC as crosslinker was also explored, and in particular enables the formation of polymeric nanoparticles of controlled sizes by the control of size of droplets.

- Emulsification droplet coalescence

  This is an alternative methodology that includes the emulsion droplet coalescence as a mean to induce formation of chitosan nanoparticles. The

procedure uses paraffin and Span 83 as reagents to obtain W/O emulsion. The emulsion is then mixed with another emulsion of NaOH that causes the solidification of chitosan nanoparticles.[153] The formation of nanoparticles is based on random collision of the droplets when the emulsions are mixed and consequent coalescence.

All these different techniques open the door to little variations of the procedures to covalently attach chitosan to alginate polymer. In fact the above examples show that both alginate and chitosan are able to react in presence of EDC forming covalent compounds, but there are very few studies on their ability to bind together. One of the most challenge is represented by the pH considering that solubilization of alginate suffers an acidic environment and EDC need slightly acidic condition to work. Recent advances in micro and nanoparticles formation from biodegradable polymers implemented the investigation of W/O emulsions method. In a typical procedure a certain amount of polysaccharide (as chitosan, alginate, starch) dissolved in water or other aqueous solvent is slowly dropped in a solution containing organic solvent. Once the emulsion was formed, another emulsion is formulated in the same way in presence of the counterpart component. Interactions based on random collision between droplets favor the reaction between the macromolecules.

# 1.5 Aim of this study

This Thesis was developed at the Laboratory of Physical and Macromolecular Chemistry in the Department of Life Science in collaboration with the Department of Chemical and Pharmaceutical Science.

The growing interest in nutraceutics due to the demonstrated beneficial effects of phytochemicals on human body is a driving force in the research field of new delivery systems. Actually the low solubility in water, the poor absorption in the gastro-intestinal tract, the low stability and the easy oxidation are limiting factors in the use of nutraceuticals. The possibility of an efficient entrapment, delivery and bioavailability of nutraceuticals represents a current relevant challenge for researchers. In this scenario biodegradable polymers as alginate and chitosan thanks to their characteristics of non toxicity, biocompatibility, mucoadhesion are very attracting for the formulation of new carriers for oral administration of nutraceuticals.

The aim of my PhD project is the formulation and characterization of new delivery systems based on covalent interaction between alginate and chitosan. The possibility to form a covalent linkage between the carboxyl units of alginate and the amine groups of chitosan using EDC/NHS as zero-length crosslinking agents will be investigated in order to obtain nanoparticles with improved stability and resistance. Moreover the covalent crosslinking should confer rigidity to the polymeric network limiting the leakage of the entrapped nutraceuticals. In the Thesis different methodologies of nanoparticle preparation will be explored including reaction in water, reaction in food grade macroemulsion and reaction in nanoemulsion. In particular nanoemulsions are a promising technology because they allow to perform the reaction within the nano sized water droplets thus limiting the interaction between polymers and giving the best result in terms of reduced sizes and stability of the nanoparticles. The systems will be fully characterized in size, stability, morphological shape, encapsulating properties and eventual toxicity. Inclusion of resveratrol and quercetin will be critically discussed and the antioxidant activity after the entrapment will be evaluated.

# Materials & Methods

# 2

# 2.1 Materials

## 2.1.1 Polymers :

- Alginate Ultrapure (NovaMatrix). Apparent viscosity : medium viscosity > 200 mPa*sGuluronic content > 60%.

- Chitosan Ultrapure (NovaMatrix). Apparent viscosity : low viscosity 20-200 mPa*s Deacetylation 75-90 %.

## 2.1.2 Components of food grade emulsions :

- Sunflower oil.
- Lecithin (Lecinova).
- L-α Phosphatidylcholine (PC): Sigma-Aldrich Co.(St Louis, Mo).

## 2.1.3 Components of not food grade emulsions :

- Cyclohexane: Sigma-Aldrich Co.(St Louis, Mo).
- Hexanol: Sigma-Aldrich Co.(St Louis, Mo).
- Triton X-100: Sigma-Aldrich Co.(St Louis, Mo).
- Tween 80: Galeno, (Carmignano, PO, Italy).
- Span 80: Galeno, (Carmignano, PO, Italy).

## 2.1.4 Normal reagents:

- (EDC) *N*-(3-Dimethylaminopropyl)-*N*'-ethylcarbodiimide hydrochloride: Sigma-Aldrich Co.(St Louis, Mo).
- NHS (*N*-Hydroxysuccinimide): Sigma-Aldrich Co.(St Louis, Mo).
- Hydrochloric Acid (HCl) : Sigma-Aldrich Co.(St Louis, Mo).
- Sodium Chloride ( NaCl), : Sigma-Aldrich Co.(St Louis, Mo).
- Acetone: Sigma-Aldrich Co.(St Louis, Mo).
- Methanol : Sigma-Aldrich Co.(St Louis, Mo).

## 2.1.5 Other reagents:

- DPPH (2,2-diphenyl-1-picrylhydrazyl radical): Sigma-Aldrich Co.(St Louis, Mo).
- Amberlite AD2: Sigma-Aldrich Co.(St Louis, Mo).
- MTT (3-[4,5-dimethylthiazol-2-yl]-2,5-diphenyltetrazolium bromide): Sigma-Aldrich Co.(St Louis, Mo).

## 2.1.6 Nutraceuticals :

- *Trans*-Resveratrol, 3,4',5-Trihydroxy-*trans*-stilbene: Acef (Fiorenzuola d'Arda PC), Italy
- Quercetin, 3,3',4',5,6-Pentahydroxyflavone: Sigma-Aldrich Co.(St Louis, Mo).
- Ascorbic acid: Farmalabor ( Canosa di Puglia, BT), Italy

# 2.2 Polymer characterization

## 2.2.1 Alginate

### 2.2.1.1 Viscometry

Reduced capillary viscosity was measured using a Schott-Geräte AVS/G automatic apparatus mounting an Ubbelohde type viscometer. Measurement (see figure 2.1) was performed at 25°C on alginate salt solutions (0.1 M NaCl). The intrinsic viscosity [η] value was determined by extrapolating the reduced specific viscosity ($\eta_{sp}/c$) values to zero concentration using the Huggins equation:

$$\frac{\eta_{sp}}{c} = [\eta] + k' \cdot [\eta]^2 \cdot c \qquad (5)$$

Where *k'* is the Huggins constant.

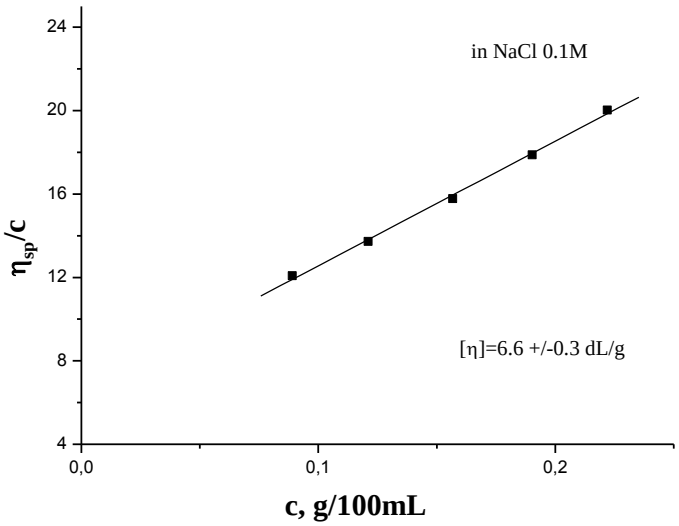


**Fig.2.1** Extrapolation of [η] in alginate NaCl 0.1 M solution.

Intrinsic viscosity [η] for a given polymer of molar mass *M* under fixed solvent conditions (i.e.: solvent type and temperature) follows a simple power law of MHS equation (3) where *k* and *a* are given parameters for a specific solute-solvent system. The <Mw> of alginate calculated from viscosity measurements is $1{,}96 \times 10^5$ g/mol. The molar mass was estimated using the MHS parameters reported elsewhere.[154]

### 2.2.1.2 Determination of Guluronic/Mannuronic ratio

$^1$H-NMR measurement was carried out at 80°C on a Varian spectrometer (11.74 T) operating at 500 MHz for $^1$H equipped with a model L650 Highland Technology pulsed field gradient (PFA) amplifier (10 A) and a standard 5 mm indirect detection PFG probe. Spectrum was recorded in $D_2O$. The polymer was exchanged three times in the proper deuterated solvent before running the measurement.

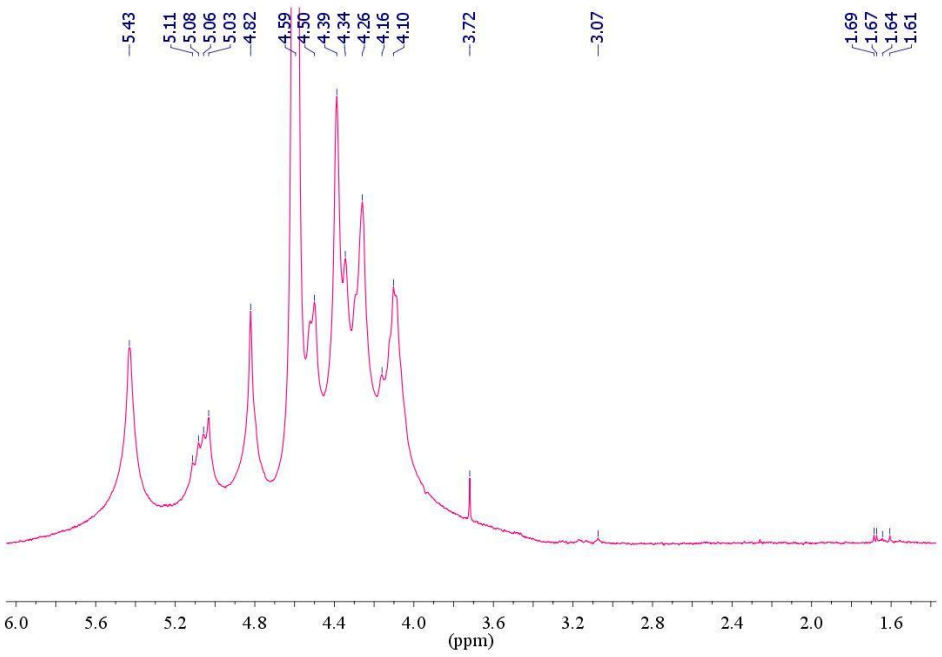


**Fig.2.2** $^1$H-NMR spectrum of alginate recorded at 80° C in $D_2O$

Signals recorded for alginate in the anomeric region (see figure 2.2) are located at 5.43 and at 5.06 ppm. The protons are assigned to the total guluronic (G) and mannuronic

(M) residues respectively. From the integrated area, a ratio G/M content of 70/30 is obtained.[155]

## 2.2.2 Chitosan

### 2.2.2.1 Viscometry

Reduced capillary viscosity was measured using a Schott-Geräte AVS/G automatic apparatus mounting an Ubbelohde type (Schott) viscometer. Temperature was maintained at 25 ± 0.1 $^{O}$C using a thermostated water bath. Measurements were performed on chitosan solutions in 0.1 M NaCl at pH 4 (see figure 2.3). The intrinsic viscosity [η] value was determined by extrapolating the reduced specific viscosity ($\eta_{sp}/c$) values to zero concentration by the use of the Huggins equation (5).

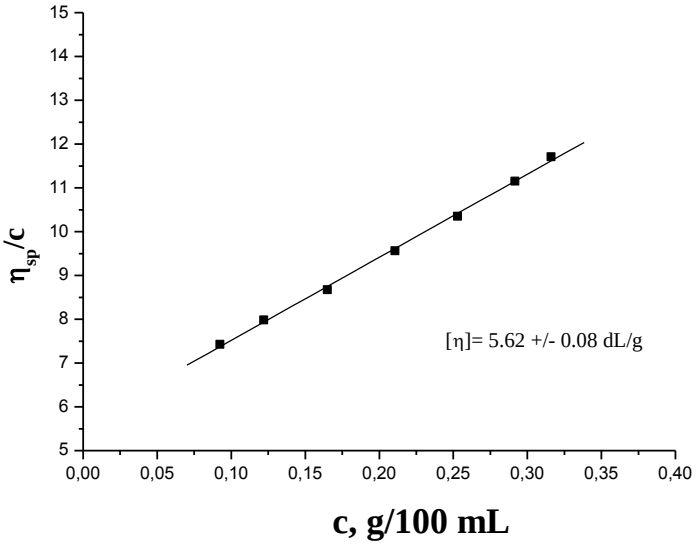


**Fig 2.3** Extrapolation of [η] in chitosan NaCl 0.1M solution.

The <Mw> of chitosan calculated from viscosity measurements according to MHS equation (3)[156,157] is 2,61x10$^5$ g/mol in fair agreement with the value declared by the producer (2,6x10$^5$).

## 2.2.2.2 Determination of acetylation degree

$^{1}$H-NMR measurements were carried out at 80°C on a Varian spectrometer (11.74 T) operating at 500 MHz for $^{1}$H equipped with a model L650 Highland Technology pulsed field gradient (PFA) amplifier (10 A) and a standard 5 mm indirect detection PFG probe. Spectra were recorded in $D_2O/CD_3COOD$ at pD =4. The polymer was exchanged three times in the proper deuterated solvent before running the measurements.

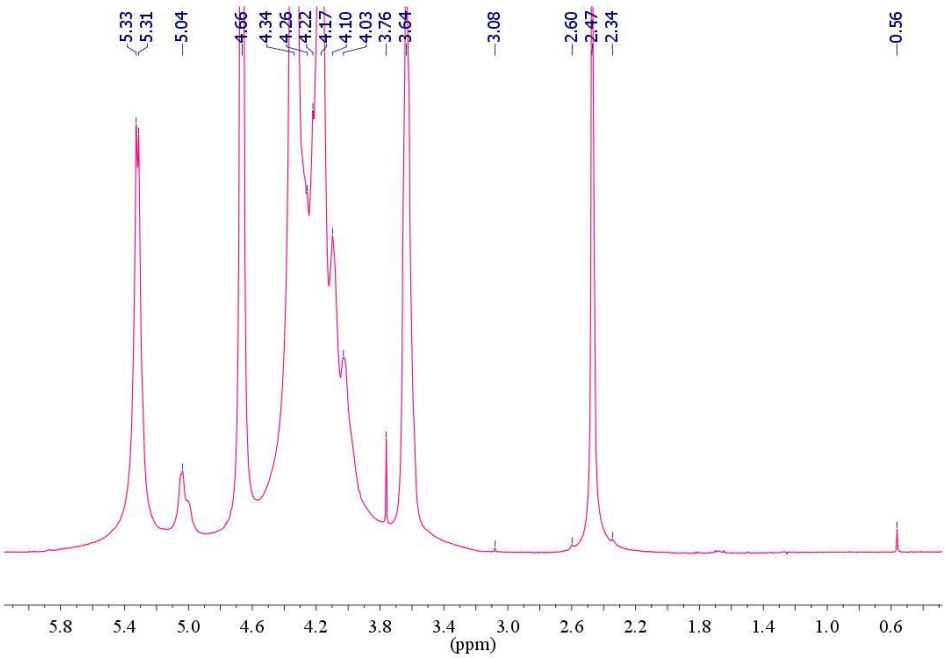


**Fig.2.4** $^{1}$H-NMR spectrum of chitosan recorded at 80° C in $D_2O/CD_3COOD$ (pD ~4)

$^{1}$H-NMR spectrum of chitosan (see figure 2.4) shows signals located at 5.33 and 5.04 ppm which are assigned to the anomeric proton resonances of the glucosamine residue (Glc-$NH_2$) and to the undeacetylated residue (GlcNAc), respectively.[158] Acetylation degree estimated from the ratio between the areas of the assigned peaks is 20%, in agreement with the technical data sheet.

# 2.3 Nanoparticles formation

## 2.3.1 Alginate-chitosan nanoparticles: preparation in water

The first approach for the synthesis of nanoparticles made of alginate and chitosan covalently crosslinked consists in the use of water as solvent for the reaction between the two polymers. In the formulation, the final total concentration of polymers was fixed at 0,2 % weight/volume (w/v). At first 2,5 ml of aqueous solution of chitosan 0,2 % w/v was prepared and the pH was adjusted at 4,5 with 0,1 M HCl. In another becker, 2,5 ml of water solution of alginate at a concentration of 0,2 % w/v were prepared. To this solution 18 μl of a EDC solution in water at a concentration of $3,5*10^{-3}$ mol/ml and 5 μl of a NHS solution in water at the concentration of $2,03\ 10^{-3}$ mol/ml were added. The final number of moles of EDC ($6,3\ 10^{-5}$ mol) was calculated to be in little excess respect to the moles of chitosan repetitive units ($2,3\ 10^{-5}$ mol), and final moles of NHS are calculated to be approximately 1/5 of final EDC moles ($1,05\ 10^{-5}$). The alginate aqueous solution was then dropped slowly in the chitosan solution under stirring and cooling at 0 °C with a ice-bath. The reaction was stirred at 0 °C for 48 h. Finally the solution was filtered using Nitrocellulose filters with decreasing pore diameters (Millipore) (0,8 μm 0,4 μm and 0,2 μm) to remove insoluble material.

## 2.3.2 Alginate-chitosan nanoparticles: preparation in food grade W/O macroemulsion

The aim of this study is to explore the possibility to obtain alginate-chitosan nanoparticles in macroemulsion. Macroemulsion-based systems can be fabricated using relatively simple processing operations and commercially available ingredients. They are currently used as delivery systems in many commercial applications. In our case the W/O emulsion was selected as a suitable system able to limit the reaction between alginate and chitosan at the internal aqueous droplets of the emulsion thus

enabling the formation of smaller nanoparticles and reducing the aggregation of the formed particles. Being the nanoparticles conceived for application in food field, the emulsion was prepared using food grade components. Water and polymers have been used as hydrophilic phase, sunflower oil as lipophilic phase and commercial lecithin or phosphatidylcholine (PC) as emulsifiers for W/O emulsions.

### 2.3.2.1 Alginate-chitosan nanoparticles: preparation using lecithin as emulsifying agent for W/O macroemulsion

At first, 2,5 ml of sunflower oil was poured in a becker and heated at 70 $^{o}$C, 0,8 g of lecithin were then added slowly to reach a final concentration of 2% on the total volume of emulsion. Mixing was maintained at 70 $^{o}$C until the complete dissolution of lecithin. In the meantime a water solution (0,75 ml) of chitosan at a concentration of 0.2 % (w/v) was prepared and pH was adjusted to 4.5 with HCl. After cooling, the water solution of chitosan was introduced under stirring in the oil phase at room temperature. An aqueous solution of alginate (0,2% w/v, 0,75 ml) containing 100 μL of crosslinker zero length EDC (3,5 $10^{-3}$ mol/ml) and 20 μL of NHS (2,03 $10^{-3}$ mol/ml). was added and the total aqueous phase volume was adjusted with water to a final volume fraction of 37,5% on the total emulsion volume. The final concentration of EDC is in great excess (10 times greater) respect to the moles of chitosan present in the mixture. The shear rate was increased and maintained for 24 h until a stable milky emulsion has formed. The emulsion was then diluted by adding a 5 time volume of water respect to the total emulsion volume. The addition of internal phase in excess causes a phase inversion and facilitates the following steps of filtration according to the demulsification process of surfactant-stabilized emulsions.

Porous membrane (Nitrocellulose and Durapor Millipore) filters with decreasing sizes of pores from 0,8 nm to 0,22 nm, have been used to separate the emulsion, filtering one time for type and pore size of the filters. Sample was finally dialyzed with membranes with a small cut off (3 kDa) against a solution of water. Totally 5 washing cycles of dialyses were made.

### 2.3.2.2 Alginate-chitosan nanoparticles: preparation using phosphatidylcholine (PC) as emulsifying agent for W/O macroemulsion

The reaction in emulsion using food lecithin as a emulsifying agent revealed some problems of analysis of the polymeric products. Being known that lecithin is a mixture of different components and analyzing its FT-IT spectrum we identified in PC the major component of our lecithin. So we decided to use pure PC as emulsifying agent instead of lecithin to avoid the presence of impurities in the final system. In particular being known from the lecithin technical data sheet the presence of 3g/100g of organic P we calculated that we need a percentage of 1,4% (w/v) of PC in the final emulsion volume to have the same emulsifying effect of lecithin considering a total volume of 4 ml of emulsion and a proportion of 6,25:3,75 oil:water.

The emulsion was prepared using 2,5 ml of sunflower oil as continuous oil phase. The oil was heated at 70 $^{o}$C and 0,056 g of PC was added to reach the the proportion calculated above. After cooling of the oil phase and emulsifying agent, the internal water phase (1,25 ml) made of chitosan at 0,2% w/v was dropped in the continuous phase, under rapid stirring. Then a water solution of alginate (1,25 ml) with a final concentration of 0,2% w/v containing 100 μl EDC 3,5 $10^{-3}$ mol/ml and 20 μl 2,03 $10^{-3}$ mol/ml was dropped in the emulsion. The emulsion was left to react for 24 h cooled in ice and under stirring. In this condition the emulsion seems to be instable as droplets of water were formed in the bottom of the becker. Nevertheless the preparation followed the same protocol described in the case of lecithin. The emulsion was diluted 5 times with water and then filtered using durapor and nitrocellulose type filters with decreasing pore sizes.

## 2.3.3 Alginate-chitosan nanoparticles: preparation using not food grade W/O nanoemulsion

The dimensions of the water droplet in the emulsion can have a pronounced influence on the functional properties and stability of the emulsion and on the final sizes and stability of the nanoparticles. Nanoemulsions can be produced with droplets of dimensions such as small that they do not scatter light appearing fully transparent. The advantage in using not food grade components in the preparation of the nanoemulsion is that they are pure and therefore they ensure an elevate control on the final composition of the emulsion. The drawback is the necessity to remove completely the toxic solvents from the nanoparticles.

### 2.3.3.1 Alginate-chitosan nanoparticles: preparation using Triton X-100 as emulsifying agent for W/O nanoemulsion

The protocol for the formation of the nanoemulsion consists of two steps: the first is the preparation of two separated emulsions, one containing chitosan and the other containing alginate and EDC/NHS. The second step involves the mixing of the two emulsions in a single emulsified phase.

At first, 6,4 ml of cyclohexane were poured in a becker and 3,2 ml of hexanol were added slowly under stirring. Then 2,4 ml of water and chitosan at a concentration of 0,2% (w/v) were added dropwise to the oil phase and the stirring rate increased. Cyclohexane/hexanol/water were used in fixed ratios of 11:6:4 respectively in all the two emulsions prepared.

The final step includes the addition of Triton X-100 drop by drop until to reach a transparent emulsion (2-2,5 ml for the volume considered here). The turning of the emulsion from milky to transparent is clearly visible. At this point the first emulsion is ready.

For the preparation of the emulsion containing alginate the procedure is similar. A volume of 6,4 ml of cyclohexane was poured in a becker, 3,2 ml of hexanol were added

under stirring and 2,4 ml of water containing 0,2 % (w/v) alginate and 26 μl of EDC at the concentration of 3,5 $10^{-3}$ mol/ml and 10 μl of NHS at the concentration of 2,03 $10^{-3}$ were dropped slowly. After that, Triton X-100 was dropped in the emulsion until the transparence was reached.

The emulsions containing alginate and chitosan were finally mixed in a single emulsion phase and left at ambient temperature for 48 h under stirring, thus allowing enough time for the mixing of the water droplets and for the coupling reaction to occur.

After this time, a volume of acetone equal to that of the reaction mixture was added to precipitate the polymers. The sample was centrifuged at 3000 rpm for 10 minutes and the pellet recovered, suspended in water and precipitated with 5 ml of acetone for 4 times. After the last precipitation step with acetone, the pellet was air-dried under a $N_2$ flow. The dried pellet was resuspended in 15 ml of water and sonicated for 15 minutes. The aqueous polymer suspension was then poured in a becker containing Amberlite XA2, preventively washed with methanol and water as reported in the technical data sheet. The resin has the capacity to remove traces of organic compounds and surfactants from the aqueous environment. In particular a dried weight of 1g of Amberlite AD2 is able to retain 0,37 g of Triton X-100. After 4 hours of slow stirring the resin was filtered off and the amount of Triton X-100 in the sample was analyzed by UV-Vis measuring the absorbance at 224 nm and calculating the concentration of surfactant using a calibration curve obtained by known concentrations of Triton X-100. The washing steps were repeated until full removal of the surfactant (usually 2-3 washing cycles). At the end of the washing steps, the sample is ready to be characterized. To obtain a more concentrated water solution of nanoparticles and to avoid the presence of nanoparticle aggregates the sample was freeze-dried and the alg-chito pellet was hydrated in a lower volume of water and centrifuged at intermediate speed (10000 rpm) for 10 minutes after the Amberlite treatment. Specifically using 10 ml of water to suspend the pellet we obtained a solution of 390 μg/ml of polymers.

### 2.3.3.2 Alginate-chitosan nanoparticles: preparation without crosslinkers using Triton X-100 as emulsifying agent for W/O nanoemulsion

The system in emulsion formulated with Triton X-100 as emulsifying agent, cyclohexane as continuous phase and hexanol as cosurfactant was prepared with the procedure described above but in absence of the crossilinker agents (EDC, NHS). At first 6,4 ml of cyclohexane were poured in a becker, then 3,2 ml of cosurfactant hexanol were added and 2,4 ml of water containing chitosan at the concentration of 0,2% (w/v) were added to the organic solution under vigorous stirring. The ratio between water/oil/cosurfactant was maintained at a constant value of 4/11/6. A solution of Triton X-100 was finally dropped until to reach a transparent emulsion (usually 2-2,5 ml are needed). Another emulsion was prepared with the same modality and ratio between components, but using a water solution of alginate 0,2 % (w/v) instead of chitosan. The alginate emulsion was then dropped into the chitosan emulsion. The final emulsion was kept under stirring for 48 h at room temperature. The polymers matrix was then precipitated using a volume of acetone equal to that of the emulsion prepared. After a centrifugation of 10 minute at 3000 rpm the pellet was recovered, resuspended in water and reprecipited four times with 5 ml of acetone. At the end the pellet was dried using a nitrogen flow, 15 ml of water were added and the suspension was sonicated for 15 minute. After sonication the suspension was washed using Amberlite AD2 preventively washed with methanol and water. The number of washing steps depends on the amounts of Triton X-100 present in suspension. Finally, to eliminate aggregates of nanoparticles the hydrated sample was centrifuged at an intermediate speed (10000 rpm) for 10 minutes.

### 2.3.3.3 Alginate-chitosan nanoparticles: preparation using Tween80-Span80 as emulsifying agents for W/O nanoemulsion

Crosslinked alginate chitosan nanoparticles were prepared also in a different W/O nanoemulsion. The continuous phase is cyclohexane also in this case, but we used a mix of emulsifying agents that better stabilize the emulsion respect to a single one. In particular a mixture of Tween 80 and Span 80 in ratio 6,5:3,5 was used as emulsifying agents for the formulation of the nanoemulsion. The following procedure was optimized. At first Tween 80 and Span 80 were mixed in proportion of 6,5:3,5 under agitation. A volume of 8 ml of cyclohexane was poured in a becker and then 1 ml of the mixture of emulsifying agents was added drop by drop to the cyclohexane under stirring. In this case to have a stable emulsion we have reduced the total aqueous volume phase at 640 μl thus to have a final ratio of cyclohexane/water of 8:0.64. Consequently, we have increased the final concentration of polymer in the water phase to 0,5 % w/v. 320 μl of water were dropped very slowly in the cyclohexane/surfactant mixture followed by 320 μl of water solution of alginate (1%, w/v) containing 26 μl of EDC 3,5 $10^{-3}$ mol/ml and 10 μl of NHS 2,03 $10^{-3}$ . A similar emulsion was prepared using chitosan (8 ml of cyclohexane, 1 ml of the mix Tween 80:Span 80 ratio 6,5:3,5, 320 μl of water and 320 μl of chitosan 1% (w/v) in aqueous solution). Then the emulsion containing alginate was dropped into the emulsion formulated with chitosan under stirring. The final nanoemulsion prepared was left under stirring for 48 h at room temperature. After this time, an identical volume (respect to the total volume of emulsion) of acetone was added to precipitate the polymers. The suspension was centrifuged at 3000 rpm for 10 minutes and the pellet was recovered. Then the precipitated polymers were resuspended in water and the precipitation-centrifugation cycle was repeated for further four times. After the last acetone washing the pellet was dried under a $N_2$ flow. Water was finally added to resuspend the pellet and the solution was sonicated for 15 minutes. The sample was then washed several times with Amberlite AD2 resin to ensure the complete removal of residues of cyclohexane, acetone and surfactants as described above. The progress

of surfactants removal was monitored at the UV-Vis. Spectra were registered in the range of 200-500 and the decreasing in absorbance at 230 nm was followed after each washing cycle. Finally, to eliminate aggregates of nanoparticles the hydrated sample was centrifuged at an intermediate speed (10000 rpm) for 10 minutes.

### 2.3.3.4 Alginate-chitosan nanoparticles: preparation without crosslinkers using Tween80-Span80 as emulsifying agents for W/O nanoemulsion

To compare results obtained from emulsion in which the crosslinkers EDC and NHS are present, a similar emulsion in absence of crosslinkers was formulated. The procedure adopted for the formulation of the emulsion includes the same steps described above, but alginate is not preventively activated with EDC and NHS. Briefly, 1 ml of Tween80-Span80 mixed in proportion 6,5:3,5 is added to a solution of 8 ml of cyclohexane, then 320 μl of water were added under stirring to the organic solution followed by 320 μl of alginate 1% (w/v). A second emulsion of chitosan was prepared following the same procedure. At the end the alginate emulsion was dropped in the chitosan emulsion, and the resulting final emulsion was kept under vigorous stirring for 48 h. Then, acetone in ratio 1:1 respect the final volume of emulsion was added to precipitate the polymer matrix. The mixture was centrifuged at 3000 rpm for 10 min. The pellet was suspended in water and the precipitation-centrifugation cycle was repeated for further four times. After the last acetone washing the pellet was dried under a $N_2$ flow. Water was finally added to resuspend the pellet and the solution was sonicated for 15 minutes. To remove organic contaminants the suspension was washed using Amberlite AD2 resin for many times checking the elimination of tween80-span80 at the UV-Vis at the wavelength of 230 nm, as described above.

Finally, to eliminate aggregates of nanoparticles the hydrated sample was centrifuged at intermediate speed (10000 rpm) for 10 minutes.

# 2.4 Nanoparticles characterization

## 2.4.1 Determination of particle size

The sizes of the nanoparticles were evaluated using the Nanoparticle Tracking Analysis (NTA) Halo$^{TM}$ LM10 of NanoSight Ltd Lysaner Way, UK, recently acquired by Malvern instruments. The instrument has a laser device that contains a solid state single-mode laser diode (635 nm). The technique provides that small particles in a liquid sample which pass through the beam pat are directly visualized from the operator as small points of light moving under Brownian motion.

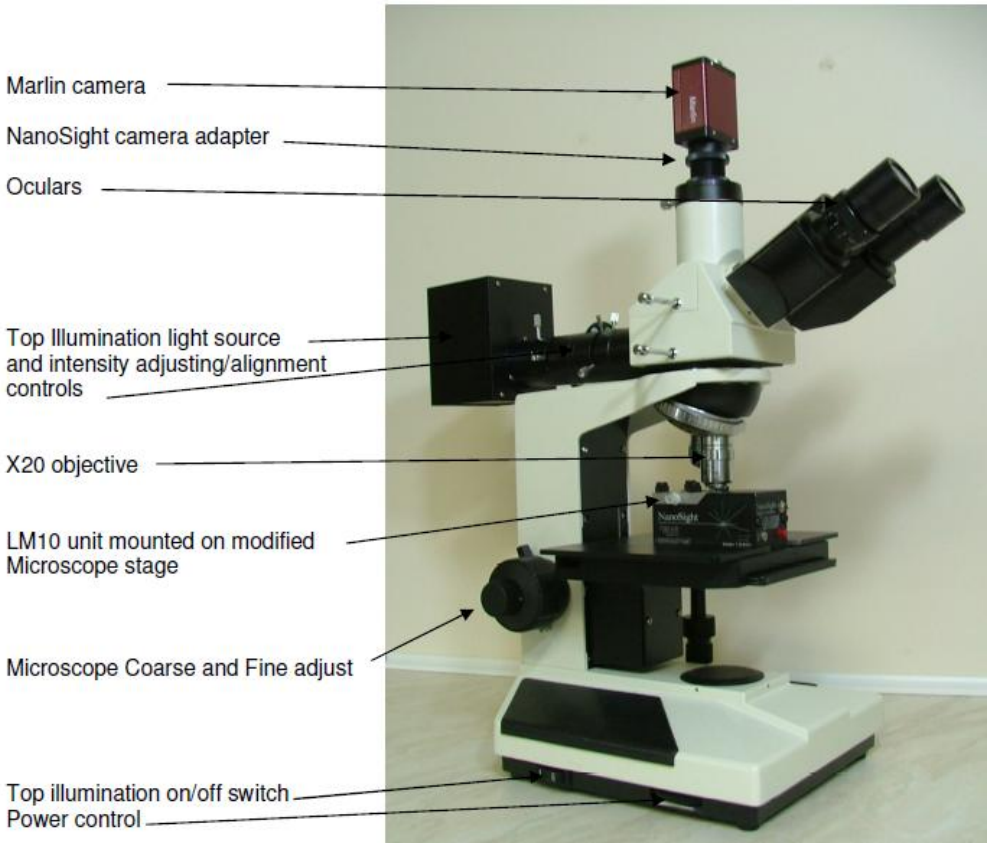


**Fig.2.5** Image of the NTA LM10 instrument.

Diffused light scattered by the particles could be processed according to the Mie theory analyzing the light scattering intensities for the determination of particles sizes.

A similar theorization involves considerable information about optical properties of sample, solvent and so on. A valid option is to analyze trajectories of nanoparticles moving under Brownian motion for an appropriate period of time exploiting the capacity of NTA to visualize the sample in real time. In fact the NTA software has the capacity to recognize and track individual nanoparticles and to relate the Brownian movements with the particle size according to the Stokes-Einstein equation:

$$\mathrm{Dt} = \frac{\mathrm{K_B T}}{6\,\pi\eta \mathrm{r_h}} \qquad (6)$$

Where $K_B$ is Boltzmann's constant, T is temperature, $\eta$ is solvent viscosity, Dt is the diffusion coefficient, $r_h$ the hydrodynamic radius.

The results obtained from NTA have been also compared to data obtained from DLS, a widespread technique used for determination of nanoparticle sizes. The instrument used was a Malvern Zetasizer nano ZS (Malvern Instruments, Worcestershire U.K). DLS analysis is based on dynamic laser light scattering. A monochromatic light generated by a laser hit the sample causing the scattering of light in all directions. The scattered light is collected and the resulting optical signals shows random changes due to the random movements of nanoparticles in and out of the laser beam, thus the scattered light fluctuates, and the frequency of this fluctuation is correlated to the size of the nanoparticles. Signals are then interpreted in term of autocorrelation function (data are processed with a correlator that enables to obtain the autocorrelation function as a function of delay time). Although DLS is a very useful and accessible device, it presents several drawbacks strictly correlated to the methodology used. Indeed, deriving the determination of particle sizes from fluctuation in scattered light and being the scattered light proportional to the sixth power of the particle diameter, the presence of large particles strongly influences the measurement. This event can affect the accuracy of size determination.[159] Nanoparticles analyzed from NTA are tracked and visualized separately for the generation of the particle size distribution. This represents an important advantage respect to the distribution profile analyzed from DLS. In fact, DLS analyzes particles simultaneously and this can generate an error

in the measurement if a small number of highly scattering large nanoparticles is present.

### 2.4.5 Determination of particle stability

Nanoparticles solutions in water have been stored at ambient temperature and the NTA measurement of stability were conducted every week for a total of 14 day to check any variations in size due to destabilization or aggregation processes as a consequence of aging. Stability of nanoparticles solutions was also verified subjecting the sample to centrifugation at a low speed of rotation (3000 rpm) and at a intermediate speed of rotation (10000 rpm) for 10 minutes. Centrifugal force accelerates sedimentation of aggregates. All the samples were then analyzed using NTA.

### 2.4.2 Spectroscopic analysis (FT-IR)

FT-IR spectra were recorded using a Thermo Scientific IS50 Nicolet FT-IR 550 Avatar 320 on the range of 4000-600 $cm^{-1}$. The samples were prepared mixing the lyophilized powder with finely powdered potassium bromide (KBr). The pellet is then pressed and air dried, finally it is located in the holding for the analysis. Spectra of raw materials and powder of samples have been acquired.

### 2.4.3 Determination of particle morphology: transmission electron microscopy (TEM) and scanning electron microscopy (SEM)

Alginate chitosan nanoparticles were examined by transmission electron microscopy (TEM). All the measurements were carried out using an EM 208-Philips TEM (Eindhoven, Netherland) equipped with a Quemesa camera (Olympus Soft Imaging Solution, Munster, Germany). The analysis were performed at Electronic Microscopy Center (Department of Life Science of University of Trieste). The samples for the analysis were prepared following a negative staining: 10 μl of sample were deposited on a carbon coated copper grid, then 10 μl of uranyl acetate (1% in water) were added as contrasting agent. After 10 minutes, the time needed for deposition of the uranyl acetate, the excess uranyl acetate was absorbed with filter paper and the sample was kept 20 minutes to dry completely.

Further information about nanoparticles morphology has been acquired from SEM after an air drying process of the sample. The dry powder was examined by scanning electron microscopy (SEM) Leica Stereocan 430i (Leica Cambridge Ltd, Cambridge, UK). The sample is mounted on a stub of metal coated with gold and observed with the microscope. The analysis were performed at Electronic Microscopy Center (Department of Life Science of University of Trieste). The sample was metalized using S150A Sputter Coater metallizer.

### 2.4.4 Spectroscopic analysis (UV-Vis)

UV-Vis spectra were acquired with a Perkin Elmer Lambda 35 UV-Vis. Spectroscopic analysis was carried out in solutions inserted in quartz cuvettes with 1 cm of optical path.

## 2.4.5 In vitro toxicity test: MTT assay

The viability of Caco-2 cells (human epithelial colorectal adenoma carcinoma cells, employed as model of intestinal epithelium) in the presence of alginate chitosan nanoparticles was evaluated using a standard test. Specifically, MTT assay was used as test for the measurement of cell viability and proliferation. The technique is based on the evaluation of mitochondrial reductase enzyme activity after incubation of nanoparticles with cells. Tetrazolium salt (MTT) a water soluble yellowish probe, in fact is reduced to insoluble MTT –formazan (see figure 2.6) of dark purple color, during normal metabolic activity .

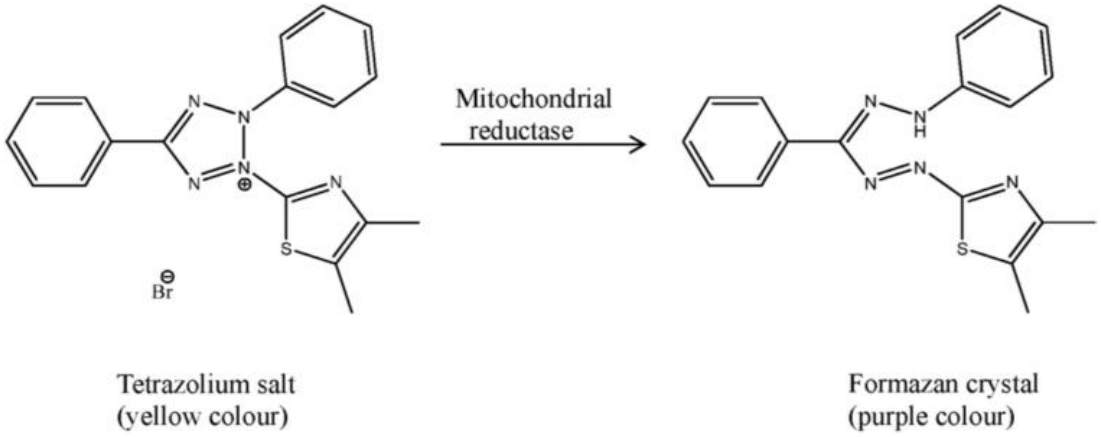


**Fig.2.6** Reduction of MTT to MTT formazan by the mitochondrial reductase.

The resulting MTT formazan can be dissolved and quantified spectrophotometrically at the wavelength of 540 nm. In case of apoptosis or necrosis or in general in case of mortality processes due to a toxic action of external compounds (alginate-chitosan npts resulting from Triton X-100 nanoemulsion and alginate-chitosan npts deriving from Tween80-Span80 nanoemulsion in this case) the mitochondrial activity is reduced. This leads to a reduction of MTT- formazan formation and consequently a reduction of UV-Vis absorbance.

Cells were plated in a sterile 96-well tissue culture plate (20000 cells/well), in 100 μl of complete Eagle's MEM (Minimum Essential Medium). Water suspension of nanoparticles were filtered using 0,2 μm sterile filters to ensure the sterility of the

sample before the contact with cells. The wells with 10 μl of diverse concentrations of nanoparticles were incubated in triplicate for 24 h. In particular the concentrations tested were 0,75 μg/ml, 3,75 μg/ml, 7,5 μg/ml for nanoparticles formulated using Triton X-100 as emulsifying agent and 2 μg/ml, 10 μg /ml, 20 μg/ml for alginate-chitosan nanoparticles obtained from emulsion with Tween80-Span80. In parallel in the same plate a positive reference of 10 μl of water was incubated with cells too. After 24 h, MTT was dissolved in water at a concentration of 5 mg/ml and 10 μl were incubated for 4 hours with cells (added of nanoparticles). After 4 h when a purple precipitate is visible, medium is removed and 50 ml of DMSO were added in every well. The 96 well plate is inserted in a microplates readers and absorbance at 540 nm read and recorded.

## 2.4.6 Loading of nutraceuticals in the nanoparticles

### 2.4.6.1 Loading of resveratrol

The loading ability of the nanoparticles was determined on samples prepared by resuspension of the nanoparticles in water. The established protocol is described below. At first a stock solution of resveratrol (10 mg/ml in ethanol) was prepared. Then the solubility limit of resveratrol in water was determined. At this purpose, 50 μl of stock solution (excess resveratrol) were added to 1 ml of water. The sample was stored for 24 h at ambient temperature, time necessary for the precipitation of insoluble components. Then the sample was centrifuged at 3000 rpm for 10 minutes to complete the precipitation process. Supernatant was collected and resveratrol quantified spectrophotometrically, adding 40 μl of the supernatant to 3 ml of water, and recording the UV-Vis spectrum in the interval of 200-500 nm. Absorbance at 307 nm (maximum absorbance value of resveratrol) was read and the concentration of resveratrol calculated using a calibration curve determined in ethanol. To verify the validity of the method, samples were centrifuged at higher rotation speed (20000 rpm for 10 minutes). The output value was the same of that obtained at lower speed

rotation and, therefore, the lower speed rotation was selected to avoid precipitation of nanoparticles. In this condition the maximum solubility of resveratrol in water is 1,3 μg/ml. For the determination of the amount of loaded resveratrol in alginate-chitosan nanoparticles obtained from emulsion in presence of Triton X-100 as emulsifying agent, 50 μl of resveratrol stock solution were added to different concentrations (52, 36, 26, 16, 5 μg/ml) of nanoparticles suspended in a final volume of 1 ml of water.

The same procedure was used in the case of alginate-chitosan nanoparticles obtained from emulsion in presence of Tween80-Span80 as emulsifying agents but using the following concentrations of nanoparticles: 73, 51, 36, 22, 7 μg/ml.

The samples were left to stabilize for a night enabling the excess of resveratrol to precipitate on the bottom of the vial. Samples were then centrifuged at 3000 rpm or 10000 rpm for 10 min as described above. 40 μl of supernatant were taken and added to 3 ml of water. Finally the UV-Vis spectrum was recorded and the absorbance was read at 307 nm to calculate the amount of resveratrol present in the samples (values were subtracted of the resveratrol absorbance in water solution).

### 2.4.6.2 Loading of quercetin

The loading ability of the nanoparticles was determined on samples prepared by resuspension of the nanoparticles in water. The procedure adopted to encapsulate and measure the amount of encapsulated quercetin is slightly different. The established protocol is described below. At first a stock solution of quercetin (10 mg/ml in DMSO) was prepared. Then the solubility limit of quercetin in water was determined (5μg/ml). At this purpose, 65 μl of stock solution (excess quercetin) were added to 1,3 ml of water. The sample was stored for 24 h at ambient temperature, time necessary for the precipitation of insoluble components. Then the sample was centrifuged at 3000 rpm for 10 minutes to complete the precipitation process. Supernatant was collected and quercetin quantified spectrophotometrically, without further dilution, recording the UV-Vis spectrum in the interval of 200-500 nm. Absorbance at 372 nm (maximum

absorbance value of quercetin) was read and the concentration of quercetin calculated using a calibration curve determined in ethanol. The resulting absorbance was then compared with the absorbance of the same sample centrifuged at higher rotational speed (20000 rpm for ten minutes) to exclude any possible interference of small crystals still present in solution. In this conditions the solubility of quercetin in water is 5 μg/ml. After having verified the total accordance between the results obtained we proceeded with the analysis on the samples containing the nanoparticles. Five aqueous dilutions of nanoparticles in a final volume of 1,3 ml were added of 65 μg of the quercetin stock solution. Specifically for alginate-chitosan nanoparticles deriving from emulsion in which Triton X-100 was used as emulsifying agent the concentrations of nanoparticles used are 68, 52, 36, 21, 5 μg/ml, instead for alginate-chitosan nanoparticles deriving from emulsion in which tween80-span80 were used as emulsifying agent the concentrations used are 95, 73, 51, 29, 7,3 μg/ml. The samples were left to stabilize for a night enabling the excess of quercetin to precipitate on the bottom of the vial. Samples were then centrifuged at 3000 rpm or 10000 rpm for 10 min as described above and the supernatant was analyzed. The UV-Vis spectrum was recorded in the interval 0f 200-500 nm and the absorbance was read at 372 nm to calculate the amount of resveratrol present in the samples and values were subtracted of the resveratrol absorbance in water solution.

### 2.4.7 Radical scavenger activity: DPPH assay

Then antioxidant activity of nanoparticles loaded with resveratrol was evaluated by the diphenylpicryl-hydrazyl (DPPH) assay. This methodology is commonly used for the estimation of the antioxidant properties of several substances. DPPH is in fact a stable free radical, thanks to the delocalization of the unpaired electron (see figure 2.7) on the all structure. This peculiar electronic configuration confers to DPPH dissolved in ethanol a deep violet color with an absorption maximum at 522 nm. When DPPH is reduced it loses the violet coloration.

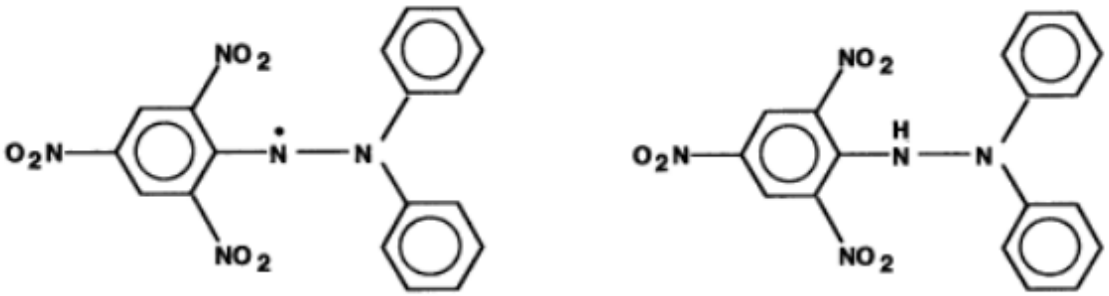


**Fig.2.7** Left: structure of DPPH. Right: structure of reduced form of DPPH.

The method is a useful way to determine if alg-chito resveratrol-loaded npts have the ability to reduce DPPH and thus a potential scavenging activity. If resveratrol acts as a scavenger, DPPH loses its color and the absorbance at 522 nm decreases. A stock solution (1 mg/ml) of DPPH in ethanol was prepared and 24 μl of the stock solution were added to different volumes of loaded resveratrol npts suspension (30 μl, 40 μl, 50 μl) diluted in a final volume of 1 ml of water:ethanol 1:1 thus realizing different concentration of resveratrol-npts. (1,6 2,1, 2,6 μg/ml of npts). The absorbance at the fixed wavelength of 522 nm was then measured every 5 minutes for 25 minutes until the discoloration process was complete.

## 2.4.8 Protection of quercetin from oxidation

A procedure usually adopted to protect quercetin from oxidation is the use of the water soluble ascorbic acid. The protocol provides the addition of quercetin (as described in paragraph relative to quercetin loading) to the highest concentrated sample of nanoparticles. Two different concentrations (3 and 7,4 μg/ml) of ascorbic acid were added to samples. Samples were then stored for 5 days checking the stability of the peak at 372 nm and compared to samples prepared in absence of ascorbic acid. Experiments were conducted in triplicate.

# Results & discussion

# 3

# Premise

This chapter is constructed following the evolution of the different protocols and experimental conditions which have been tested and optimized in order to obtain alginate-chitosan nanoparticles. Indeed, different procedures for the synthesis of stable nanoparticles, formed by covalently crosslinked alginate and chitosan have been examined, the most relevant of which will be presented and described in the next pages. Therefore, the architecture of the chapter follows the temporal succession of the modifications of the synthetic protocol aimed to reach the final goal.

Every formulation attempted and the relative results obtained, represented an important link to develop the subsequent system. So all the improvements and modifications derive from a critical evaluation of the previous systems. The chapter starts describing the first attempts of reaction between alginate and chitosan in water in presence of the crosslinking agents; results relative to this method will be briefly summarized. The instability of the system obtained in this conditions has prompted the investigation of new procedures. So the attention has moved towards the formulation of alginate-chitosan nanoparticles in emulsion exploiting two different food grade W/O macroemulsion as a microreactor to obtain nanoparticles. Results will be presented with a short description and discussion.

Finally the chapter focuses on a further optimization of the process represented by the optimization of two different types of stable W/O nanoemulsions. These systems present the best characteristics if compared to the previous ones. A depth description of the results obtained and of the experimental conditions optimized regarding the last two systems will be presented and discussed. The properties and characteristics of the obtained crosslinked alginate-chitosan nanoparticles will be examined and illustrated critically. This last part is in fact the fulcrum of the Thesis, but for a full comprehension is important to present all the steps that led us to the final process optimization.

## 3.1 Alginate-chitosan nanoparticles: preparation in water

The first attempt to couple alginate carboxyl units with chitosan amine functions was performed in aqueous environment. As explained in the Introduction, in fact, the electrostatic interaction occurring between carboxylates alginate and amines of chitosan is responsible of the process of polyelectrolyte complexation named complex coacervation. The interaction is strongly influenced by the pH, molecular weight and concentration of the polymers. If the interaction is strong, the possible effect is the formation of a macrogel. Controlling the parameters mentioned above it is possible to obtain micro or nano structures, but the formed network is usually weak and loses its integrity rapidly.[102] So we thought that the use of EDC/NHS as covalent crosslinker agents may reinforce the weak ionic network resulting in stable nanoparticles. At first, an aqueous solution of chitosan (0,2%w/v) was prepared. The pH of the water solution was preventively acidified at a value of 4.5- 5 with HCl 0,1 M. Then a water solution of alginate (0,2% w/v) previously added of EDC and NHS was added. EDC belongs to the family of carbodiimides which are commonly used as condensing agent in peptide synthesis. Carbodiimide is a generic term referring to unsaturated molecules having the following structure RN=C=NR'.

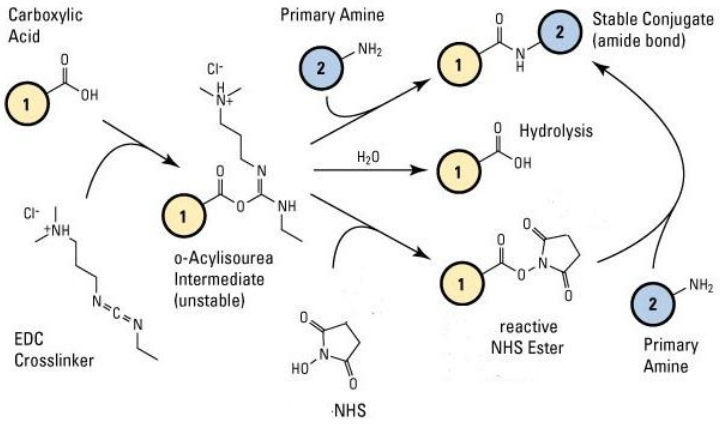


**Fig.3.1** Schematic reaction of EDC and NHS in presence of carboxylic acid and amine.

The reaction scheme (see figure 3.1) involves the attack of the nucleophilic carboxylate ion (carried by alginate) to the electrophilic carbon atom of the carbodiimide. The

resulting activated O-acylisourea adduct is then attacked by the primary amine (chitosan in our case) forming an amide derivative. EDC is the most frequently used carbodiimide for amide bond formation. It is a water soluble molecule very reactive especially in a pH range of about 3,5-4,5. One of the main problem during the reaction is the possible formation of the N-Acylurea adduct. In our procedure the pH was fixed at 5 and in these conditions the hydrolysis of the O-acylisourea is fast, leading to a lower yield of coupling. The addition of N-Hydroxysulfosuccinimide (NHS) reduces the deactivation improving coupling efficiency and reducing the possibility of rearrangement to N-acylurea derivative. In our preparation, EDC and NHS are firstly incubated with alginate (the molecule bearing the carboxyl groups) and then water solution containing the polymer and the crosslinking agents were finally added to chitosan. In the final mixture the amount in weight of the two polymers was the same. The reaction vessel was kept in ice under stirring for 48 h. After that time, the mixture presented some macro-gel aggregates probably due to the strong interaction between alginate and chitosan. Macro-gel were removed by filtering the suspension using nitrocellulose filters with a decreasing pore diameters from 0,8 μm to 0,4 μm and 0,2 μm.

### 3.1.1 Determination of particle size

The sizes of nanoparticles have been determined using Nanoparticles Tracking Analysis (NTA). The formulation suspended in water, obtained as described above, was loaded into the sample chamber using a syringe. The sample was fluxed slowly avoiding formation of bubbles. Once the sample was equilibrated in the chamber it is possible to proceed with the measurements of the nanoparticle size. The instrument is able to measure and calculate the mean diameter of a nanoparticle solution with a concentration between$10^6$- $10^9$ nanoparticles per ml. The size distribution profile (see figure 3.2) of the system shows an average diameter of the nanoparticles of 200 nm (standard deviation ($\sigma$)= ± 63 nm. The size distribution is, however broad and shows the tendency of the nanoparticles to form aggregates with size in the range of 500 nm.

In addition we have to consider that the larger particles have been removed during the filtering procedure.

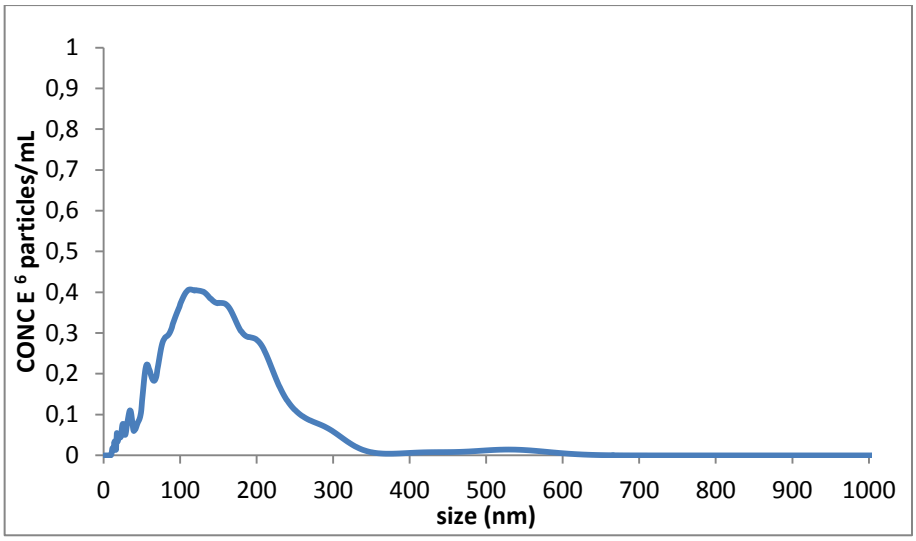


**Fig.3.2** Size distribution of nanoparticles resulting from NTA analysis.

### 3.1.2 Determination of particle morphology

The shape and morphology of the material obtained from the reaction in water was investigated by TEM. One drop of the filtered sample was deposited on a carbon coated copper grid, stained with uranyl acetate and, after evaporation of water, examined by TEM. The TEM image presented in figure 3.3 shows a not well defined aspect of the matrix and the presence of raw material. Probably the ionic interaction between alginate and chitosan is the predominant force of interaction in the system thus impeding the covalent reaction between polymers and the formation of stable and well defined nanoparticles. Alternatively, a too high degree of covalent crosslinking between the polymers generates a rigid linear structure. In addition the high vacuum required by TEM favors the aggregation within the matrix.

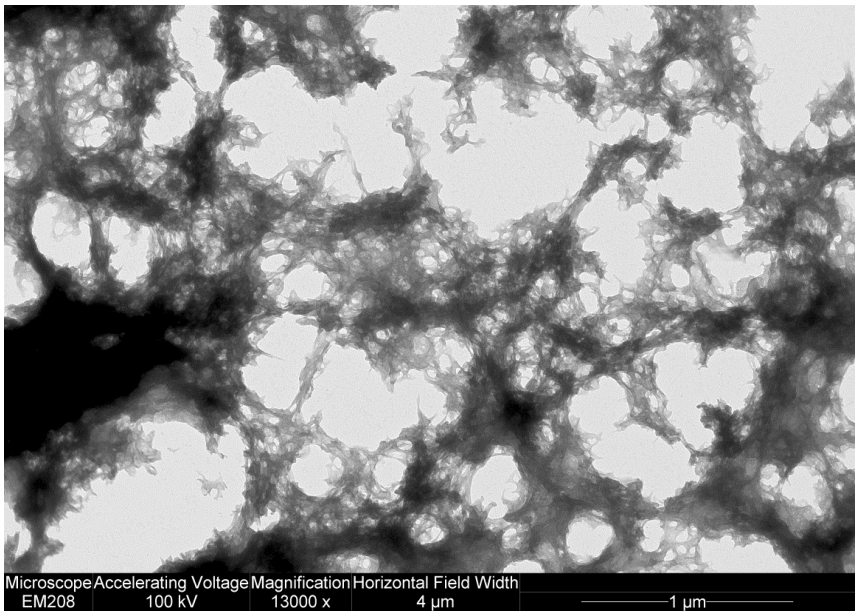


**Fig.3.3** TEM image of alginate-chitosan matrix deriving from reaction in water.

The sample was also investigated performing a SEM analysis on the filtered material. The image (see figure 3.4) confirms the data obtained by TEM showing the predominance of aggregated non-structured material.

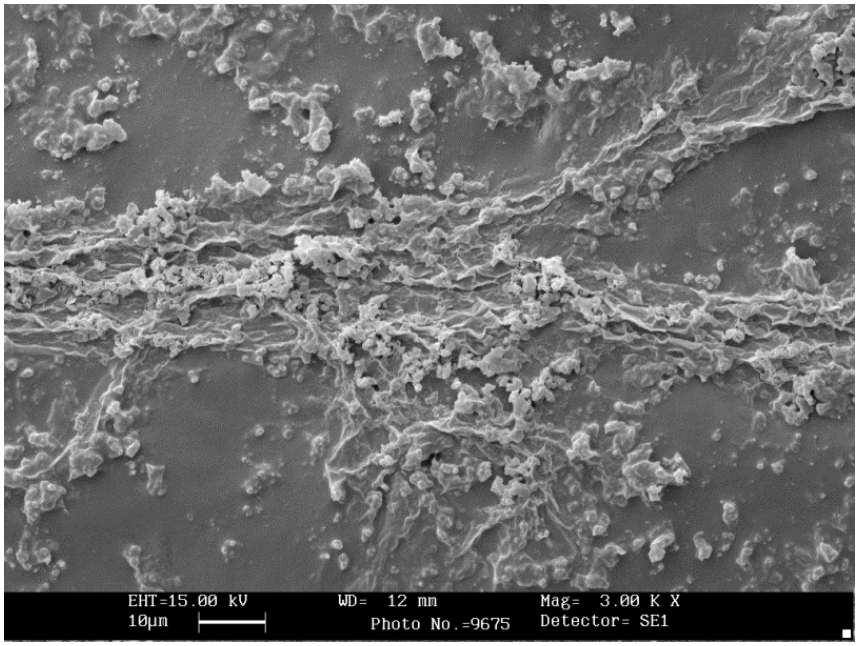


**Fig.3.4** SEM image of alginate-chitosan matrix deriving from reaction in water.

Overall the results obtained from NTA and electronic microscopy show that the reaction between alginate and chitosan in water leads to the formation of aggregated polymeric materials and not of nanoparticles.

## 3.2 Alginate-chitosan nanoparticles: preparation using lecithin as emulsifying agent for W/O macroemulsion

To prevent the aggregation phenomena observed in the samples obtained from the reaction in water, we decided to perform the reaction between alginate and chitosan in a different system. In particular we explored conditions in which the interaction between the polymers can be limited. Emulsions for instance represent an interesting strategy to confine a limited amount of reactants in a small and insulated environment. In our case, the reaction between the polymers occurs in an aqueous medium and, therefore, using W/O macroemulsion the reaction is confined in the water droplets of the emulsion which contain a limited amount of polymers although an equilibrium within droplets with exchange of material is present. Being the final use of the nanoparticles conceived for food application, the components of the emulsion were selected within food grade components. The first step is the selection of the emulsifying agent and of the continuous phase. Generally vegetable oils can represent a good choice for formation of both W/O and O/W emulsion systems. Among this class numerous articles have explored the use of sunflower oil, olive oil, castor oil, soybean oil and peanuts oil as continuous or internal phase.[160,161] In this work after a first attempt using castor oil, sunflower oil was selected as external phase of the emulsion. Regarding the emulsifying agent, relevant articles show the use of polyglycerol polyricinoleate (PGPR)[162] or lecithin[163] as active surface agents. Lecithin is usually applied in food industry as emulsifier and as agent to regulate viscosity and thus was selected as potential emulsifying agent. Lecithin is a combination of different phospholipids mixed to other components such as triglycerides and fatty acids and can be used to obtain both W/O and O/W emulsions depending on the ratio between external and internal phase. Although the HLB of commercial lecithin is not declared, it

is known[164] that this value depends on the composition of lecithin but usually has an intermediate value between that required for O/W and W/O. Different concentrations and ratios between oil and water and emulsifying agent have been tested, in according to the diagram phase, before to set the right conditions and ratio between internal and continuous phase. At the end a ratio of 6,25:3,75 oil: water and a 2% concentration of lecithin were set as the best condition. The procedure for the formation of emulsion is briefly described below.

The chitosan aqueous phase was prepared by dispersing 0,2% (w/v) polymer in water at pH 5-5,5 under stirring. The oil phase was prepared by mixing lecithin at the concentration of 2% (on the total volume of emulsion) with sunflower oil. Mixing was performed at 70 $^{o}$C until a complete dissolution of lecithin. After cooling, the water phase was introduced under shear in the oil phase at room temperature. Then, pH was adjusted to 5,5 with HCl.

A solution of alginate (0,2% (w/v)) in water preventively activated with EDC and NHS was then added to the emulsion to obtain a volume fraction of dispersed water phase of the 37,5 % respect to oil phase. In the final water phase the amount of the two polymers was the same expressed in weight.

The shear rate was increased and maintained for one day until a stable milky emulsion has formed. After this time which should allow the reaction between the two polymers and the formation of the nanoparticles, the emulsion must be broken to recover the nanoparticles. Several techniques are described in literature to destabilize and break emulsion as micro-wave radiation[165] or demulsification based on freeze and thaw method[166], but these procedures seemed do not work on our system.

After different attempts, the separation of phases was achieved combining two different procedures: phase inversion of emulsion and filtration. In fact the phase inversion can represent a strategy to destabilize the emulsion. Filtration seems to produce the same effect, in particular it seems that hydrophobic membranes produce demulsification of oil in water emulsion due to the coalescence of oil droplets in the membrane pores.[167] So we first inverted the emulsion from W/O to O/W by diluting with a five times volume of water and then the emulsion was filtered using hydrophobic and hydrophilic membranes of decreasing sizes pores. In particular, the

filtration was performed using filters with pore size of 0.8 μm, 0,4 μm and 0.22 μm, filtering one time for type of filter and for pore size.

### 3.2.1 Spectroscopic analysis (FT-IR)

Initially FT-IR spectra were performed directly on the matrix obtained by lyophilization of the solution after filtration. However, filtration was not able to completely remove lecithin and crosslinkers. in fact the FT-IR spectrum of the sample not purified shows a very complex pattern. An Attempt to purify the samples was did using pre packed column of Sephadex G 25 but this led to a further dilution of the polymer suspension and, moreover, aggregated matrix of alginate and chitosan had the tendency to obstruct the pores of the column. Finally we have selected dialyses as a possible approach for purification. Dialysis was performed in dialyses bag with a small cut off (3 kDa ) against a solution of water. After 5 washing cycles of dialyses, the sample was freeze-dried and analyzed.

The Infrared spectra were performed on lecithin powder, on the pure polymers and on the final alginate-chitosan matrix deriving from the reaction in emulsion. All the samples for analysis have been prepared in KBr tablets.

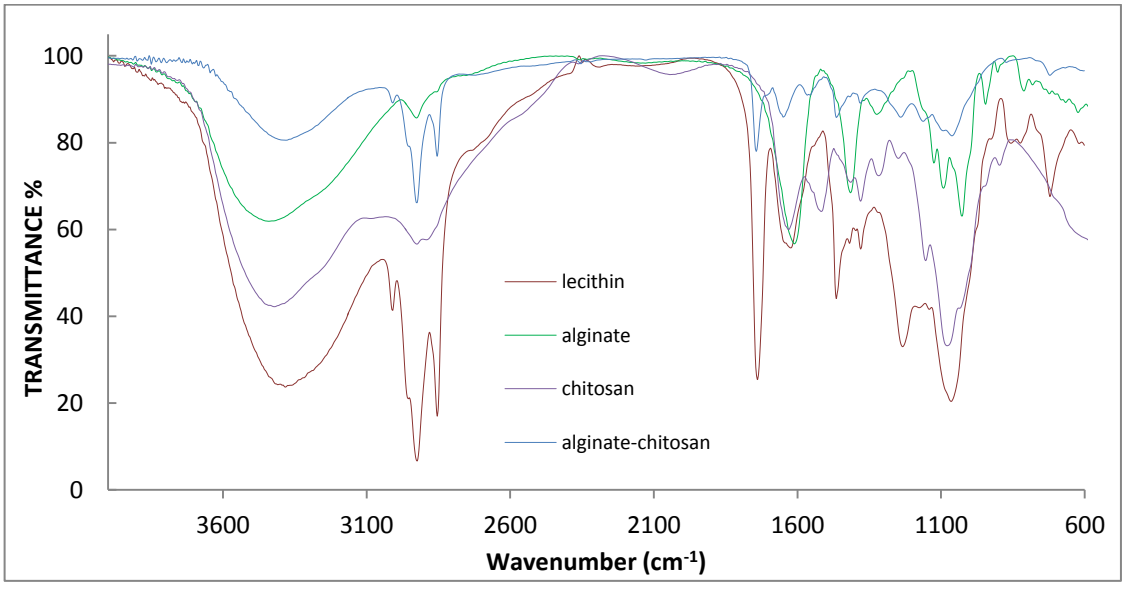


**Fig.3.5** FTIR spectra of pure polymers, lecithin and alginate-chitosan after reaction.

The FT-IR spectrum (see figure 3.5) of lecithin (purple track) shows the typical absorption bands of this surfactant. In particular the peak at 3282.61 $cm^{-1}$ is due to the stretching OH and the peaks at 3010, $cm^{-1}$, 2958 $cm^{-1}$ and 2924 $cm^{-1}$ are due to the asymmetric stretching of the =CH-, and to the asymmetric and symmetric stretching of the CH groups respectively. At 1739 $cm^{-1}$ there is the typical band of the stretching of the carbonyl groups of the fatty acids, the signals at 1624 $cm^{-1}$ and 1464 $cm^{-1}$ correspond to the CH scissoring, while the peak at 1380 $cm^{-1}$ is due to the $CH_3$ symmetric bending, finally the absorption bands at 1234-1065 $cm^{-1}$ are the typical asymmetric and symmetric stretching of the phosphate group.

The FT-IR spectrum of the alginate-chitosan matrix (blue track) deriving from the reaction in emulsion is essentially dominated by the resonances of the lecithin which is still present in the sample. The clear identification of the polymers and in particular of the eventual characteristics bands of the amide bond is not possible.

Indeed, the peak at 1649 $cm^{-1}$ could be identified as the amide bands (bands I) but the attribution is ambiguous because alginate and chitosan present also peaks close to this value (alginate at 1613 $cm^{-1}$ and chitosan at 1639 $cm^{-1}$ ). The band at 1554 $cm^{-1}$ instead can be interpreted as the amide band II and it is certainly a new band, but being lecithin still present is not possible to attribute the eventual covalent bond to alginate and chitosan interaction. In fact as underlined, lecithin includes different substances potentially bearing carboxyl and amine functions that can also react forming amides. An important observation is the absence of the characteristic and intense peaks of EDC in the range of 2700-2000 $cm^{-1}$, meaning that the purification steps were able to completely remove the crosslinking agent.

### 3.2.2 Determination of particle size

Nanoparticles prepared in emulsion and purified by dialysis were characterized in terms of size and size distribution with NTA. Figure 3.6 presents the results obtained.

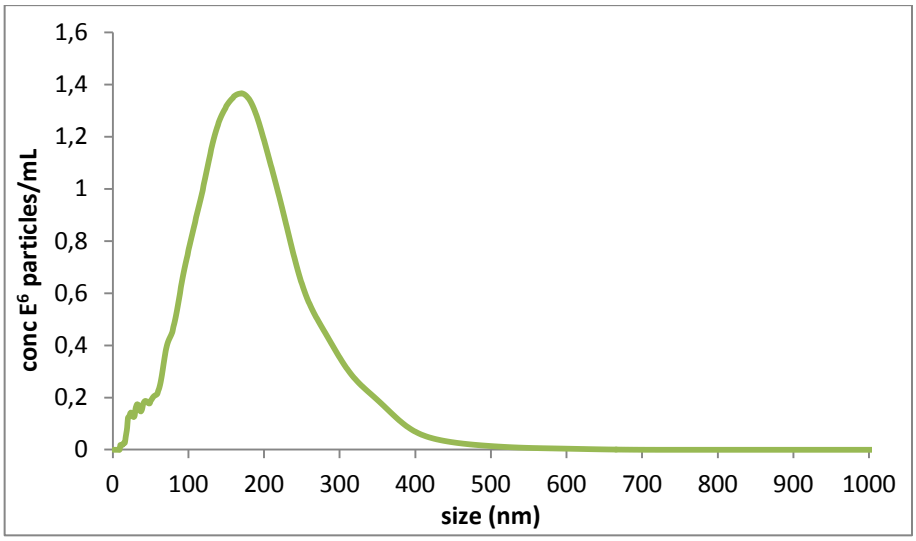


**Fig.3.6** Sizes distribution of alginate-chitosan nanoparticles from W/O macroemulsion resulting from NTA analysis.

The average size distribution of the nanoparticle is centered at 200 nm ($\sigma = \pm 46$) and the curve is simmetrically distributed around the average value.

### 3.2.3 Determination of particle morphology

Samples were analyzed in form and shape using transmission electron microscopy (TEM). The image (see figure 3.7) obtained reveals the presence of some nanoparticles. The major amount of material, however, does not present a well defined structural arrangement, but it is aggregated in non uniform way.

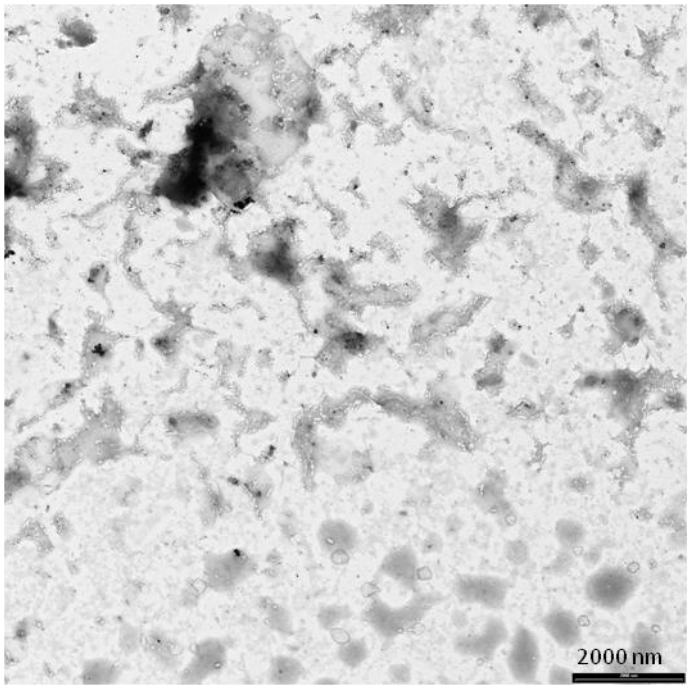


**Fig.3.7** TEM image of alginate-chitosan matrix deriving from W/O macroemulsion.

Overall, also with this system we were not able to obtain nanoparticle. In addition we have to consider that from FT-IR spectra is visible the presence of lecithin. Dialysis in fact is not able to remove completely lecithin and this can influence the final composition and also the type of interactions within the sample. Indeed, examples of chitosan-lecithin interactions are well described in literature. Sonvico et al. first [168] and other groups then [169] developed a method to produce chitosan-lecithin nanoparticles for encapsulation of drugs. The formation of nanoparticles is based on electrostatic interaction between the negatively charged lecithin and the positively charged chitosan. Considering this further element we cannot exclude that the particles observed with NTA and partly with TEM may derive from a chitosan/lecithin interaction.

The fact that lecithin is a mixture of different components represents also a problem for the reaction between alginate and chitosan. In fact, substances present in lecithin and bearing amine functions can act as competitor of chitosan in the coupling reaction. In general, too many variables complicates the comprehension of the processes involved in this type of emulsion. To better understand the system it is, therefore, necessary a selection of pure components in order to simplify the systems.

## 3.3 Alginate-chitosan nanoparticles: preparation using PC as emulsifying agent for W/O macroemulsion

The use of lecithin, despite the formation of a stable macroemulsion, revealed some critical issues deriving from a possible involvement in a ionic interaction with chitosan. As referred above, lecithin consists of a complex mix of components. In particular the 70 % is made of phospholipids[170] and among these, phosphatidylcholine (PC) is the greater component. A comparison of the FT-IR spectrum of lecithin with the PC and phosphatdylethanolamine (PE) ones, revealed that our lecithin is mostly composed from PC. To understand if the PC alone has the capacity to stabilize the emulsion, we prepared an emulsion in the same condition of the previous one using PC instead of lecithin as emulsifier agent. The attempt was made with the identical ratios between emulsion components used in the case of lecithin. We only calculated the amounts of PC from the percentage of phosphoric group present in lecithin. In the final composition of emulsion a 1,4 % of PC is present.

Unfortunately the resulting emulsion is not stable and the water droplets coalesce forming a precipitate. In any case sample was diluted five times with water and then the emulsion was filtered using hydrophobic and hydrophilic membranes of decreasing sizes pores. In particular, the filtration was performed using filters with pore size of 0.8 μm, 0,4 μm and 0.22 μm, filtering one time for type of filter and for pore size. The FT-IR spectrum performed on the filtered matrix is not well resolved and identification of the components is not possible.

### 3.3.1 Determination of particle size

NTA analysis (see figure 3.8) of the sample obtained shows a broad distribution of sizes and low concentration of particles in the sample. Probably the high hydrophobic behavior of PC has negative effects on the stability of emulsion destabilizing the system.

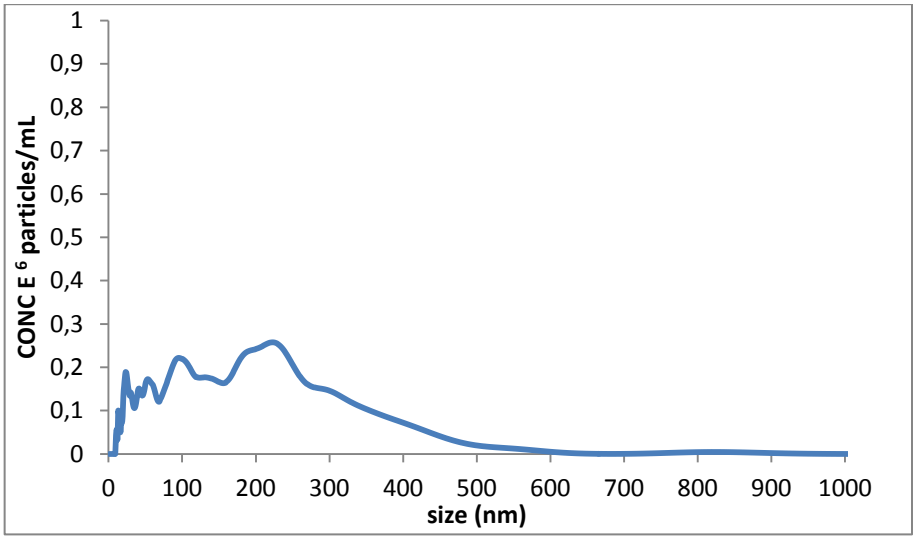


**Fig.3.8** Sizes distribution of nanoparticles resulting from NTA analysis in presence of PC.

As a conclusion of this part, the results obtained from food grade emulsion have been useful to design the characteristics of the next emulsion. In particular it will be desirable

- A reduction of the water droplet size in the emulsion to form smaller nanoparticles.
- The use of more pure components (organic solvents) in order to avoid complications deriving from impurities.
- The definition of a relatively simple and efficient purification process.
- The use of non ionic emulsifying agent to avoid direct interactions with the polymers.

## 3.4 Alginate-chitosan nanoparticles: preparation using Triton X-100 as emulsifying agent for W/O nanoemulsion

The procedure developed for the formation of alginate-chitosan nanoparticles in the internal droplets of the W/O nanoemulsion was conceived to obtain a stable system using not food grade components, and in particular the behavior of pure organic components was explored. This choice was motivated by the problems encountered in the analysis and characterization of systems formulated with food grade components, due to the presence of large amounts of impurities. Organic solvents and reagents give the possibility to work with pure components without any contamination of raw materials. In literature several articles report the possibility to use cyclohexane as continuous phase.[171] As underlined in the introduction in the formulation of a stable emulsion it is important to know the required HLB of the continuous phase. Cyclohexane, for example needs a value of HLB close to 10. Triton X-100 is a common emulsifying agent, frequently used as emulsifier in presence of cyclohexane as continuous oil phase. Triton X-100 is a polyoxyethylene derivative (see figure 3.9) belonging to the non ionic surfactant family.

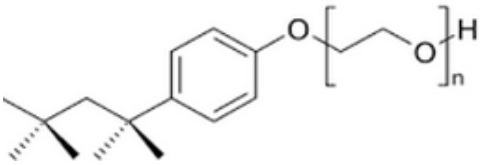


**Fig.3.9** Structure of Triton X-100

The choice of a non charged surfactant is justified by the presence of two charged polymers (alginate and chitosan); a further charged component in the emulsion can complicate the reaction interacting with the polymers. Triton X-100 has a HLB of 13, a value too high for cyclohexane, and an hypothetic emulsion formulated in such a way can undergo phase inversion. To obtain a stable emulsion it is, therefore, necessary to add a further component lowering the HLB to a value close to 10. To this aim, usually, a blend of Triton X-100 and hexanol[172] is used. The co-surfactant, in this case a linear alcohol like hexanol with an HLB of 6, acts as a HLB lowering agent. Selected the components to be used for the formulation of the emulsion and calculated the single volume fractions to obtain a value of HLB close to 10, the final composition may be

fine-tuned to set the best condition. In particular, the optimization of component ratio was achieved referring to the phase diagram reporting the three components (oil, water, surfactant). The region explored was the part of the diagram in which cyclohexane is present in large amount being the continuous phase, hexanol is the second component respect to the total volume fraction, the surfactant is present in a relative high amount to stabilize the emulsion, and, finally, the aqueous phase is present in small amount to avoid phase inversion of the emulsion.

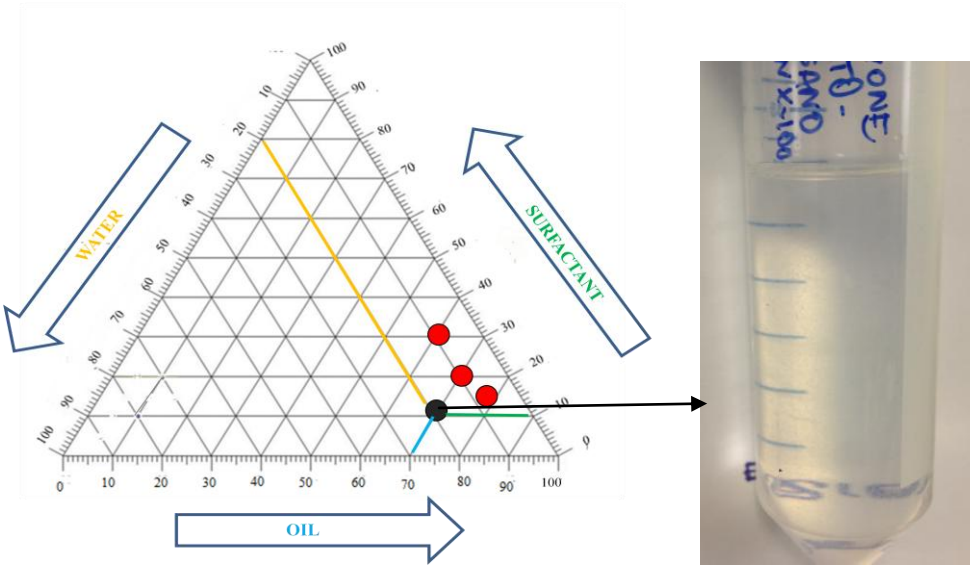


**Fig.3.10** Left: phase diagram showing the components ratios tested (red points) before to select the best one (black point). Right: final aspect of emulsion.

Figure 3.10 shows the phase diagram used to optimized the composition of the emulsion and the mixtures tested (red and black points). All the points tested fall in the W/O nanoemulsion region and the final composition chosen is very close to that reported by J. Zhi and al..[173] This work describes the *in situ* preparation of chitosan/$Fe_3O_4$ magnetic nanoparticles in W/O nanoemulsion with a good control of nanoparticle size and homogeneity thanks to the use of the internal water droplets of the nanoemulsion as nanosized reactors. In particular, a solution of chitosan and ferrous salt was prepared in water and then mixed with cyclohexane and hexanol in a fixed W/O ratio of 4/17. In the final step of nanoemulsion formulation, Triton X-100 was added under a vigorous stirring until the system became transparent. Then, magnetic chitosan nanoparticles were precipitated with a rapid change of pH adding NaOH to the emulsion and were crosslinked with glutaraldehyde. An article of the

same authors[174] describes the formation of chitosan nanoparticles using a slightly different procedure. At first, two emulsions, one containing chitosan and the other glutaraldehyde, were independently formulated in the same condition as above. Then the emulsion containing glutaraldehyde was added dropwise in the emulsion containing chitosan and kept under stirring enabling to the water droplets of the two different emulsions to collide and to exchange their components putting in contact the polymer with the glutaraldehyde. This process allows the formation of crosslinked chitosan-glutaraldehyde nanoparticles. The article reports also that the crosslinked chitosan nanoparticles are able to absorb and concentrate furosemide from a water solution, thanks to the hydrophobic interactions established between chitosan and furosemide. Inspired by these works we decided to explore a similar methodology for the preparation of alginate-chitosan crosslinked nanoparticles exploiting the water pool of nanoemulsion as nanoreactors. Two emulsions have been formulated using the following cyclohexane/hexanol/water ratios: 11/6/4 and titrating with Triton X-100 under stirring until a clear solution was obtained. In this condition and in the absence of polymers, measurement of aqueous droplets of the emulsion recorded by DLS shows a mean diameter of 58 nm with a low polydispersity index (0,25). The final Triton X-100 ratio was about 1/3 respect to cyclohexane. The first emulsion was prepared using a water solution (pH= 5) of chitosan at a 0,2 w/v concentration and the second one was prepared using a water solution of alginate at a 0,2 w/v concentration added of the zero length crosslinkers EDC (26 μl at the concentration of 3,5 $10^{-3}$ mol/ml) and NHS (10 μl at the concentration of 2,03 $10^{-3}$).

In our preparation EDC and NHS are firstly incubated with alginate (the molecule bearing the carboxyl groups) and the water solution containing the polymer and the crosslinking agents was used to form the emulsion which was finally added to the emulsion containing chitosan (see figure 3.11). After coalescence of the water droplets of the two emulsions the reaction takes place probably between the mannuronic (M) functions of alginate, being less rigid than G blocks, and the amine functions of chitosan. The emulsion containing alginate and EDC/NHS was then added dropwise in the emulsion containing chitosan and the system was maintained under stirring for 48 hours to ensure efficient collision between the drops of alginate and chitosan and to

let the crosslinking reaction to occur thus forming crosslinked alginate-chitosan nanoparticles.

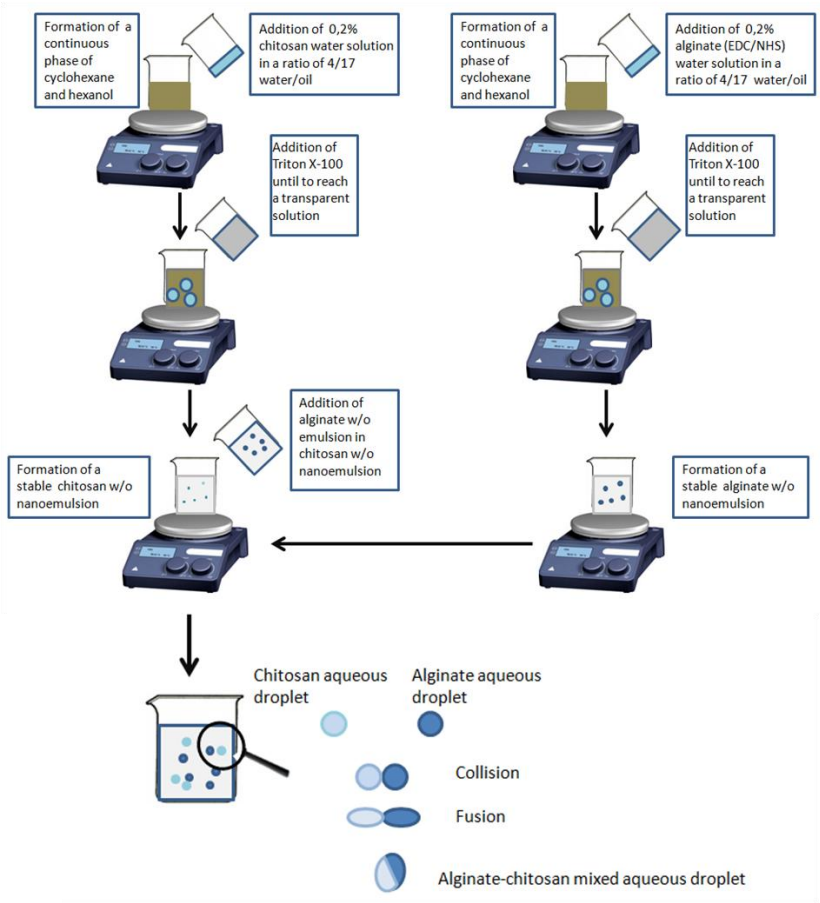


**Fig.3.11** Schematic representation of the protocol used to form alginate-chitosan nanoparticles in w/o nanoemulsion using Triton X-100 as emulsifying agent.

The step following the reaction between the two polymers in the nanoemulsion was the recovery and purification of the nanoparticles. This step was problematic and took several time and attempts to find a convenient procedure. In the first attempt the emulsion was broken by addition of water and the organic solvent was evaporated under reduced pressure leaving a water solution of nanoparticles containing also hexanol and Triton X-100. Removal of these two components was then attempted by repeated dialysis against water or water/ethanol mixtures and by treatment with Amberlite AD2 (see below). However, with these methods the full removal of Triton X-100 was not obtained. At the end, the most convenient procedure was found to be the precipitation of the polymeric fraction from the emulsion with acetone which being

miscible with water can penetrate in the water droplets causing the precipitation of alginate-chitosan nanoparticles.[175] Acetone is also useful because it dissolves all the organic components included emulsifying agent, determining the formation of two well distinguished phases: the precipitated polymer matrix and the organic solution. Therefore, the emulsion was treated with acetone and centrifuged. The liquid phase was discharged and the pellet was resuspended in water and precipitated again with acetone for five times. After the last precipitation the pellet of polymers was dried with a $N_2$ flow and resuspended in water. Totally about 70% (6,5 mg) of initial polymers is recovered. To remove completely the traces of organic solvents and Triton X-100, Amberlite AD2, was used. As stated in the technical data sheet, Amberlite AD2 is a polystyrene resin which is used in "very sensitive analytical procedures to detect organics in the environment or to concentrate them from a water solution". In fact this resin is very efficient in adsorbing hydrophobic molecules on the polystyrene surface thanks to van der Waals forces. The resin is also able to remove traces of Triton X-100 still present in the nanoparticles water suspension with an adsorbing capacity of 0,37 g of surfactant per g of dry resin:

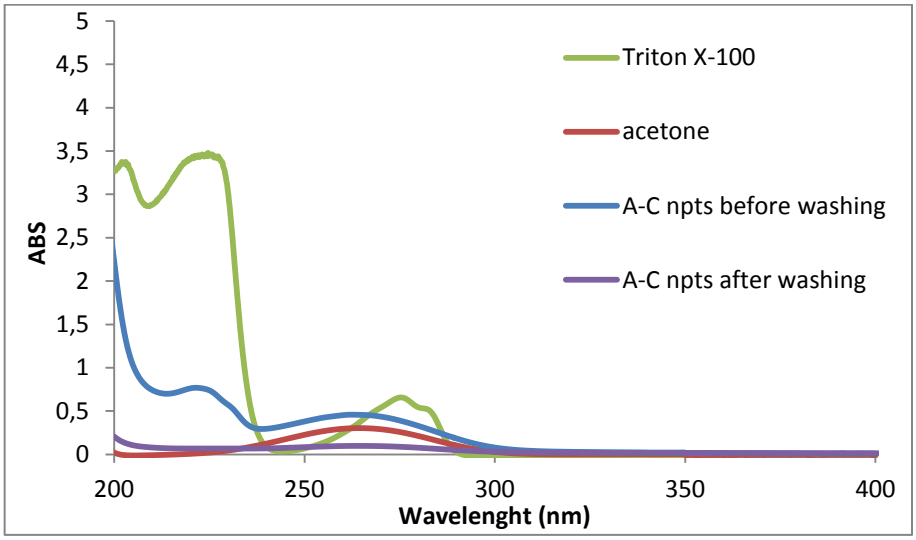


**Fig.3.12** UV-Vis spectra of water solution of Triton X-100, acetone and nanoparticles suspension before and after treatment with Amberlite AD2.

The purification step was followed by UV-Vis spectroscopy. As is possible to see in figure 3.12, Triton X-100 has a UV-Vis spectrum with two absorbance maxima (green

track) at 273 nm and 224 nm (the most intense peak). The water suspension of nanoparticles (blue track) before to be washed with Amberlite AD2 still contains traces of acetone and Triton X-100. The signal relative to Triton X-100 at 273 nm is covered by the broad peak due to acetone still present in little amount in the water suspension, but the presence of Triton X-100 is clearly deducible from the peak at 224 nm. Using a calibration curve, obtained by measuring the absorbance at 224 nm of solution at known concentration of Triton X-100, it also possible to calculate the amount of Triton X-100 still present in the water suspension of nanoparticles and to proceed with the washing steps until all the Triton X-100 is removed. Usually the total removal of the surfactant requires 2 or 3 steps of washing with the resin and the UV-Vis spectrum obtained at the end of the treatment showing the absence of Triton X-100 is reported in figure 3.12 (violet track).

After the nanoparticles sample was completely purified from organic solvents and emulsifying agent, it was possible to proceed with further analysis.

### 3.4.1 Determination of particle size

In all the applications related to nanoparticles, the particle size is the most important parameter to know. One popular method widespread in the last period is the NTA, a versatile technology that enables a direct visualization of the sample thanks to a camera connected to the sample chamber. The measurements were performed at ambient temperature and represent the medium value of three different measurements of three different batches. Figure 3.13 shows the results obtained. The mean diameter of the nanoparticles is 215 nm ($\sigma$= ±49 nm). The curve appears simmetrically distributed around this central value. A little amount of nanoparticles seems to be present at very low diameter values, between 10-60 nm, but this region is in the proximity of the detection limit of the instrument (40 nm for polymers) so the signal can be due to background noise as also suggested from the low concentration reported.

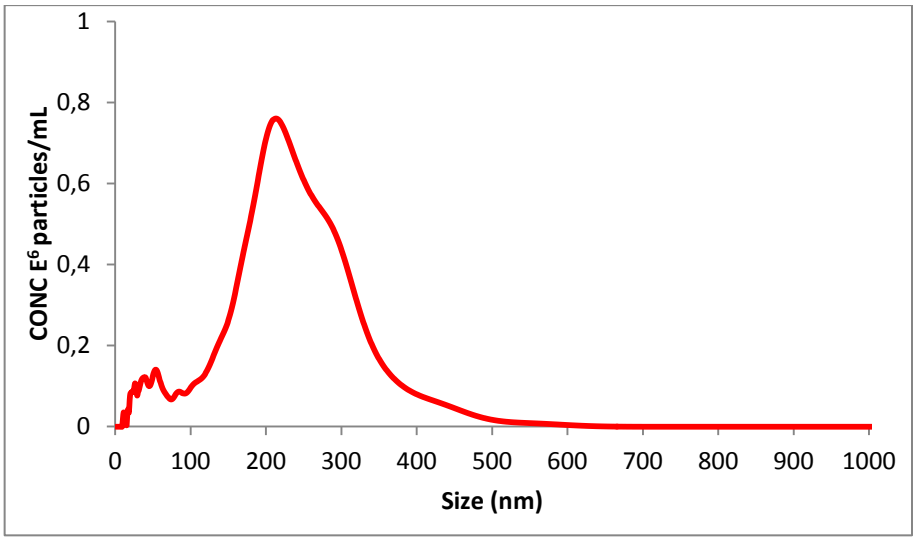


**Fig.3.13** Particle size of nanoparticles obtained from NTA.

The size distribution of the nanoparticles obtained is comparable to those reported in the literature for similar polymeric formulation.[176] The sizes appear acceptable and well reproducible from different batches.

## 3.4.2 Determination of particle stability

To verify the stability of the nanoparticle suspension the mean nanoparticle diameter was measured (by NTA) on the same samples over 1 week and 2 weeks in order to understand if any structural change or degradation process occur in the system. In particular we measured the mean diameter maintaining the same dilution of the sample which was conserved at room temperature during all the experiment. Figure 3.14 reports the result obtained.

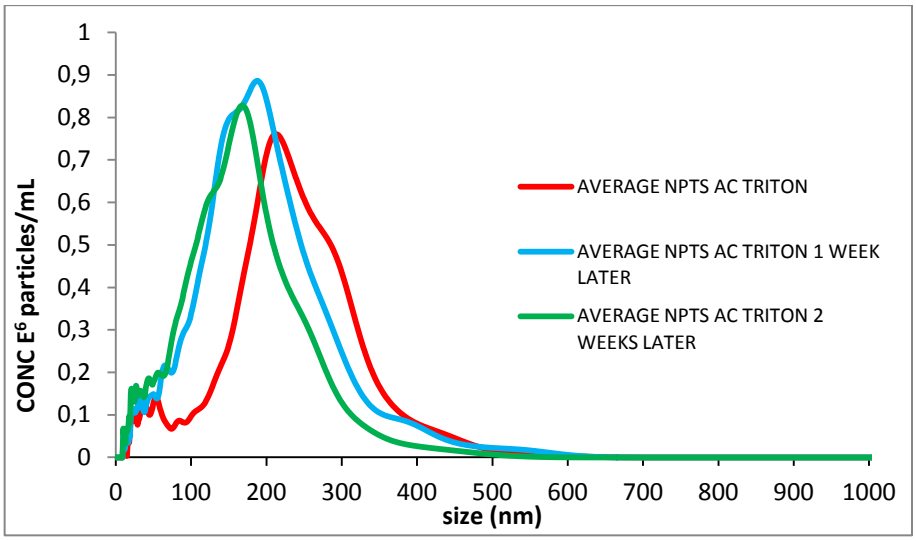


**Fig.3.14** Diameter distribution curves measured for the same sample after 1 and 2 weeks of aging. Each curve is the average of three independent measurements.

From the curve obtained (see figure 3.14) it is possible to observe a clear reduction of the particle size after one week even more evident after two weeks from preparation. This phenomenon could be the result of a partial disruption of the nanoparticles or, more likely, an event of aggregation and consequent precipitation of the biggest nanoparticles. In this case, indeed, the removal due to aggregation/precipitation of the larger nanoparticles will result in a shift of the mean diameter toward lower values. This hypothesis is also supported by an analogous size decrease observed after a centrifugation step of the sample, carried out on the same day in which the batch is prepared. Indeed, centrifugation of a freshly prepared sample at 10000 rpm for 10 minutes precipitates the aggregated particles separating them from the smallest ones which remain suspended in water. The results are shown in figure 3.15 and comparing the size distribution curve (green track) resulting from centrifugation with the one measured after two weeks of aging (see red track in figure 3.14) there is a good correspondence in term of mean diameter and shape of the curves. This suggests that the centrifugal force accelerates the sedimentation process of aggregated nanoparticles present in suspension, thus representing a useful approach to detect and remove the presence aggregated nanoparticles from the suspension. Moreover, the centrifuged sample is stable at room temperature during time not showing appreciable modification of the nanoparticle man diameter after 14 days of aging.

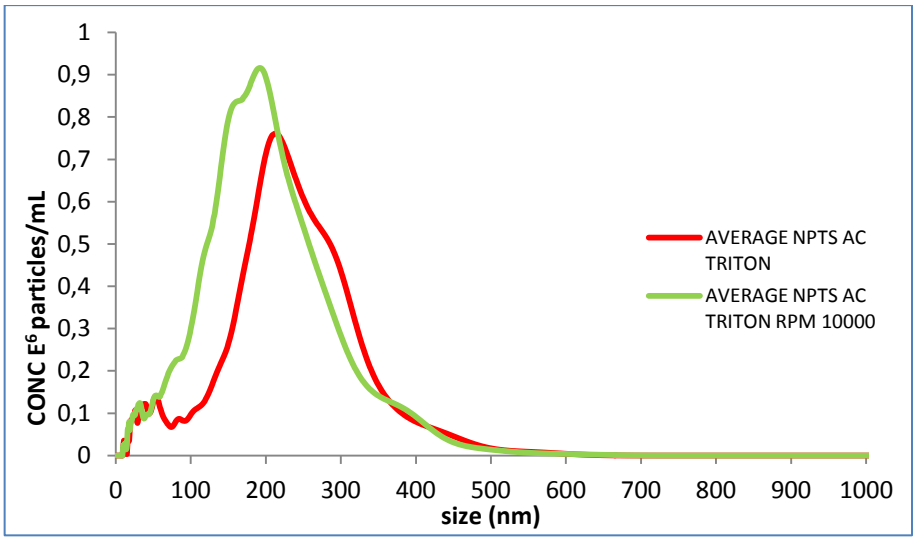


**Fig.3.15** Average size of nanoparticles measured using NTA before and after centrifugation

### 3.4.3 Spectroscopic analysis (FT-IR)

From the FT-IR spectra is possible to found a confirmation about the presence of both alginate and chitosan in the final composition of the nanoparticles and to formulate some hypotheses about an eventual interaction. In particular comparing the spectra of the final alginate-chitosan matrix with alginate and chitosan powder, some considerations can reinforce the hypothesis of an interaction without, however, a real evidence confirming the formation of the amide bond. Figure 3.16 reports the FT-IR spectra obtained in KBr pellet for chitosan, alginate and the alginate-chitosan nanoparticles and tables 3.1 and 3.2 show the assignments of the bands to chitosan and alginate respectively.

| Table FTIR Bands of Chitosan with assignments | |
|---|---|
| Chitosan vibration ($cm^{-1}$) | assignment |
| 3600-3100 | O-H overlapped to the N-H stretch |
| 3000-2800 | C-H asym stretch |
| 1631 | C=O amide Ⅰ, |
| 1515 | Amide Ⅱ band, symmetric $NH_3^+$ bending |
| 1415 | $-CH_2$ bending |
| 1380 | $CH_3$ symmetrical deformation |
| 1249 | C-O-H group |
| 1153-1049 | C-C-O stretch |

**Tab.3.1** FT-IR bands of chitosan

| Table FTIR Bands of Alginate assignment | |
|---|---|
| Alginate vibration ($cm^{-1}$) | assignment |
| 3600-3200 broad | OH, stretch |
| 3000-2800 | C-H asym and sym stretch |
| 1610 | $CO_2$- asymmetric |
| 1415 | $CO_2$- symmetric |
| 1320 | C-O stretching |
| 1160-1026 | C-C-O stretch |
| 944 | O-H bend |

**Tab.3.2** FT-IR bands of alginate

The Infrared spectrum of the chitosan reveals the typical chitosan absorbance peaks: the bands appearing from 3750 to 3000 $cm^{-1}$ are due to the stretching vibrations of O-H groups overlapped to stretching vibration of N-H. Absorption in the range of 1680-1470 $cm^{-1}$ indicates vibrations of carbonyl groups, in this specific case the secondary amide due to the partial acetylation of chitosan has a frequency of 1631 $cm^{-1}$.[177] The peak at 1515 $cm^{-1}$ instead can be attributed to the protonated amine group overlapped to the amide Ⅱ signal. The absorptions at 1380 $cm^{-1}$ and 1415 $cm^{-1}$ are relative to the bending vibrations of $CH_3$ and $CH_2$ respectively. The band at 1249 $cm^{-1}$ is the absorption peak of the stretching vibration of the C-O-H group. The bands located at 1153-1026 $cm^{-1}$ are related to C-O-C vibrations. The alginate FT-IR spectrum shows a broad peak around 3500 $cm^{-1}$ relative to the O-H stretching and H bonded, the peaks at 2923 $cm^{-1}$ and 2858 $cm^{-1}$ instead are due to the C-H asymmetric and symmetric stretching. At 1610 $cm^{-1}$ and 1415 $cm^{-1}$ there are the characteristic bands of alginate ($COO^-$ asymmetric and symmetric stretching). The peak at 1320 $cm^{-1}$ corresponds to C-O stretching, peaks at 1166 $cm^{-1}$ and 1126 $cm^{-1}$ are due to the C-C-O stretching. The last peak at 944 $cm^{-1}$ is due to the O-H bending. In the spectrum of the lyophilized matrix after reaction between alginate and chitosan it is evident the presence of the characteristic peaks of the polymers.

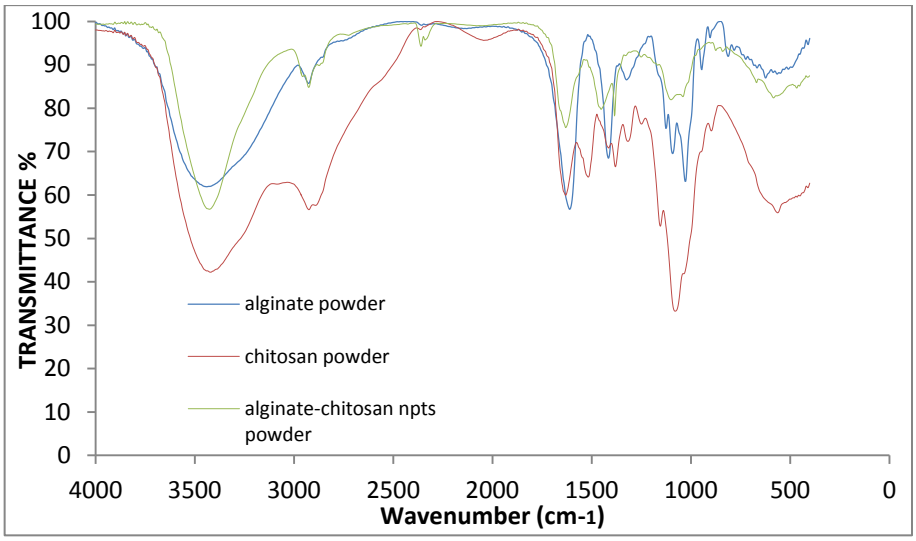


**Fig.3.16** Comparison of FT-IR spectra obtained from alginate and chitosan powder, and alginate-chitosan covalent matrix after reaction.

In particular the presence of an intense peak at 1635 $cm^{-1}$ can be the result of the addition of alginate and chitosan characteristic peaks (1631 $cm^{-1}$ for chitosan and 1610 $cm^{-1}$ for alginate) or it can be considered as the amide I band. The absence of a peak at 1530 $cm^{-1}$ suggests the absence of the protonated amine of chitosan possibly due to a large involvement of the amine in the reaction of amidation. In conclusion the analysis of the FT-IR spectrum of the polymer nanoparticles confirms the presence of the two polymers but cannot give a clear-cut demonstration of the formation of the amide bond. Regrettably, attempts to characterize the nanoparticles using NMR failed due to a too low solubility in water and other NMR solvents (MeOH, DMSO, etc.)

## 3.4.4 Determination of particle morphology

The morphology, shape and size of the nanoparticles were investigated using TEM and SEM microscopy. To perform TEM a droplet of water suspension of nanoparticles was poured on a copper grid and contrasted with uranyl acetate. After complete evaporation of water, the sample is ready to be introduced in the chamber for the analysis.

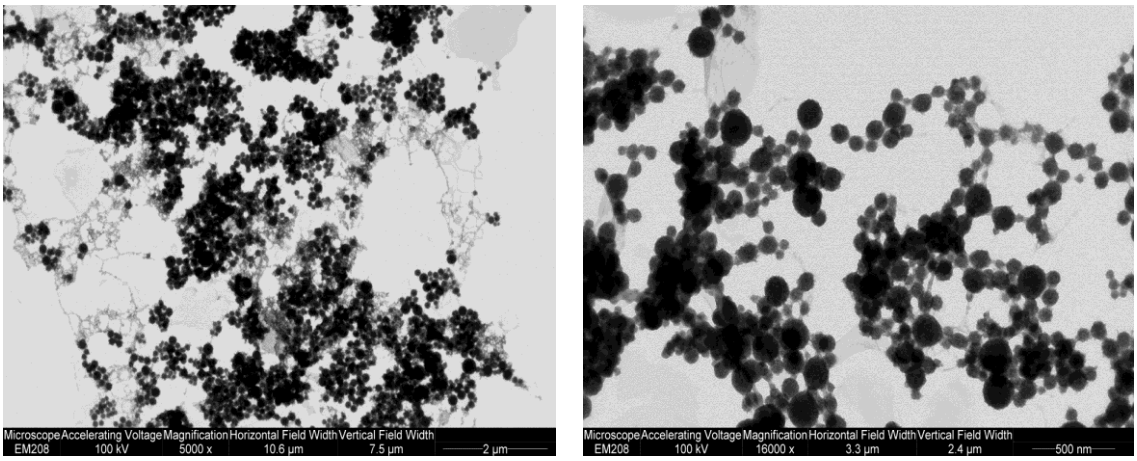


**Fig.3.17** TEM images of covalent alginate-chitosan nanoparticles at different magnification.

Nanoparticles appear with a spherical shape (see figure 3.17) and the image reveals a good distribution of the mean diameter with the particles being quite homogenous in sizes. The mean diameter measured by analyzing 70 nanoparticles using a digital micrograph program is 96 nm ($\sigma$= ± 27 nm (see figure 3.18).

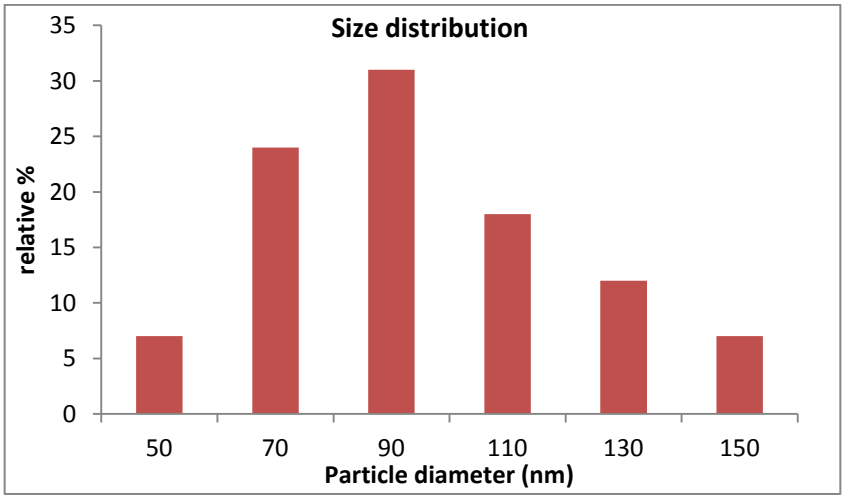


**Fig.3.18** Size distribution of particles measured with Micrograph program.

The average diameter is smaller when compared with that obtained from NTA. However, this is likely the effect of the measurement conditions. Indeed, TEM analysis is performed under high vacuum and the drying of the sample results is a general shrinkage of the nanoparticles.[178] This shrinkage effect underlines the swelling properties in water environment for the crosslinked nanoparticles. The TEM image

recorded at higher magnification (see figure 3.17, right) shows well shaped spherical nanoparticles. In this case it is possible to observe some clusters of nanoparticles that probably reflect the agglomeration process observed with NTA.

The topology of nanoparticles has been explored using SEM microscopy which shows the tridimensional structure of the nanoparticles. The resulting figures for the system composed of alginate-chitosan nanoparticles show a clear aggregative process of the nanoparticles. The sample presents a large amorphous structure made by fused nanoparticles as is clearly seen on the surface where the spherical shape of the nanoparticles is maintained (see figure 3.19, left).

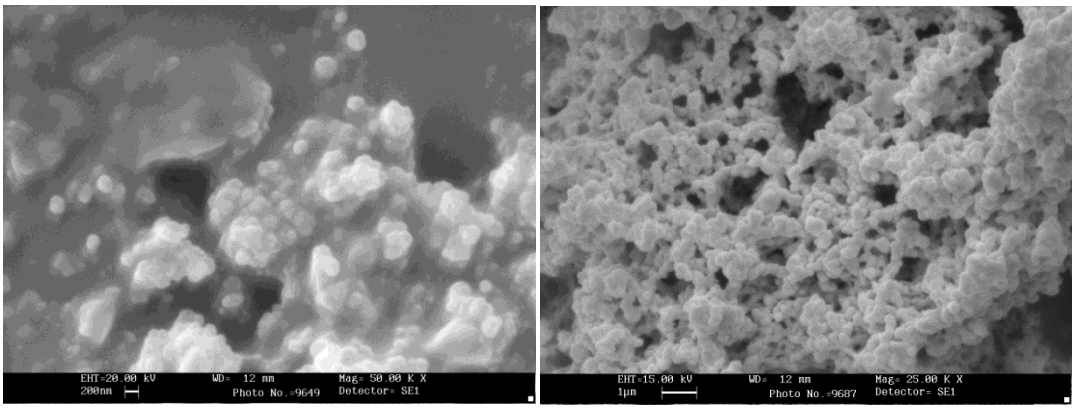


**Fig.3.19** SEM images of covalent alginate-chitosan nanoparticles.

## 3.4.5 In vitro toxicity test: MTT assay

In order to evaluate the possible toxicity of the nanoparticles prepared with the protocol described above the MTT toxicological assay was set on Caco-2 cells. The MTT assay is a valid method to check the proliferation of cells and therefore an eventual mortality in case of toxic action of external agents, the nanoparticle suspensions in this case. This study represents a preliminary information about toxicity of the polymeric matrix forming the nanoparticles *in se* or on the toxic action due to organic residues of solvent or surfactant. In fact these factors may potentially have a key role in the mortality of cells. In particular three dilutions of alginate-chitosan nanoparticles have

been tested with Caco-2 cell line in order to highlight possible effects of the sample concentration.

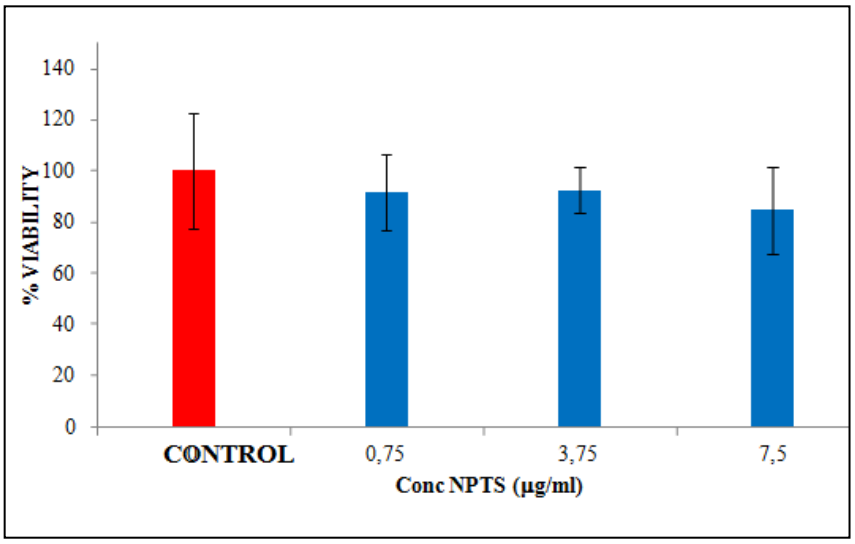


**Fig.3.20** Histogram relative to % viability of Caco-2 cells after exposition to different concentrations of alginate-chitosan nanoparticles.

The results of the toxicity test is shown in figure 3.20. Comparison of the cell viability after exposure to the 3 different concentration of nanoparticle sample (blue) with the control experiment (red) does not manifest evident changes in proliferation of cells. Therefore, a toxic action of the nanoparticles can be excluded at least at the concentrations tested. The nanoparticles (also considering the standard deviation) show a value of cell vitality comparable with compounds normally referred as non toxic for cells.[179] However, a slightly lower value of cell viability, although within the experimental error, observed at the highest concentration tested suggests that some toxicity may manifest at higher concentration. This opens the way to further studies aimed to test a wider concentration range of nanoparticles.

### 3.4.6 Encapsulating properties of the nanoparticles

The design of polymer nanoparticles manifesting encapsulation ability is of fundamental importance in drug delivery. Several reviews and articles have explored the possibility of alginate and chitosan derivatives to encapsulate and retain bioactive drugs or peptides.[180] In general hydrophilic biopolymers are investigated for the ability to load a water soluble drug. The encapsulation of a hydrophilic charged drug is based on ionic interactions occurring among opposite charges carried by the biopolymer and the drug. However, preparation of the polymeric carrier directly in water in the presence of the drug usually results in a low encapsulation. So many efforts were addressed on the preparation of nanoparticles using emulsification techniques. In the case of alginate nanoparticles, for example, emulsification followed by gelation with $Ca^{2+}$ ions showed a low encapsulation efficiency and a fast release for the high porosity of alginate matrix. The coating of the alginate nanoparticles with chitosan improves the encapsulation efficiency by modifying the surface properties of the nanoparticles.[181] However, in some cases the loading ability remains low probably for the several stages usually included in the protocol for the preparation of the nanoparticles that determine a loss of loaded molecules. Our purpose is to explore the ability of alginate-chitosan crosslinked nanoparticles to encapsulate hydrophobic drugs. It's well recognized the ability of chitosan to establish hydrophobic interactions with lipophilic molecules, thanks to the presence of a little amounts of acetylated functions, and this property seems to be strictly related with the molecular weight with hydrophobic interactions increasing with the molecular weight.[182] In the protocol developed to evaluate the encapsulating properties of alginate-chitosan nanoparticles, the bioactive compounds are not loaded in the initial step of emulsion formulation. In fact being the lipophilic compounds, the possibility to lose the drug in the continuous phase of the nanoemulsion during nanoparticles formation is very high. To avoid this problem and also the risk of bioactive molecules loss during the purification procedure, the bioactive molecules were added directly to the water suspension of nanoparticles in the final step, after nanoparticles have been purified from organic solvent, taking

advantage of chitosan hydrophobicity.[183] Being the final system not a rigid matrix, the chitosan hydrophobic moieties have a certain tendency to place themselves in the core of the structure if exposed in aqueous environment. Resveratrol and quercetin in particular, are the lipophilic compounds selected to investigate the entrapping properties of the nanoparticles. Literature reports [20,38,50,101] describe several carriers explored for the encapsulation of these polyphenols, but researches on alginate-chitosan covalent carriers are lacking.

### 3.4.6.1 Loading of resveratrol

Resveratrol represents a molecule of great interest in nutraceuticals for its antioxidant properties. It belongs to the class of the stilbenes and specifically is a 3,4',5 – Trihydroxystilbene (see figure 3.21). The antioxidant activity is reported only for the *trans* form of the compound. Different authors have described the positive beneficial effect of a daily consumption of resveratrol and several carriers were explored with encapsulation purpose.[10]

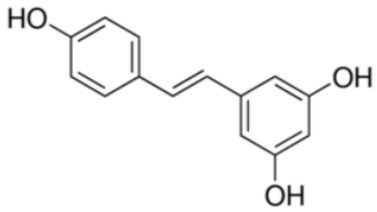


**Fig 3.21** Structure of resveratrol.

Recently the technologies related to encapsulation of bioactive molecules into different polymer matrices to enhance stability have been developing rapidly. Chitosan and alginate being safe polymers can represent potential carriers for resveratrol. In particular literature reports recent investigation on resveratrol-loaded chitosan-TPP microspheres[184] and alginate sub-micro-spheres.[184] Yield in encapsulation is highly variable and depends from different parameters.

In this Thesis the experiments to verify the encapsulating properties of alginate-chitosan nanoparticles were conducted spectrophotometrically because resveratrol

presents an easily detectable absorbance band in the UV range with a maximum at 307 nm. Before to proceed with the measure of the encapsulation capacity of the nanoparticles it was necessary to develop a procedure to determine the solubility limit of resveratrol in water. At this purpose, an aqueous suspension was prepared in which resveratrol was added in excess (0,5 mg/ml). After 24 h of equilibration time, necessary to permit to the excess resveratrol to precipitate, the sample was centrifuged at 3000 rpm for 10 min, and a small volume of supernatant was diluted in water and inserted in the couvette for the UV-Vis measurements (see figure 3.22, blue track). It is important to highlight that the system needs a given time (before centrifugation) to ensure nucleation and growth of the crystals in accordance with the Ostwald ripening process. In fact at first many small crystals having a higher solubility respect to larger ones are formed. Hand to hand these small crystals grow forming larger crystals which precipitates out of solution. Control experiments in our conditions showed that 24 h of aging are sufficient to ensure a complete precipitation of the insoluble material giving a saturated water solution of resveratrol.

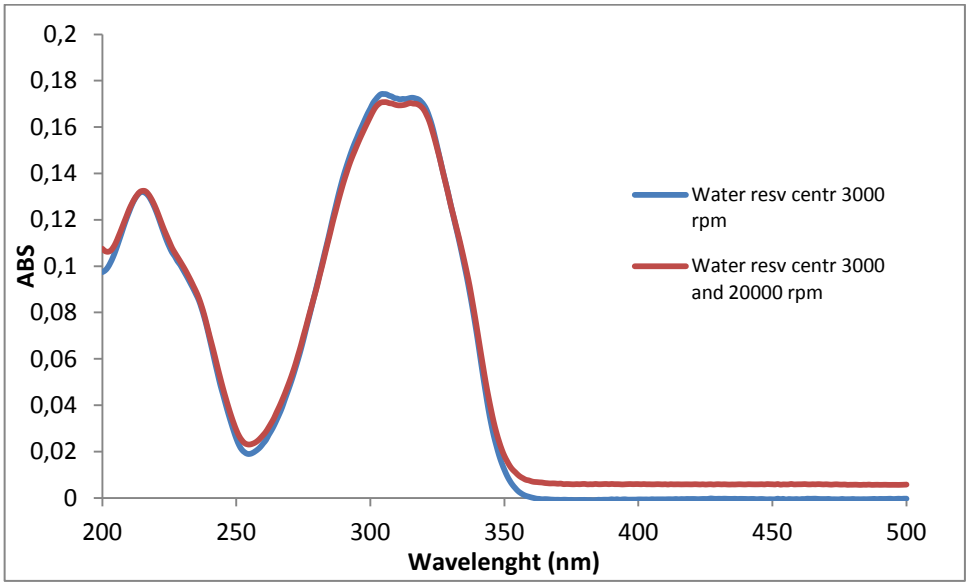


**Fig.3.22** Validation of the procedure to measure the solubility limit of resveratrol.

After this first centrifugation step, the speed of rotation was increased to confirm the complete precipitation of the insoluble portion of resveratrol, avoiding possible false positive results due to small crystals of resveratrol still present in suspension. The

absorbance of resveratrol at 307 nm after centrifugation at 20000 rpm (red track) was the same as in the case of centrifugation at lower speed indicating that centrifugation at 3000 rpm is sufficient to ensure complete precipitation of the insoluble portion of resveratrol. This absorbance value corresponds to a solubility limit of 1,3 μg/ml calculated using a calibration curve measured in ethanol. For the experiment with the nanoparticles a similar protocol was used. An excess of resveratrol (0,5 mg/ml) was added to the nanoparticle suspension and, after 24 h of aging, the water suspension was centrifuged at 3000 rpm and the UV-Vis spectrum was recorded. In this way the trapping ability of the nanoparticles can be easily evaluated from the absorbance value at 307 nm respect to that obtained in water.

The results of these experiments carried out at different concentration of nanoparticles are shown in figure 3.23. As expected increasing the concentration of nanoparticles the measured absorbance at 307 nm increases indicating that the nanoparticles are able to entrap resveratrol increasing its concentration above its solubility limit in water. The correlation between resveratrol absorbance and nanoparticle concentration is almost linear for the first four points and departs from linearity in the most concentrated sample (black point). Considering the linear part of the curve we can calculate an entrapping efficiency of 1,4 μg of resveratrol per 1 μg of nanoparticles. Instead if we consider the black point (the most concentrated sample) the value of entrapped resveratrol is of 2,35 μg per 1 μg of nanoparticles. As discussed before in occasion of the analysis of nanoparticles stability during time, probably the deviation from linearity in the trapping ability of the nanoparticles can be ascribed to the presence of aggregates at high concentration of nanoparticles in which resveratrol remains “entangled”. Indeed, following the evolution of the most concentrated sample (black point of figure 3.23) during a period of days (see figure 3.24), a decrease of resveratrol absorbance during the time is observed until a plateau is reached. This decrease is likely due to the precipitation of the aggregated nanoparticles present at the relatively high concentration of the sample. This is also confirmed by the fact that the samples obtained at lower concentration are stable over time.

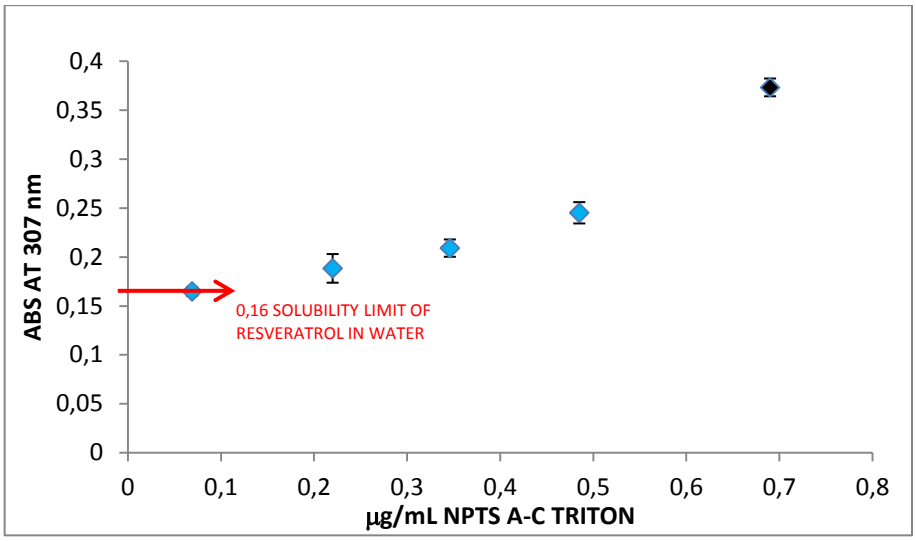


**Fig 3.23** Absorbance of resveratrol at different concentrations of alginate-chitosan nanoparticles.

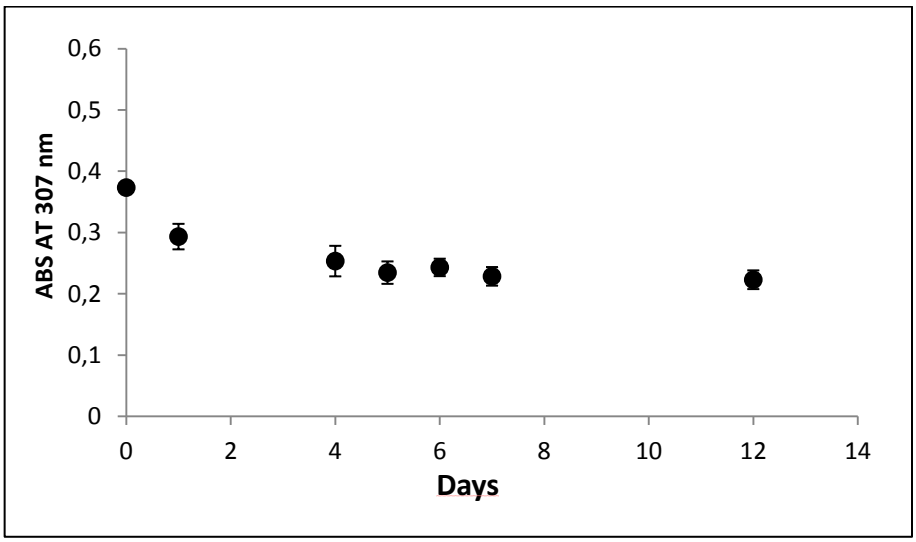


**Fig 3.24** Evolution of the highest concentrated sample (black point figure 3.23) during the time.

## 3.4.6.2 Radical scavenger activity: DPPH assay

Having demonstrated the ability of alginate-chitosan nanoparticles to entrap resveratrol, we investigated if the antioxidant ability of the molecule is retained in the nanoparticles formulation. A common test used to evaluate the ability of resveratrol to act as a scavenger is the DPPH assay. DPPH is a stable radical (thanks to a good

delocalization of the unpaired electron in the structure) with an oxidant ability. In a typical reaction with an antioxidant molecule, DPPH is reduced from the antioxidant molecule, which in turn is oxidized. This behavior mimics what occurs in our body between radicals and radical-scavengers as polyphenols.

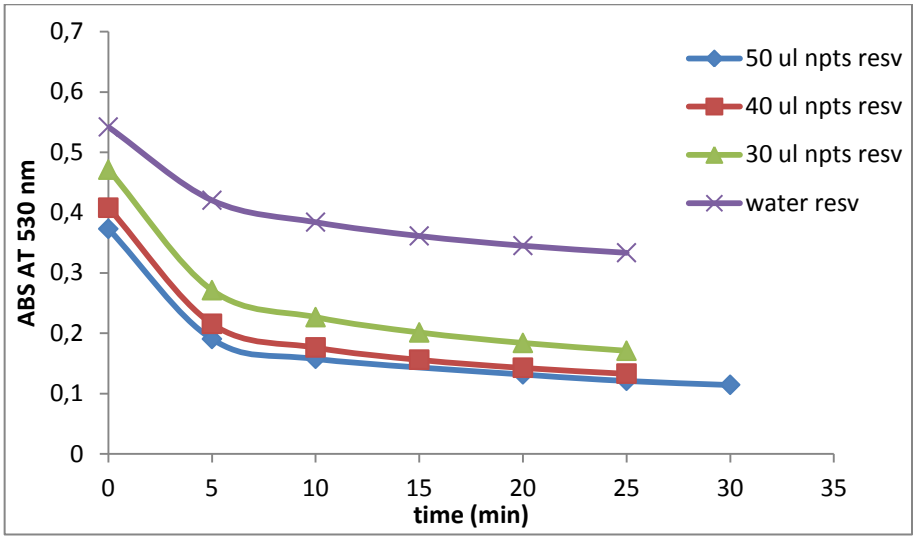


**Fig.3.25** Reduction of DPPH at different concentrations of resveratrol.

Reduction of DPPH is followed by the loss of the typical violet color detectable in the visible spectra at 530 nm. If resveratrol encapsulated in the alginate-chitosan nanoparticles is able to act as scavenger (how normally in the body does) thus reducing DPPH, the absorbance at 530 nm should decrease. The graph of figure 3.25 shows the results obtained in the experiment performed for 25 minutes, the time necessary to reach a plateau value for the absorbance of DPPH. Resveratrol, at the solubility limit in water (violet track) and resveratrol in nanoparticles prepared at different concentrations show a similar trend of decay. Nanoparticles having a concentration of resveratrol above the solubility limit have a lower plateau value of absorbance compared to resveratrol in water thus indicating that resveratrol entrapped in the nanoparticles preserves its antioxidant action.

### 3.4.6.3 Loading of quercetin

Quercetin (3,3',4',5,7-Pentahydroxy-flavone) is a relevant polyphenols in the field of nutraceutics (see figure 3.26) belonging to the family of flavones. It is a potent antioxidant molecule, and as reported from many works has an interesting activity against cancer.[185] However its use is limited by its extreme insolubility in water.

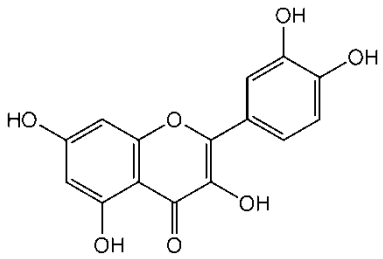


**Fig.3.26** Structure of quercetin.

Different materials and conditions have been studied to overcome this drawback and to improve water solubility of quercetin. The inclusion in nano carriers seems to represent a possible strategy. Entrapment in carrier in fact can also stabilize the molecule against rapid oxidation and degradation. The scope of this part of the project is to study encapsulation ability of synthesized alginate-chitosan nanoparticles and their capacity to retain and protect quercetin. A protocol similar to that of resveratrol was used to evaluate the encapsulation of quercetin. In brief quercetin was dissolved in DMSO at a concentration of 10 mg/ml and then added to water to reach a final concentration of 0,5 mg/ml. This oversaturated solution was incubated for 24 h and then centrifuged at increasing centrifuged forces to eliminate the insoluble portion of quercetin (see figure 3.27). As in the previous case centrifugation at 3000 rpm is sufficient to eliminate the suspended quercetin. In this condition the solubility limit of quercetin is 5 μg/ml, calculated using a calibration curve obtained in ethanol.

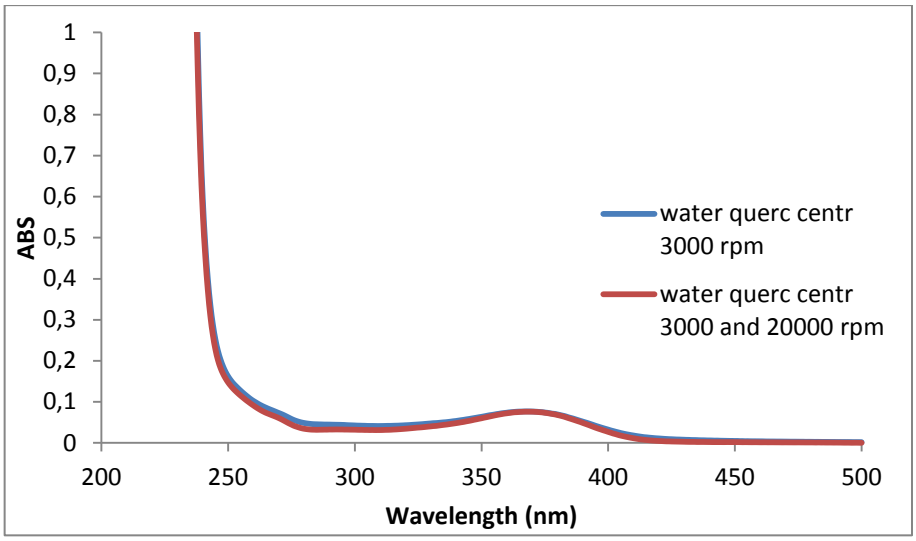


**Fig.3.27** UV-Vis spectra of quercetin solution in water after centrifugation at different centrifugal speeds.

Then, five samples with increasing concentrations of nanoparticles were incubated with the oversaturated concentration of quercetin. After the aging for 24h the suspensions were centrifuged at 10000 rpm to overcome the problems due to the possible presence of aggregated nanoparticles observed in the experiments with resveratrol at high concentration of nanoparticles. Figure 3.28 shows the dependence of the measured absorbance of quercetin in the nanoparticle suspensions after centrifugation which, in this case, is linear for all the concentrations investigated. From the data of figure it is clear that the nanoparticles are able to increase the amount of quercetin solubilized in water reasonably by entrapping the bioactive molecule thanks to hydrophobic interaction and hydrogen bonding. In these conditions the amount of quercetin entrapped is 346 ng per 1 μg of nanoparticles

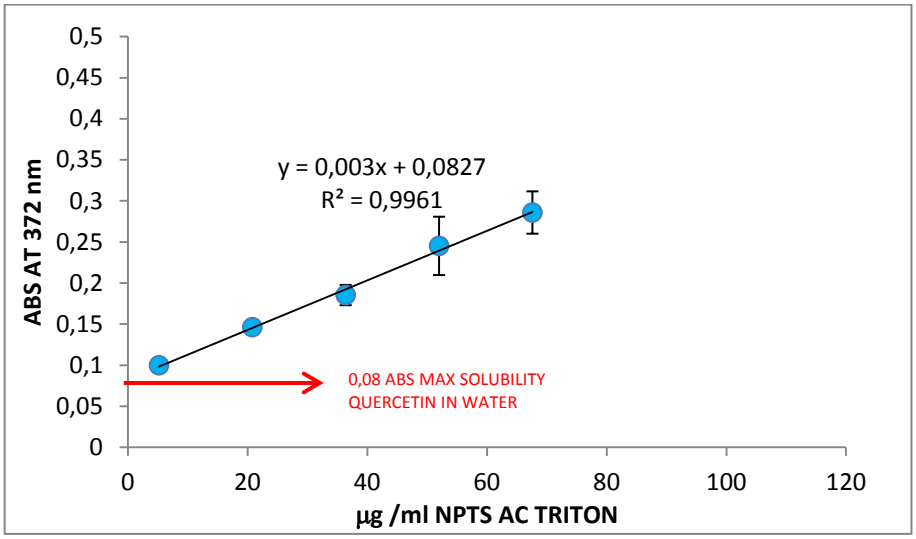


**Fig.3.28** Increasing concentration of quercetin at increasing amount of alginate-chitosan (Triton X-100) nanoparticles.

### 3.4.6.4 Stability of quercetin in nanoparticles and protection from oxidation

As a further characterization of the quercetin loaded nanoparticles and considering that quercetin is easily oxidized we monitored the stability of the bioactive molecule during time following the evolution of its UV-Vis spectra. Figure 3.29 shows that the absorbance of a quercetin solution at its solubility limit in water at 372 nm, in correspondence of its maximum absorbance, measured after three days of aging is unchanged indicating that the molecule in this condition is stable.

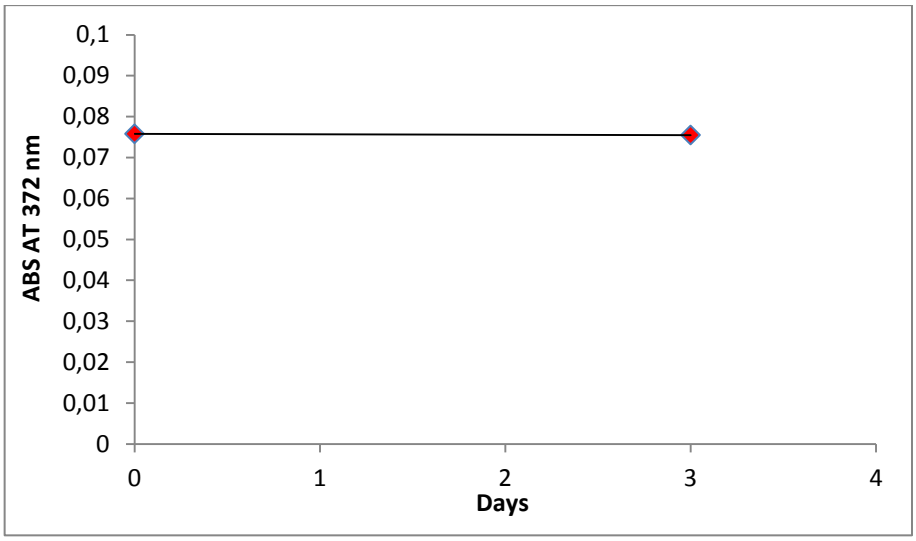


**Fig.3.29** Stability of quercetin in water.

On the other hand, the UV-Vis spectrum of quercetin loaded in alginate-chitosan nanoparticles (conc 68 μg/ml) during time shows a drastic evolution with the decrease of the absorbance at 372 nm and the appearance of a new peak at 330 nm (see figure 3.30). The time course of the absorbance at 330 and 372 nm over a period of five days is shown in figure 3.31 (left and right respectively) and shows that this phenomenon reaches a plateau after about 4 four days.

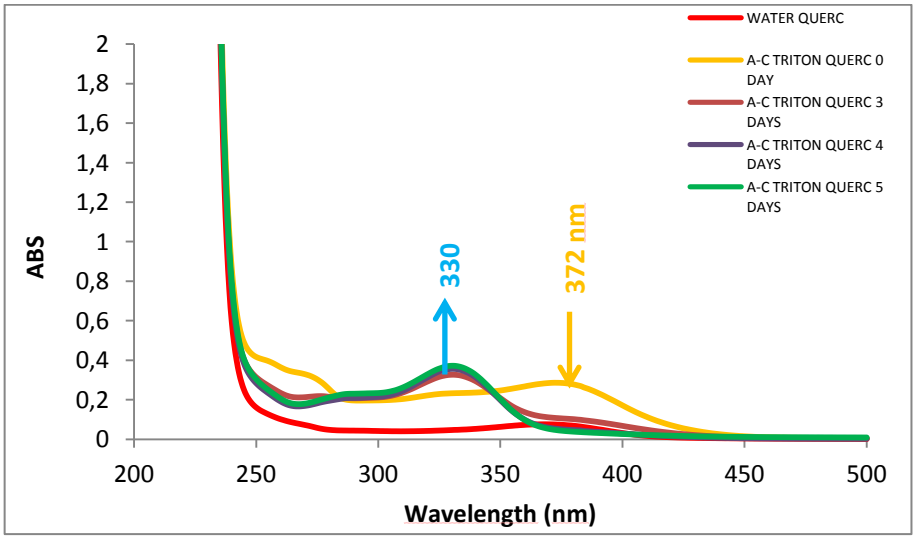


**Fig.3.30** Time evolution of the UV-Vis spectra of quercetin entrapped in alginate-chitosan nanoparticles (68 μg/ml).

Analysis of the literature suggests that the spectral modifications observed are probably related to an oxidation process of quercetin.[186] Indeed, quercetin is a polyphenolic compound known to act as antioxidant with scavenging activity toward oxygen reactive species in human body. This scavenging process leads to a two electron oxidation of quercetin which is converted in an ortho-quinone derivative, named QQ (see figure 3.32).

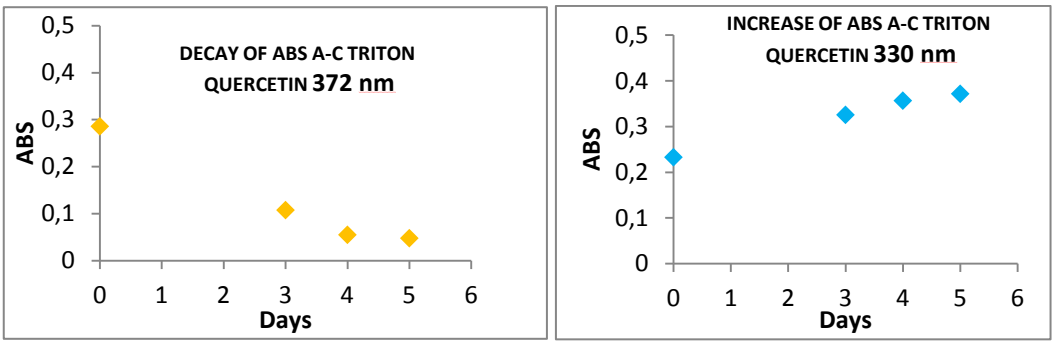


**Fig.3.31** A time course of the absorbance at 372 nm (left) and 330 nm (right) for quercetin entrapped in alginate-chitosan nanoparticles (68μg/ml).

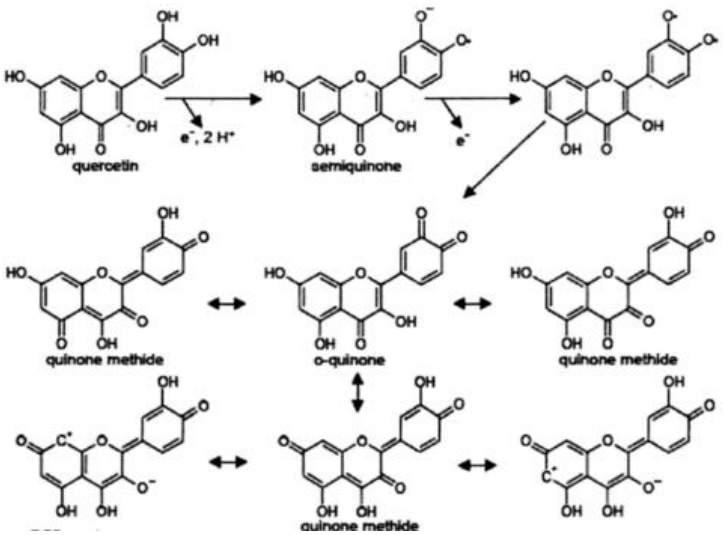


**Fig .3.32** Different oxidation states of quercetin.

The quinone (QQ) derivative yields from the oxidation of the two hydroxyl groups present in the B ring (catechol group). This oxidized molecule is present in different isomeric forms (orto quinone and many para quinone methides). This process is described[186] to lead to a spectral change of quercetin very similar to that observed in

our case and in particular to the disappearing of the peak at 372 nm and its replacement with a new absorbance peak at 330 nm. Contemporary the peak at 268 nm and a near shoulder decrease in absorbance. Therefore, we can conclude that quercetin is not stable when trapped in the nanoparticles and this is probably related to the high local concentration of the molecules in the relatively small volume of the nanoparticles. Indeed it is known that at high concentration, antioxidants molecules can undergo an auto-oxidation process.[187] Clearly, the instability of the bioactive molecule in the nanoparticles is a undesired effect also because the quinone form of quercetin is toxic being able to arylate cellular proteins and to react with the biological occurring thiols. However, the oxidation process of quercetin can be suppressed by addition of a other water soluble oxidant such as ascorbic acid which can act as protective agent toward quercetin.[188] Figure 3.33 shows the percentage of oxidation of quercetin loaded in the nanoparticles in the condition of figure 3.30 after five days in water and in the presence of a 3 μg/ml and 7,4 μg/ml of ascorbic acid. Increasing the amount of ascorbic acid the amount of oxidized quercetin decreases and at a 7,4 μg/ml it is reduced to a value close to zero. Therefore, ascorbic acid can represent a valid protecting agent for quercetin entrapped in our nanoparticles.

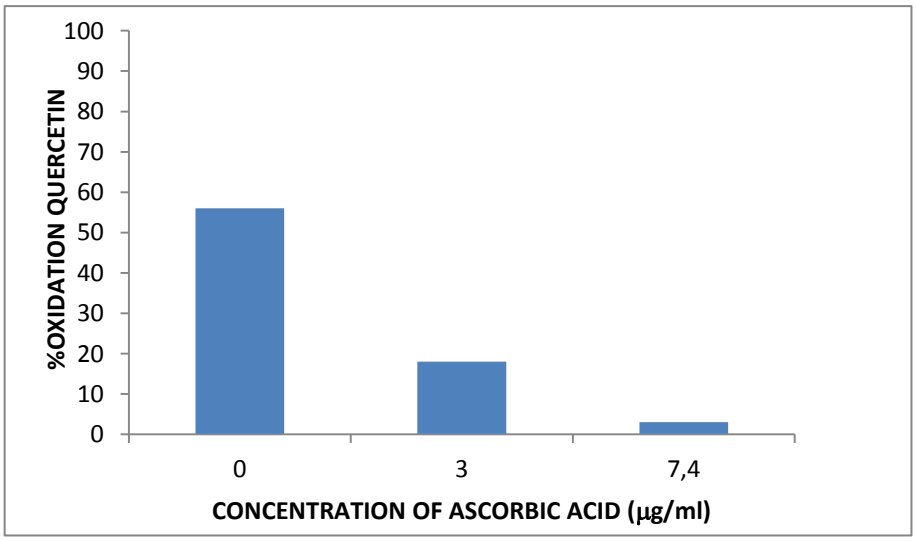


**Fig.3.33** Prevention of quercetin oxidation, adding different concentration of ascorbic acid in quercetin loaded alginate-chitosan nanoparticles.

## 3.5 Alginate-chitosan nanoparticles: preparation without crosslinkers using Triton X-100 as emulsifying agent for W/O nanoemulsion

To investigate the effect of the crosslinkers EDC and NHS on the preparation of alginate-chitosan nanoparticles an analogous set of experiments was performed in the same conditions used for the preparation of the nanoparticles in the emulsion with Triton X-100 but in the absence of EDC/NHS. Briefly a W/O nanoemulsion using cyclohexane as continuous phase, hexanol as cosurfactant and aqueous phase containing 0,2% (w/v) chitosan was prepared in ratio 17/4 of oil /water. Emulsion was then titrated with Triton X-100 until to reach a transparent nanoemulsion. At the same time and with the same procedure a similar nanoemulsion was prepared in presence of 0,2% (w/v) alginate in the aqueous phase (without the addition of EDC and NHS). The emulsion containing alginate was then added dropwise in the emulsion containing chitosan. At the end of the mixing step, the resultant emulsion was maintained under stirring for 48 h to favor spontaneous collision between droplets. The process of purification was the same adopted for the emulsion in presence of EDC and NHS. The particles were precipitated five times using acetone and then resuspended in water and washed with the polystyrene resin Amberlite AD2 for many times checking the complete removal of organic solvents and surfactant at the UV-Vis. At the end of the purification, the water suspension of nanoparticles is ready to be analyzed. Following this procedure the total polymer recovery was 70 % of which we were able to resuspend in water a 20% while the rest remains as insoluble pellet.

### 3.5.1 Determination of particle size

The ionic interaction between the opposite charges of alginate and chitosan is responsible of a process known as complex coacervation. The complexation between the two polyelectrolytes represents an advantage in the case of exposition of the final

matrix to sudden change of pH as after an oral administration. In fact, alginate is soluble at high pH and shrinks at low pH whereas chitosan dissolves at low pH and is insoluble at high pH. Moreover, the bonding with chitosan solves the problem of the porosity of the alginate network mitigating the possible leakage of drugs.[73] The complexation between the polymers usually involves a first step of a ionic gelation in which alginate is crosslinked with calcium, followed by the complex coacervation occurring between ca-alginate and chitosan. In fact calcium is essential to obtain good results in term of mechanical properties thanks to an increase of structure stability of the complex.[189] Chitosan-alginate interaction (in absence of calcium) is reported to be weak.[190] During the complexation, the acetylation degree (of chitosan) and the control of pH are key factors to maintain the chitosan dissolved: amine groups have to be charged and at high pH the number of charged amines decreases. Increasing pH, protonation also depends from the molecular weight of the polymers: the higher is the molecular weight the lower is the maximum value of pH at which chitosan is soluble. The network deriving from alginate-chitosan interaction can be described as a sequence of ionic interchain bonds alternating to regions constituted from uncoupled units of both polymers. The consideration discussed above may have a crucial role during coacervation between the polymers. In fact in the set-up of our experiments calcium is not present. However, the interaction between opposite charges carried by alginate and chitosan in emulsion is limited to the internal water droplets and the compartmentalization of the aqueous phase containing the polymers can help the formation of small size coacervates. Once the suspension was purified from the organic material, the sizes of the nanoparticles were analyzed using NTA. A comparison of the properties and the results obtained with alginate-chitosan covalent cross-linked nanoparticles with the system obtained from ionic interactions can elucidate the importance of the crosslinkers in the formulation of the nanoparticles.

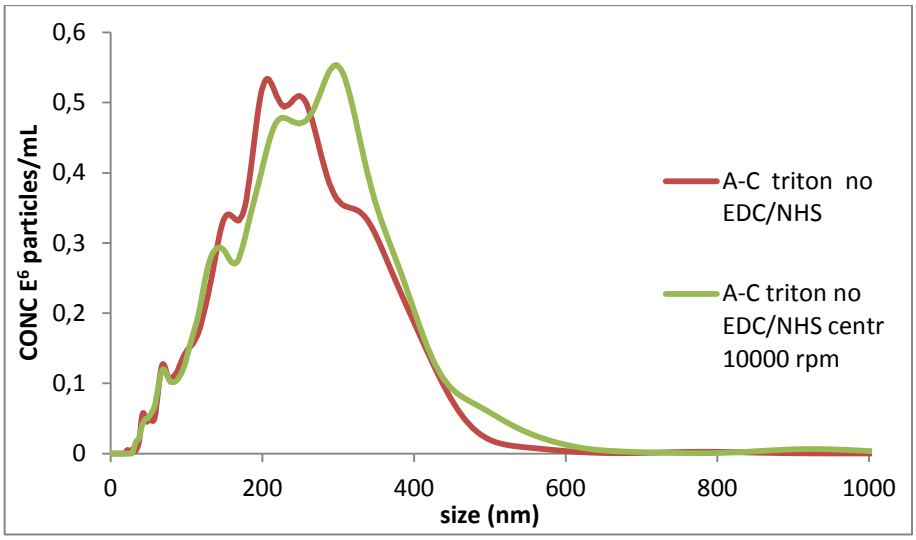


**Fig.3.34** Particle size of alginate-chitosan nanoparticles measured with NTA.

The plotted graph showing the size distribution of ionic alginate-chitosan nanoparticles (see figure 3.34), shows a broad curve if compared with the result for nanoparticles obtained in the presence of the crosslinkers (see figure 3.15). In particular, the distribution of sizes is not homogeneous with the presence of large nanoparticles or aggregates of polymers. Centrifugation of the suspension at 10000 rpm has little effect on the shape of the size distribution which, unexpectedly, moves toward a larger mean diameter. A possible explanation for this observation is that the centrifugal action can force polymers to approach each other thanks to the free charges present on the chain, determining an increment of volume of the aggregates. Despite this, the average particle size is in the range of 200-300 nm denoting the preferred formation of small particles respect to large aggregates.

## 3.5.2 Spectroscopic analysis (FT-IR)

FT-IR spectra were acquired to study the final composition of the matrix and in particular to know if alginate and chitosan are still present in the final composition despite the several washes and treatments they are exposed. Analysis by Fourier

transform infrared (FT-IR) was performed on the final ionic alginate-chitosan system and on pure alginate and chitosan polymers. Considerations about the characteristic peaks of pure alginate and chitosan have been discussed in the previous paragraph. Here are reported only the results concerning the presence of characteristic peaks in the polymeric matrix obtained by ionic interactions (see figure 3.35). Pure alginate presents characteristic vibration peaks at 1610 $cm^{-1}$ and 1415 $cm^{-1}$ due to the carboxylate group (asymmetric and symmetric $CO_2^-$ stretching respectively). Other important bands are present at the wavenumber of 1322 $cm^{-1}$ due to the skeletal vibration of the saccharide structure and at 1091-1027 $cm^{-1}$ relative to asymmetric stretching of the C-O-C system. Pure chitosan instead displays characteristic strong peaks at 1631 $cm^{-1}$ and 1515 $cm^{-1}$: the band at 1631 $cm^{-1}$ due to the stretching C=O (amide I band) and band at 1515 $cm^{-1}$ probably due to N-H peak of amine overlapped to the amide II vibration. The spectrum of ionic alginate-chitosan system has the same appearance with only few differences. The peaks of alginate (1610 $cm^{-1}$ ) and of chitosan ( 1631 $cm^{-1}$) appear overlapped in an intense peak at 1630 $cm^{-1}$. In addition it is possible to see the formation of a new peak a 1739 $cm^{-1}$ due to carboxylic acid, suggesting that a little amount of alginate is present in a protonated state. The peak of pure chitosan at 1515 $cm^{-1}$ and of pure alginate at 1415 $cm^{-1}$ compare in a single peak at 1428 $cm^{-1}$. The addition of the two bands in fact explains the increment in intensity of the peak at 1428 $cm^{-1}$ respect to peak at 1631 $cm^{-1}$ (if we compare the intensity of peaks in pure polymers).

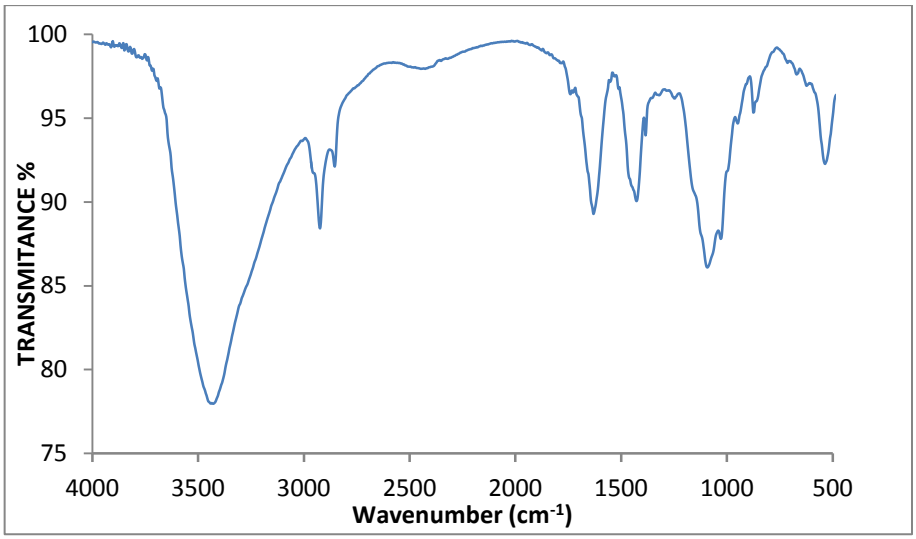


**Fig.3.35** FT-IR spectrum of alginate-chitosan ionic matrix after reaction.

## 3.5.3 Determination of particle morphology

The shape and morphology of the polymeric matrix were also studied with TEM and the images were compared with those obtained from covalent interaction in the nanoparticles described in the previous paragraph (see figure 3.17). The sample for analysis was prepared in the same condition used for the sample in presence of crosslinkers: uranyl acetate was used as contrasting agent. After air drying the sample was examined at the transmission electron microscope (TEM). The images obtained suggest that the polymeric matrix is not arranged in well shaped structures but at a first approach it appears as raw material. The presence of nanoparticles cannot be excluded, but, if present, they are entrapped in a continuous material so it is difficult to individuate them from the images (see figures 3.36, 3.37).

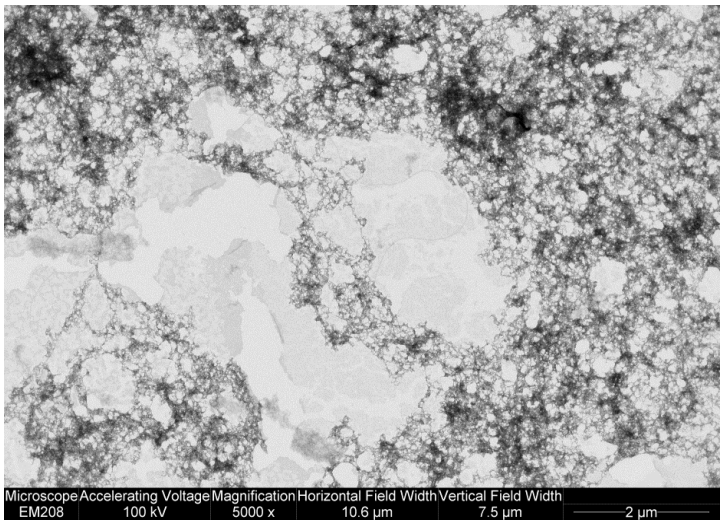


**Fig.3.36** TEM images performed on ionic alginate-chitosan sample.

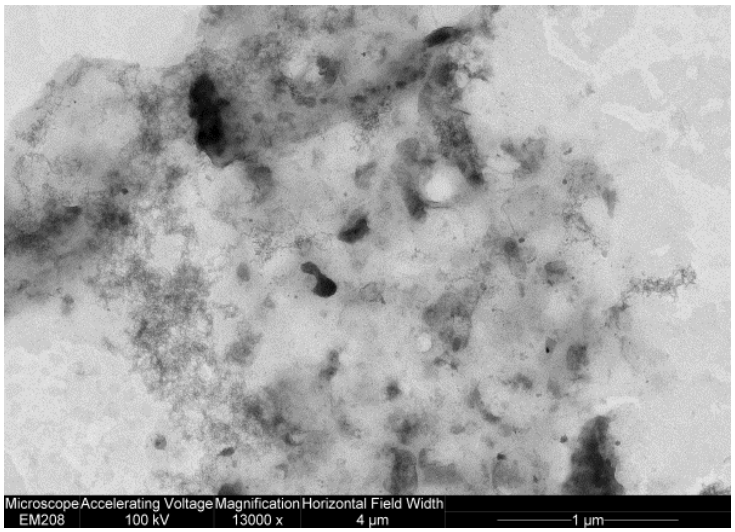


**Fig.3.37** TEM images performed on ionic alginate-chitosan sample.

At high magnification (see figure 3.37) of a restricted field, structures similar to nanoparticles with an irregular form, entrapped in the matrix can be identified. As discussed before, it is possible that electrostatic attraction between the oppositely charged groups in the polymers is limited to some portions of the polymer chains and other parts remain as loops of the single polymer giving less structured nanosystems. Moreover, the evaporation of the solvent can improve the tendency of material to shrink facilitating the formation of collapsed structures. So the first important

difference emerging between the two systems (covalent and ionic ones) is the lacking of well shaped and separated nanoparticles in the matrix.

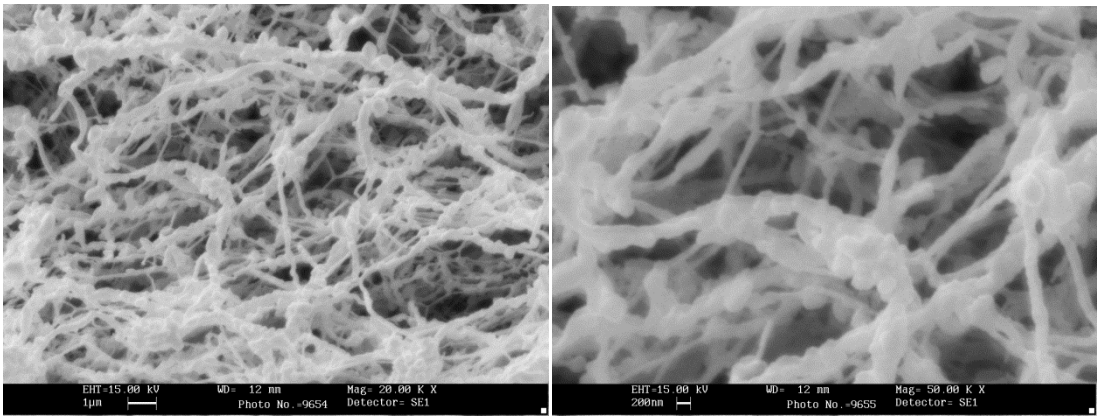


**Fig.3.38** SEM images of ionic alginate-chitosan nanoparticles.

The morphology of the system was investigated also with the scanning electron microscopy (SEM). SEM analysis of the sample validates the morphological aspect resulting from TEM. In the image (see figure 3.38) nanoparticles of 200-300 nm are visible as decoration of a filamentous network. Nanoparticles appear in a bunching state among polymer fibers. The average sizes of particles resulting from NTA is confirmed from the sizes of particles visible from SEM taking into account that these tools cause a general shrinking of the polymer material due to water evaporation.

### 3.5.4 Encapsulation properties of the nanoparticles: loading of resveratrol

Purified samples of ionic alginate-chitosan system were investigated for their ability to encapsulate hydrophobic nutraceutical resveratrol. The process of encapsulation followed the same procedure adopted for covalent cross-linked alginate-chitosan nanoparticles. The samples were prepared in triplicates at five dilutions in a fixed volume of 1 ml of final sample. Resveratrol was added in a fixed concentration of 0,5

mg/ml and after precipitation of the excess of resveratrol, the samples were centrifuged. Taking in account the problems of the relative high sizes of the nanoparticles, the samples were subjected to a intermediated speed of rotation of 10000 rpm. Then the supernatant was collected and analyzed at UV–Vis measuring the characteristic absorbance peak of resveratrol at 307 nm. For comparison a similar set of experiments using centrifugation at 10000 rpm was performed with the covalent crosslinked alginate-chitosan nanoparticles and the results are reported in figure 3.39.

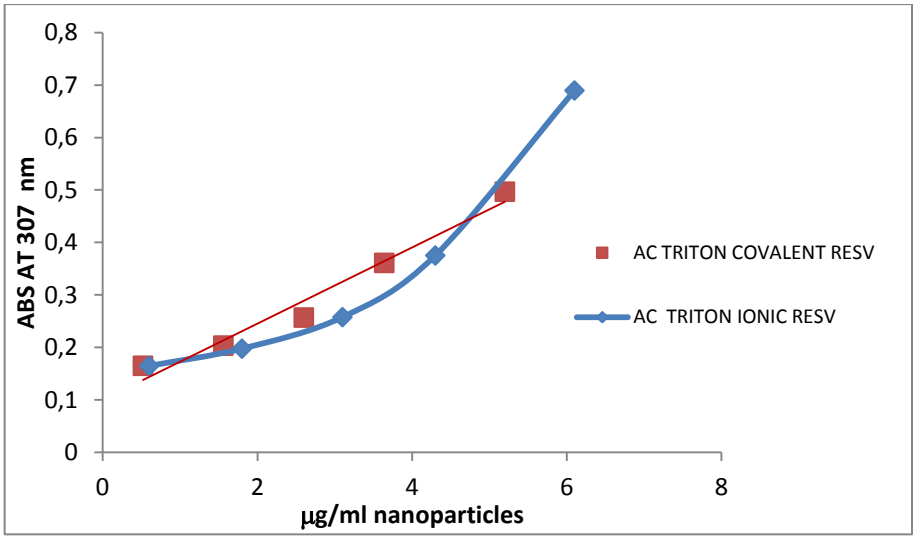


**Fig.3.39** Comparison of resveratrol absorbance between covalent and ionic alginate-chitosan samples (centrifuged at 10000 rpm).

In the case of the covalent crosslinked nanoparticles (red points) the amount of encapsulated resveratrol increases linearly with the concentration of nanoparticles in all the concentration range explored. If we compare these results with those reported in figure 3.23, which were obtained at a lower centrifugation speed (3000 rpm), it is evident that in this conditions the positive deviation from the linearity observed at high concentration disappears. This confirms the hypothesis that the observed higher encapsulation capacity was due to formation of nanoparticles aggregates which are removed by centrifugation at higher speed. On the other hand, in the case of the nanoparticles ionically bonded (blue points) a strong positive deviation from linearity at the highest nanoparticle concentration is still present, despite the centrifugation at 10000 rpm. Probably, in this case the amount of agglomerated material is much higher

respect to the covalent cross-linked nanoparticles as confirmed from the results of NTA, TEM and SEM and the centrifugation step is not sufficient to completely remove this material. As hypothesized for the crosslinked alginate-chitosan system, the aggregated nanoparticles are able to solubilize a higher amount of resveratrol thanks to chain entanglements between polymers and resveratrol. This phenomenon was also evidenced in studies about physical interaction between resveratrol and PLA.[191] On the other hand this system was not stable and loses resveratrol during time. The same phenomenon is observed also in our case. Figure 3.40 shows the evolution in time of the resveratrol content in the two systems under study measured at the highest concentration of polymers. While in the case of the covalent crosslinked nanoparticles the decrease of the concentration of resveratrol in five days is very small, the ionic system loses very quickly a high amount of resveratrol reaching after six day a plateau value smaller than that observed with covalent crosslinked nanoparticles. This rapid loss of resveratrol is indicative of a fast precipitation of the matrix and of the entangled resveratrol or of a weaker interaction of resveratrol with the network possibly due to the high porosity of alginate and to the presence of single polymer chains. In any case, however the trapping efficiency of the two systems are not very different.

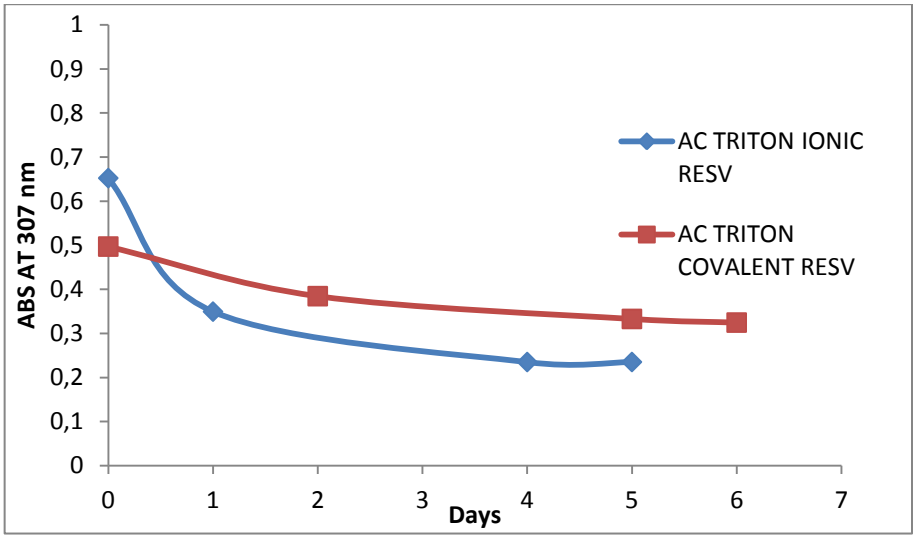


**Fig.3.40** Evolution of the absorbance at 307 nm for the highest concentrated sample (centrifuged at 10000 rpm) of covalent and ionic nanoparticles during the time.

### 3.5.5 Effect of salt concentration on the size of alginate-chitosan nanoparticles

The last aspect we have investigated to evaluate differences between ionic and covalent crosslinked manufactured nanoparticles, regards their behavior if exposed to an increasing concentration of salt. The experimental setup was optimized in presence of NaCl. A low concentration range of salt was explored to individuate possible differences in a little interval of concentration. The effect deriving from the addition of salt to a polymer solution is an aspect largely studied for the determination of the physico-chemical properties of a polyelectrolyte solution. In fact as referred in the chapter describing alginate and chitosan, the addition of salt reduces the intrinsic viscosity of polyelectrolytes. The presence of charges of the same type on the polymer chain determines an expansion of the chain due to the repulsion between nearby charges. Increasing the ionic strength, repulsion is screened, leading to a reduction of the volume occupied by polymer. Some reports suggest that the addition of salt such as NaCl on alginate and chitosan ionic complexes has a low influence on the interaction between polymers.[192] The effect on particle size (see figure 3.41) after addition of different concentrations (10, 20, 50 mM) of NaCl to ionic and covalent crosslinked systems is different. In ionic alginate-chitosan nanoparticles (green track), the addition of salt seems initially to increase the attraction between polymers thanks to a screening effect that reduces the expansion of the chains, but after a "critical" concentration value the interaction between polymers became weaker and particle size increases. This may be due to a competition of the salt for the available binding sites on the two polymers which decreases their interaction leading to the formation of larger particles. On the other hand, the covalent crosslinked nanoparticles (violet track) show a small gradual increment of sizes with the concentration of added salt. This suggests that the covalent crosslinking reinforces the network making the nanoparticles less sensitive to the added salt.

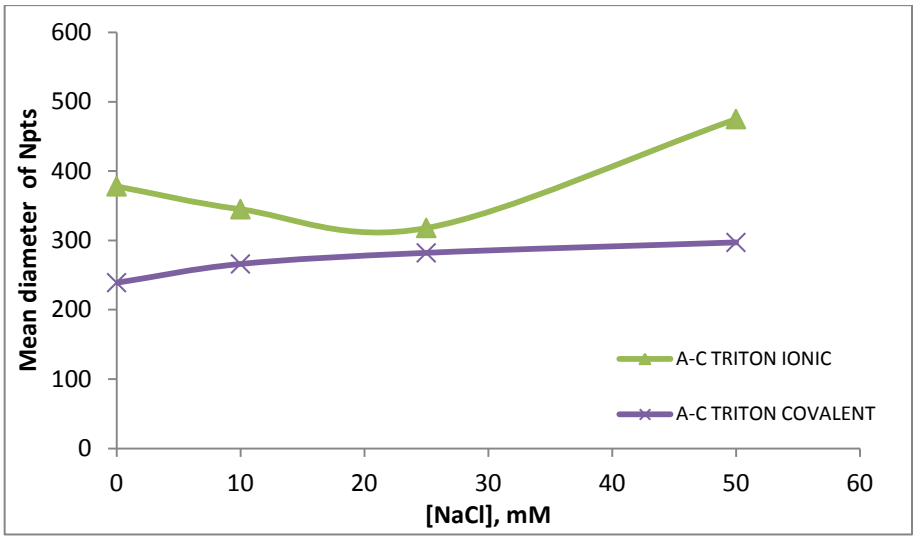


**Fig.3.41** Change in particle size after addition of NaCl on covalent and ionic alginate-chitosan nanoparticles. The sizes have been calculated considering as mean diameter the value referring to the 90% of the total particle population.

## 3.6 Alginate-chitosan nanoparticles: preparation using Tween 80-Span80 as emulsifying agents for W/O nanoemulsion

The difficulty met in purification of the nanoparticle suspension from the residues of Triton X-100 and the need to found a stable formulation for alginate-chitosan nanoparticles, led us to an examination of other possible emulsifying agents. At first, different attempts were made using Span 60 in vaseline, but the resulting solution was viscous and difficult to process. Other attempts were addressed in formulation of systems in presence of paraffin oil and Span 80 but the emulsions were milky and not transparent meaning that the water droplets were very large. After many efforts failed for the viscous behavior of mineral oil we decided to maintain cyclohexane as continuous phase. In fact, despite problems related to toxicity, cyclohexane is easily removed and forms stable W/O nanoemulsions. The emulsifying agent was instead changed. Generally a blend of emulsifying agents has the advantage respect to a single one to an easy tuning of the final HLB by modulating the proportion between the blend components. Moreover a blend of emulsifiers provides a better solubilization of water and a prolonged stability [193] of the emulsion. So the investigation was

addressed toward series of Span and Tween. After several attempts a blend between Tween 80 and Span 80 was selected. These emulsifying agents are well known for their characteristics of biocompatibility, good stability and poor toxicity. They are approved for pharmaceutical and food use and found application in several fields. Span 80 (see figure 3.42, left) is a sorbitan mono-oleate which behaves as a viscous emulsifier able to form W/O emulsion with an HLB of 4,3.

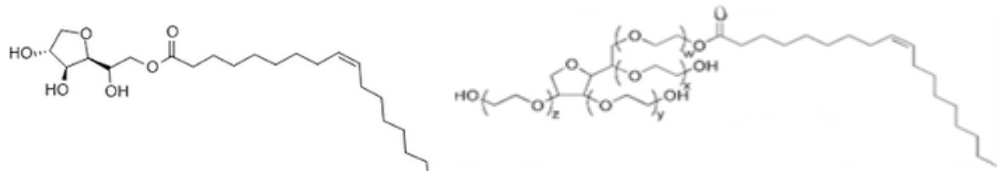

**Fig.3.42** Left: structure of Span 80. Right: structure of Tween 80.

Tween 80 instead, is a polyoxyethylene derivative of sorbitan functionalized with an oleic acid chain. The number of the oxyethylene moieties in the different chains may vary but the sum x+y+w+z = 20 (see figure 3.42, right). Tween 80 has an HLB of 15 and thus an hydrophilic behavior favoring the formation of O/W emulsions.

A blend of these two emulsifying agents is generally used to form both O/W and W/O emulsions. In particular we are interested in the formulation of a stable W/O nanoemulsion. We, therefore, started to explore the behavior of emulsifiers, using different ratios of emulsifying agents and observing the type and stability of the emulsion formed. To investigate the dispersion of water in the system, the aqueous phase was added slowly to oil phase containing the blend of surfactants according to the titration method.[194] The selected ratios tested between Tween 80 and Span 80 were 5:5, 1:9, 3:7, 7:3 and 6,5:3,5. In these conditions different phenomena have been observed: formation of gel, creaming, instability of emulsion, milky aspect. In particular, during the optimization of the emulsion composition we investigated the region of W/O nanoemulsion in proximity to a low value of emulsifying agent to simplify the consequent step of purification from surfactant. After many attempts the final ratio chosen was Tween 80/Span 80 6,5:3,5 which ensures the formation of a stable clear emulsion. The HLB of Tween 80 is 15 and so it gives a contribute of 9,7 to

the total HLB. Instead Span 80 has a HLB of 4,3 meaning that its contribute to the final HLB is 1,5. The relative high amount of Tween 80 needed to formulate the emulsion can be explained with the high solubilization capacity of this emulsifying agent that is classified as a strong solubilizer for water.[193] The final 11,3 HLB value is close to that required for cyclohexane (HLB= 10). Indeed, a good match between the HLB of the continuous phase (cyclohexane in our case) with the HLB of the emulsifying agents increases the possibility to formulate a stable emulsion.

The final composition between oil/emulsifiers/water emerging after titration and optimization using the phase diagram is 83/10/7 which corresponds to the black point in the nanoemulsion region (see figure 3.43, left).

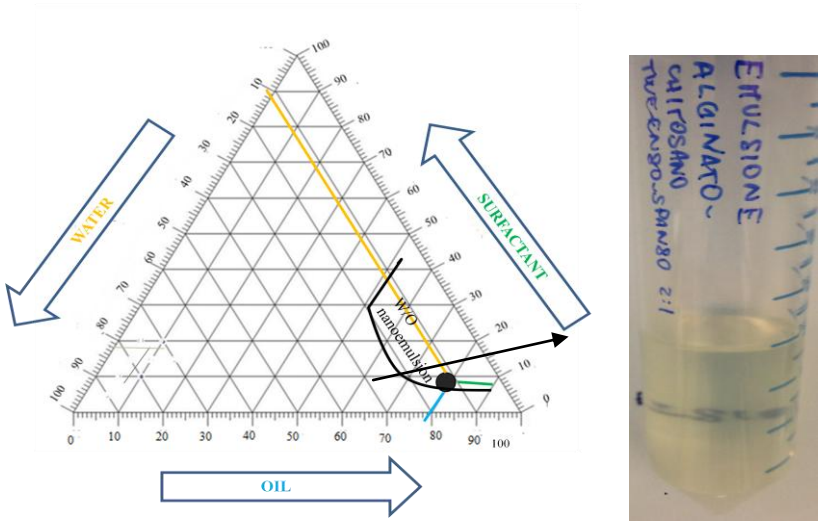


**Fig.3.43** Left: best ratio of components selected (black point). Right: final aspect of emulsion prepared referring to the phase diagram.

The established protocol for the formation of the emulsion (see figure 3.44 ) is slightly different respect to the one used for the emulsion with Triton X-100. In particular the process starts with the addition of the external phase in a becker. Then the emulsifying agent is added in the proportion indicated. The aqueous phase at pH 5 containing the polymer (chitosan) in a concentration of 0,5 (w/v) is finally added dropwise and the system was left under stirring for 48 h. A transparent yellowish solution is observed at the end of the process (see figure 3.43, right). If the solution

shows still opalescence some droplets of emulsifiers blend may help to turn the emulsion towards the transparency.

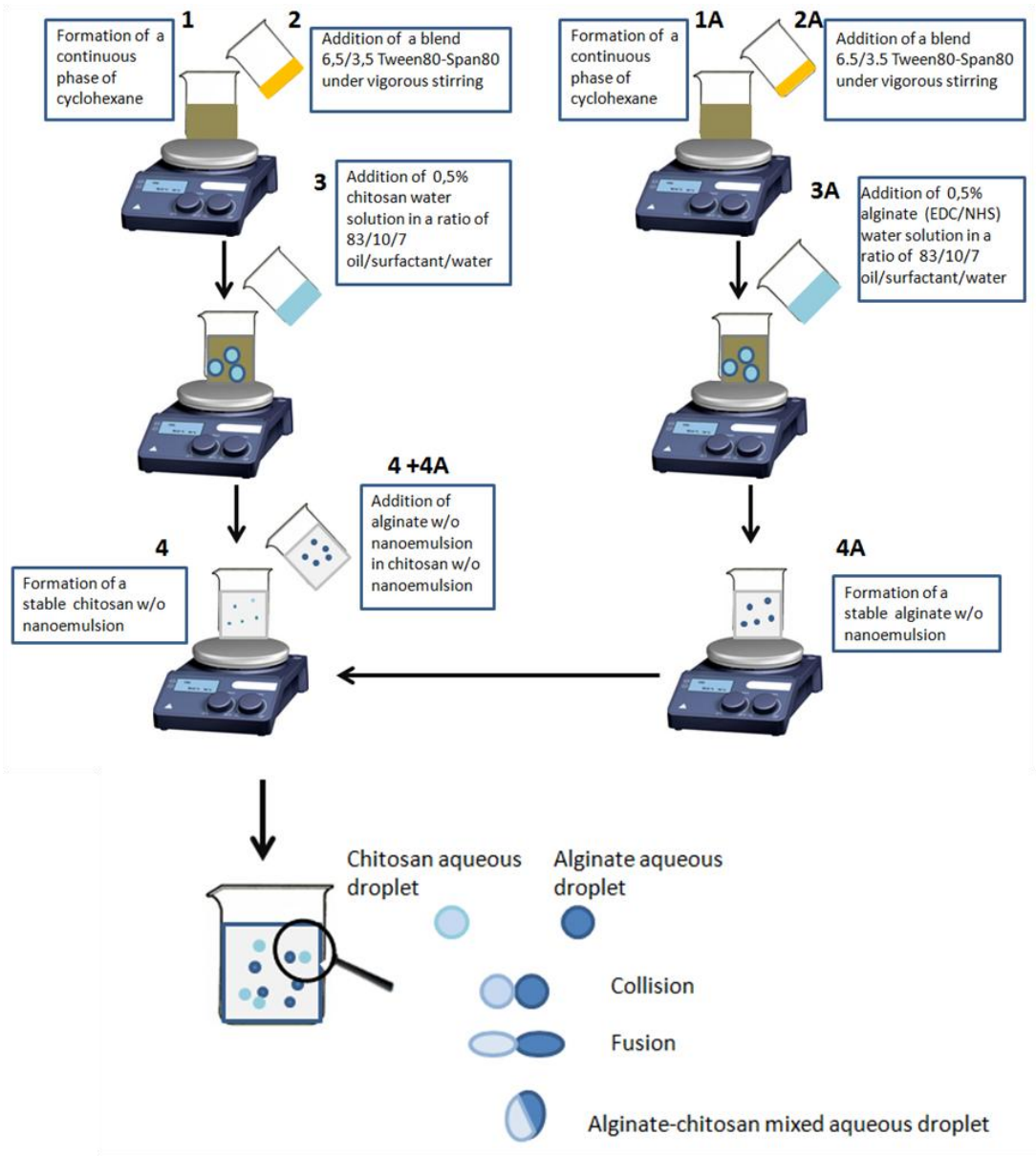


**Fig.3.44** Schematic representation of the protocol used to form alginate-chitosan nanoparticles in w/o nanoemulsion using Tween80-Span80 as emulsifying agents.

The same procedure was followed for the preparation of the emulsion containing alginate and the crosslinkers EDC/NHS preventively mixed to activate the carboxyl groups of alginate. Briefly after addition of the blend of Tween 80-Span 80 to the continuous phase, the aqueous phase containing alginate at the concentration of 0,5

(w/v), 26 µl of EDC at the concentration of 3,5 $10^{-3}$ mol/ml and 10 µl of NHS at the concentration of 2,03 $10^{-3}$ was added dropwise. Once the two emulsions were prepared, the alginate emulsion was poured drop by drop in the chitosan emulsion and the final system left to react under stirring for 48 h. During this time the droplets of the emulsions have sufficient time to collide and merge thus enabling the reaction between alginate and chitosan to occur. In the final emulsion the concentration of the two polymers in the water phase was 0,25 w/v and EDC/NHS were in large excess respect to the concentration of carboxylate groups of alginate.

Elapsed the reaction time, the emulsion was treated with acetone to precipitate the polymers. The polymeric pellet was suspended in water and re-precipitated for 5 times to ensure the complete removal of the organic solvent and surfactants. After the last wash, the polymer matrix was dried under $N_2$ flux to remove residues of acetone and then resuspended in water and treated with Amberlite AD2 resin to remove completely any traces of organic components and surfactants still present. During the purification we discovered that the resin has a better capability to adsorb Triton X-100 rather than Tween80 –Span80 , so the sample needed more washing steps (4-5) before to be purified. In any case the emulsifying agents used in this preparation are not toxic and approved in food products. Also in this case the removal of emulsifiers and acetone was checked by UV-Vis spectrometry (see figure 3.45).

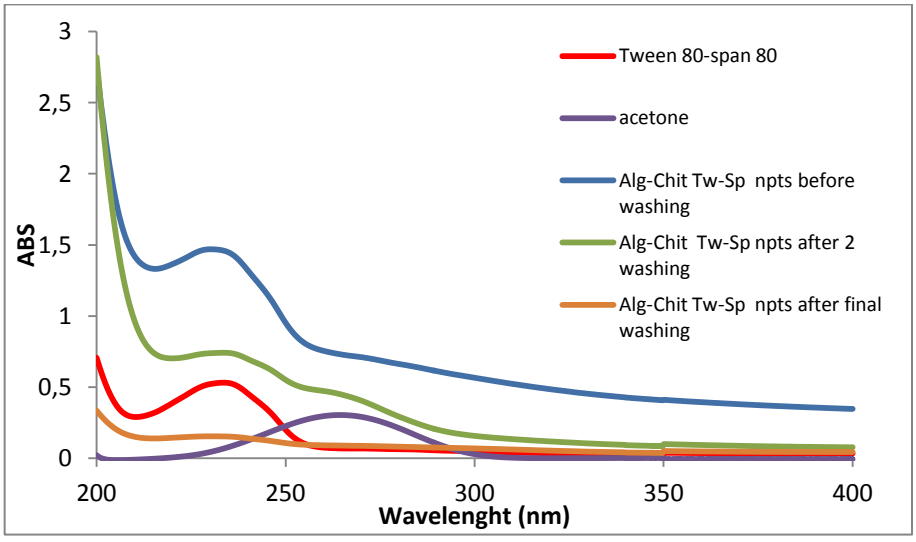


**Fig.3.45** UV-Vis spectra of water solution of Tween80-Span80 mixture, acetone and nanoparticles suspension before and after treatment with Amberlite AD2.

The graph displays the proceeding of the purification of the sample. Tween80-Span80 blend present a maximum absorption at 230 nm (red track) and acetone has a broad band at 265 nm (violet track). The sample before the washing with Amberlite AD2 (blue track) displays both the peaks relative to surfactants and acetone. After two washing steps the amount of impurities decreases (green track) and after five washing steps (orange track) the sample is completely purified and ready for further investigation and characterization.

### 3.6.1 Determination of particle size and stability

Sizes of the purified sample suspended in water were measured with NTA directly after loading the sample in the chamber. All the measurements were performed at ambient temperature. The nanoparticle diameter distribution profile of the sample is shown in the figure 3.46. All the curves are the averages of three independent measurements.

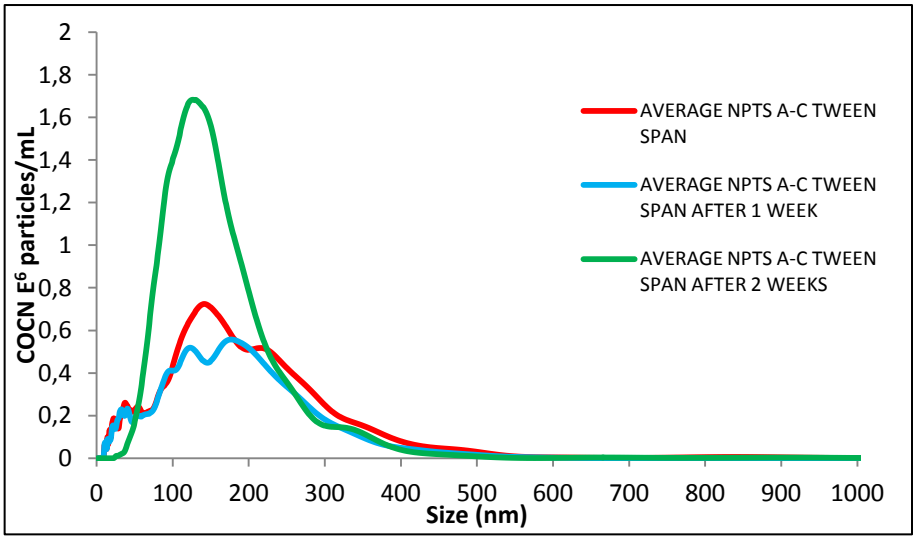


**Fig.3.46** Diameter distribution curves measured for the same sample after 1 and 2 week of aging. Each curve is the average of three independent measurements.

The curve recorded on fresh nanoparticle sample (red track) shows a monodisperse nanoparticle population with a mean diameter of about 180 nm ($\sigma$= ± 54). As in the case of the sample prepared with Triton X-100, the stability of the preparation was analyzed investigating the size changes over the time. In fact, changes in particle size

can be a valid method to detect instability of the sample (aggregation, degradation). The sample stored at ambient temperature, and analyzed after one week (blue track) shows slight changes in particle distribution while a small reduction of size becomes apparent after two weeks of aging (green track). The evident higher concentration of the sample aged two weeks is due to a different dilution of the suspension but the shape of the curve is almost the same as the other ones. As a conclusion, the sample appears stable when stored for 14 days without relevant changes in the nanoparticle size distribution. The stability and homogeneity of the sample was also investigated after centrifugation. In fact if aggregated nanoparticles are present, the centrifugal force accelerates their precipitation. So freshly prepared sample was centrifuged at 10000 rpm for 10 minutes and the supernatant was examined with NTA (see figure 3.47).

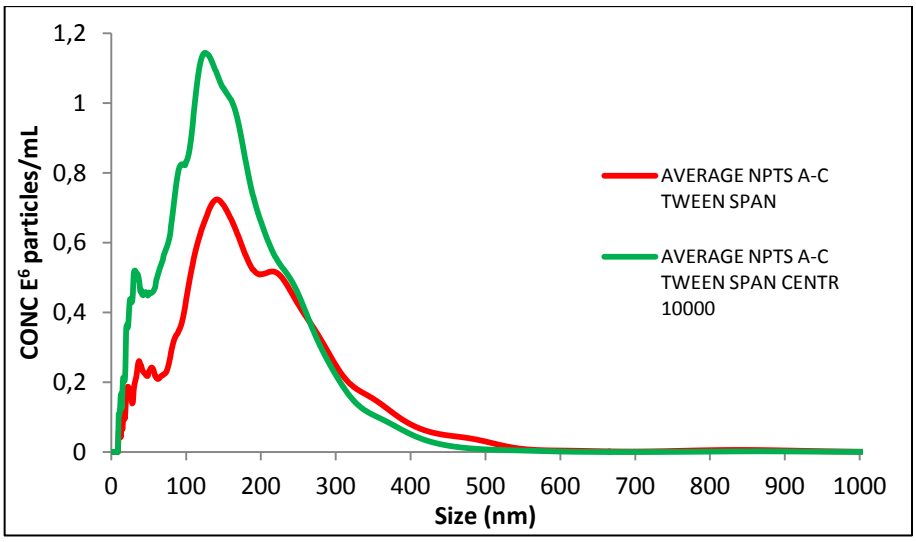


**Fig.3.47** Average size of nanoparticle measured using NTA before and after centrifugation.

Figure 3.47 shows the diameter distribution for the nanoparticle population before (red curve) and after centrifugation (green track). Apart from the different absolute intensity due to different dilution of the samples, the shape of the two curves are very similar. This confirms the good stability of the sample prepared with Tween80-Span80 and indicates that only a little amount of aggregated nanoparticles is present.

The nanoparticle samples prepared using Tween80-Span80 were also investigated using DLS, another useful tool very popular in sizes characterization, in order to validate the results gained from NTA.

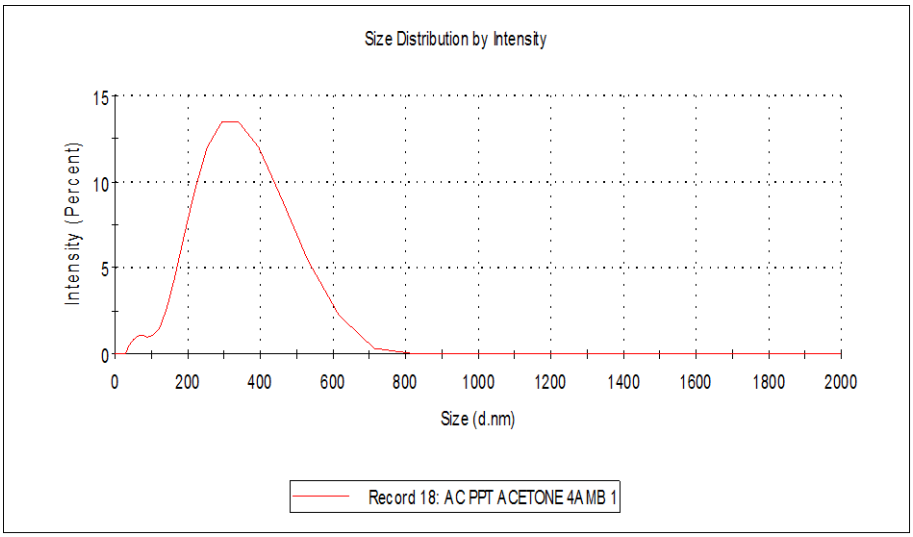


**Fig.3.48** DLS measurements on alginate-chitosan nanoparticles obtained from w/o nanoemulsion.

The results of DLS analysis (see figure 3.48) when compared with those of NTA show a similar trend of diameter distribution with a slightly broader distribution and a larger polydispersity. Also the mean diameter is slightly shifted to higher value (300 nm).

## 3.6.2 Spectroscopic analysis (FT-IR)

FTIR analysis represents a valid spectroscopic aid to evaluate possible interactions between pure alginate and chitosan after the reaction and to confirm the presence of both the polymers in the final composition of the nanoparticles. Sample was analyzed in form of pellet prepared mixing the lyophilized sample with KBr salt. The recorded spectrum (see figure 3.49) was then compared with spectra of pure alginate and chitosan. The tables 3.1 and 3.2 reported in the previous paragraph show the typical bands and relative attributions of pure chitosan and alginate.

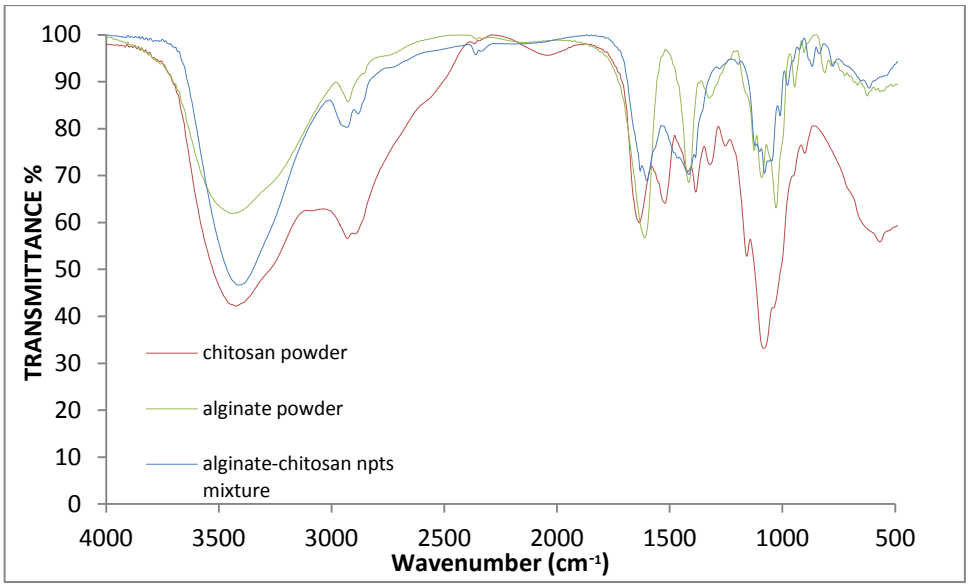


**Fig.3.49** Comparison of FT-IR spectra obtained from alginate and chitosan powder and alginate-chitosan covalent matrix after reaction using tween80- span80 as emulsifying agents.

Alginate-chitosan sample (blue track) presents a broad peak relative to O-H and N-H in the interval of 3500-3100 $cm^{-1}$. Bands due to CH stretching are also present in the range 3000-2800 $cm^{1}$. The typical bands of chitosan (red track) and alginate (green track) at 1631 $cm^{-1}$ and 1610 $cm^{-1}$ respectively appear in a single splitted peak. Also in this case the peak relative to the amine functions (1515 $cm^{-1}$) of chitosan is not present possibly for its involvement in the reaction with alginate. The peaks related to the skeleton of ring at 1160-1020 $cm^{-1}$ are instead present in the final polymeric nanoparticles. The analysis confirms that alginate and chitosan are both present but doesn't give direct information about the possible formation of the amide bond between the carboxyl groups of alginate and the amine functions of chitosan. Further attempts to obtain the desired information from NMR analysis failed due to the low solubility of the sample in the different solvents tested.

### 3.6.3 Determination of particle morphology

Further information about sizes and shape of the nanoparticle samples has been acquired from TEM analysis. TEM is a tool enabling a direct imaging of nanomaterial offering the possibility to obtain quantitative information on the size and morphology of the nanoparticles. A good image quality depends on the contrast of the sample related to the background. In our case sample has been contrasted using uranyl acetate, after that a droplet of the sample has been deposited on a copper grid coated with a thin carbon layer and allowed to evaporate.

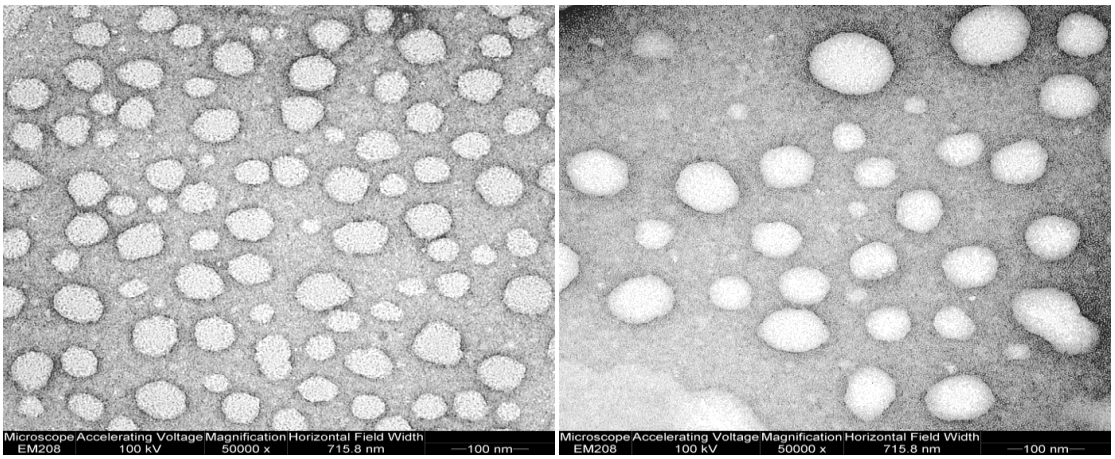


**Fig.3.50** TEM images of covalent alginate-chitosan nanoparticles at high magnification.

Digital images of the sample (see figure 3.50) show spherical nanoparticles, with a regular shape. Particles analysis is not complicated by the presence of aggregated material and the mean diameter was measured for all the particles in the image. The distribution profile of nanoparticles was obtained measuring each particle diameter using Digital Micrograph analyzer and the data were processed to obtain histogram of particle size distribution.

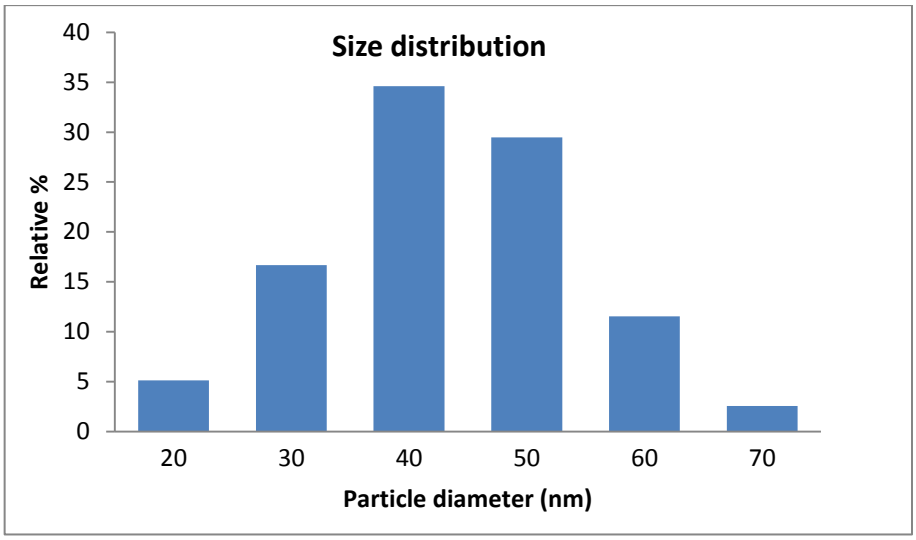


**Fig.3.51** Size distribution of particle measured with Digital Micrograph program

The resulting data (see figure 3.51) show a monodisperse profile of particle diameters with a maximum at 40 nm and a mean diameter value of 48 nm ($\sigma$= ± 11 nm). The mean diameter shows a large difference compared to the value of 200-300 nm resulting from NTA and DLS. However, in general, sizes measured by TEM are smaller than those obtained from NTA and DLS. This difference is due to the fact that DLS and NTA measure the hydrodynamic radius of the nanoparticles while TEM measures the projected area diameter of particles in a dry state. Results presented by other investigators on alginate-chitosan nanoparticles report similar discrepancy between data acquired with these techniques.[195]

### 3.6.4 In vitro toxicity test: MTT assay

Alginate and Chitosan are safe and biocompatible polymers largely employed in food and pharmaceutical fields. However, during the manipulation they can undergo modification respect to native state and the presence of residual reactants can cause toxicity. To evaluate an eventual toxic action, several technique are reported from literature thus generating a great variability of parameters to analyze. MTT assay is a popular method adopted at this purpose. MTT is a useful assay for the measurement of cell proliferation. As model cells to perform MTT assay we have selected Caco-2 cells (human epithelial colorectal adenocarcinoma cells, as a model of intestinal epithelium).

MTT is a yellowish probe converted to water-insoluble MTT-formazan of dark purple color by mitochondrial dehydrogenases of living cells. The intensity of purple color is measured colorimetrically at a wavelength of 570 nm.

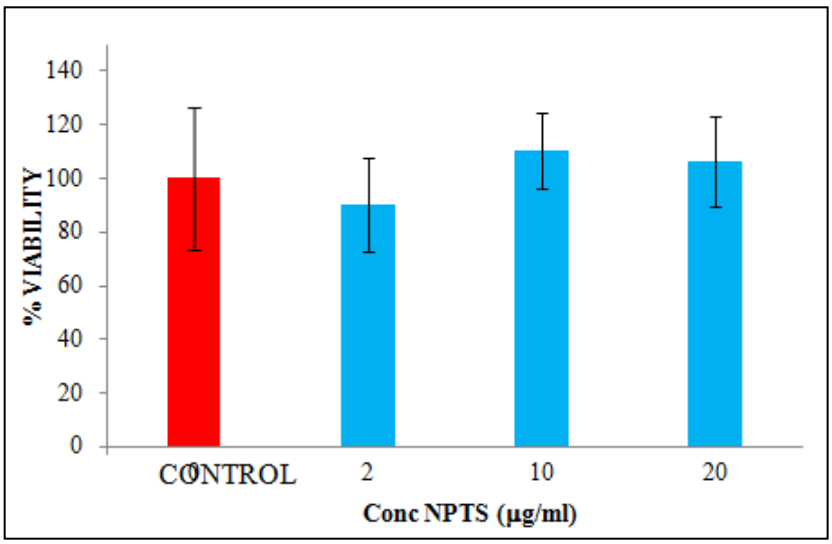


**Fig.3.52** Histogram relative to % viability of Caco-2 cells after exposition to different concentration of alginate-chitosan nanoparticles

If nanoparticles show toxicity, they interfere with the normal metabolic process of the cell, thus the conversion of MTT in MTT formazan decreases. Before the experiment, nanoparticles were filtered with 0,2 µm sterile filters to ensure sterility and 1 ml of filtered suspension was lyophilized and the residue weighed to know the amounts of polymer (20 µg/ml). Then three different dilutions of the sample (see figure 3.52) were introduced on a 96 well plate in presence of Caco-2 cell and after one day of incubation MTT was added to estimate the activity of the cell. All samples (blue) were evaluate in triplicate including a positive control (red). No evidence of citotoxicity is visible from the plotted results and a viability of about 100% of cells is reported for all the concentrations analyzed.

### 3.6.5 Encapsulating properties of nanoparticles

The investigation of encapsulating properties of alginate-chitosan covalent carriers represents part of the scope of this Thesis. The growing interest in nanotechnology is justified from the high advantages offered by nano sized carriers. The primary milestone during the manufacturing of nano carriers is the demonstration of their ability to retain and release bioactive drugs. The main interest in our case is to demonstrate the entrapment of nutraceuticals of interest in cardiovascular related diseases.

#### 3.6.5.1 Loading of resveratrol

As in the case of the nanoparticles described in the previous paragraph we investigated the encapsulation of resveratrol in our carriers once the nanoparticles have been purified from organic residues. This reduces an eventual loss of the bioactive molecule during purification. Resveratrol can establish several hydrogen bonds (for the presence of the phenolic hydroxyl groups) and thus it can form H-bonded complexes with alginate and chitosan. Moreover chitosan bears an acetylated portion that offers a hydrophobic site for the binding of lipophilic molecules. Following the protocol described in the previous chapter, in the experimental quantification of resveratrol in nanoparticles at the beginning a lower speed of rotation in the centrifugation of the samples was selected to avoid precipitation of polymers. In particular five concentrations of nanoparticles were prepared in a fixed volume of 1 ml and the same amount of resveratrol was added to each sample (final concentration 0,5 mg/ml) and after centrifugation the amount of resveratrol remained in the supernatant was determined spectrophotometrically. The results are reported in figure 3.53 where each point represents the average value of three independent measurements with relative standard deviation. From the graph is possible to observe that increasing the concentration of nanoparticles the amount of solubilized resveratrol increases well above the solubility limit in water. As in the case before, the correlation between concentration of nanoparticles and solubilized resveratrol is linear

for the first part of the graph (four points) and deviates positively at the highest concentration explored (black point). This higher value of entrapped resveratrol, is probably due to an increased interaction between resveratrol and polymers matrices which at the highest concentration form some kind of aggregates. However, this resulting entangled network of resveratrol-matrices is not stable and collapses during time as can be seen from the decrease in resveratrol concentration observed during time (see figure 3.54). The estimated value of resveratrol entrapped in nanoparticles corrected of the value deriving from the water soluble fraction of resveratrol is of 1,87 μg per 1 μg of nanoparticles.

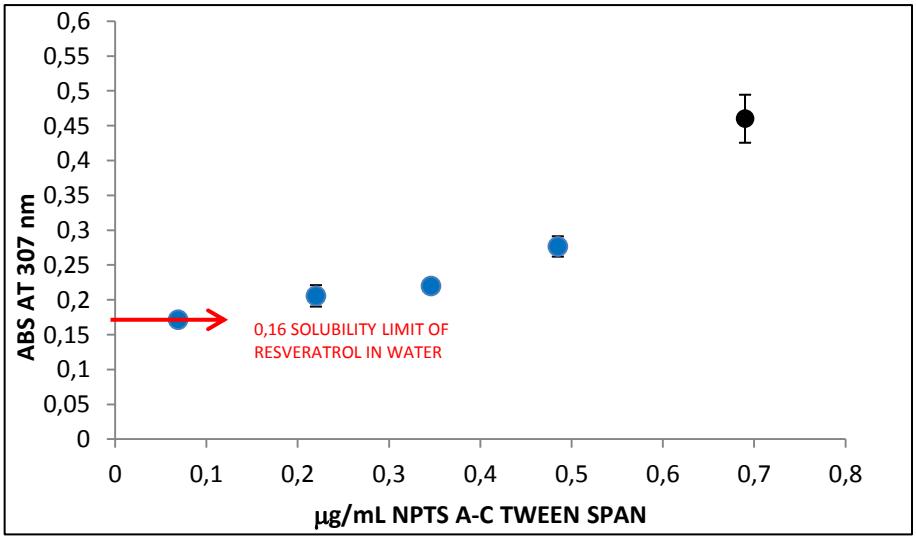


**Fig.3.53** Absorbance of resveratrol at different concentrations of alginate chitosan nanoparticles.

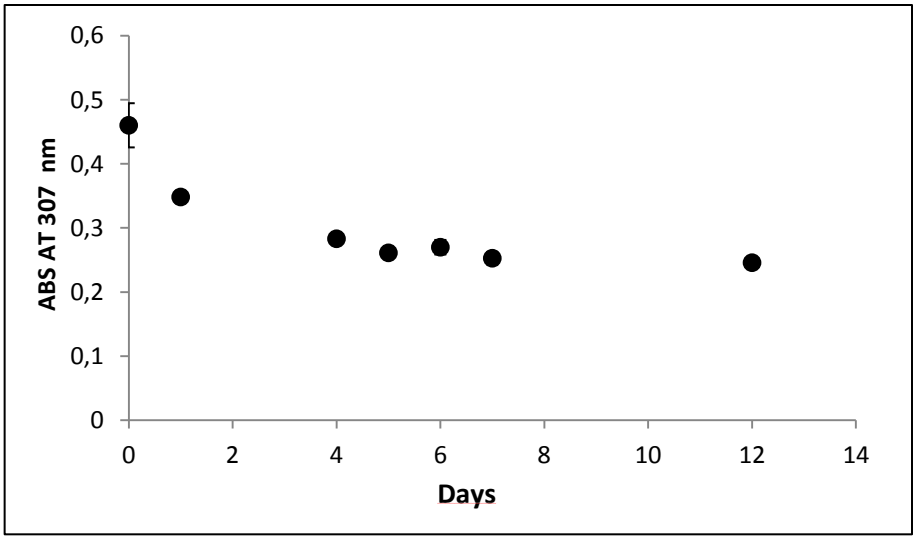


**Fig.3.54** Evolution of the highest concentrated sample (black point figure 3.53) during time.

If the samples are centrifuged at an intermediate speed value (10000 rpm) the correlation between concentration of nanoparticles and solubilized resveratrol becomes linear for all the concentration investigated (see figure 3.55, left) and the samples are stable for at least 10 days as shown in the right panel of figure 3.55 for the sample at the highest concentration of nanoparticles.

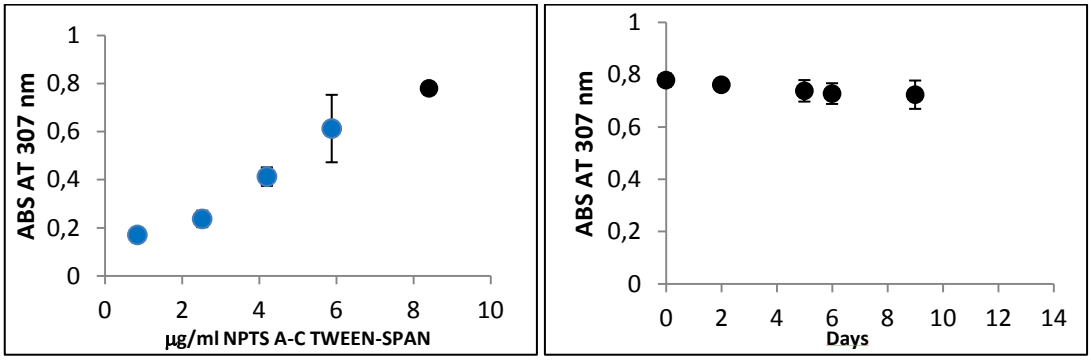


**Fig.3.55** Left: linear trend for all concentrations of A-C nanoparticles entrapping resveratrol (centrifuged at 10000 rpm). Right: stability during time of the highest concentrated sample (black point).

The described results underline the capability of alginate-chitosan nanoparticles manufactured from W/O emulsion in presence of Tween 80-Span 80 to encapsulate resveratrol.

### 3.6.5.2 Loading of quercetin

To study the encapsulation of quercetin with the alginate-chitosan nanoparticles the procedure optimized and described in the previous chapter was used. In brief, five concentrations of alginate-chitosan nanoparticles were prepared in 1,3 ml of water solution. Then an excess quercetin at a fixed concentration (0,5 mg/ml) was added to all the samples. Samples were left at ambient temperature for 24 h to enable the total precipitation of quercetin and centrifuged at an intermediate speed rotation (10000 rpm). Then the concentration of quercetin solubilized in the supernatant was determined using UV-Vis spectroscopy. The resulting data are plotted in figure 3.56.

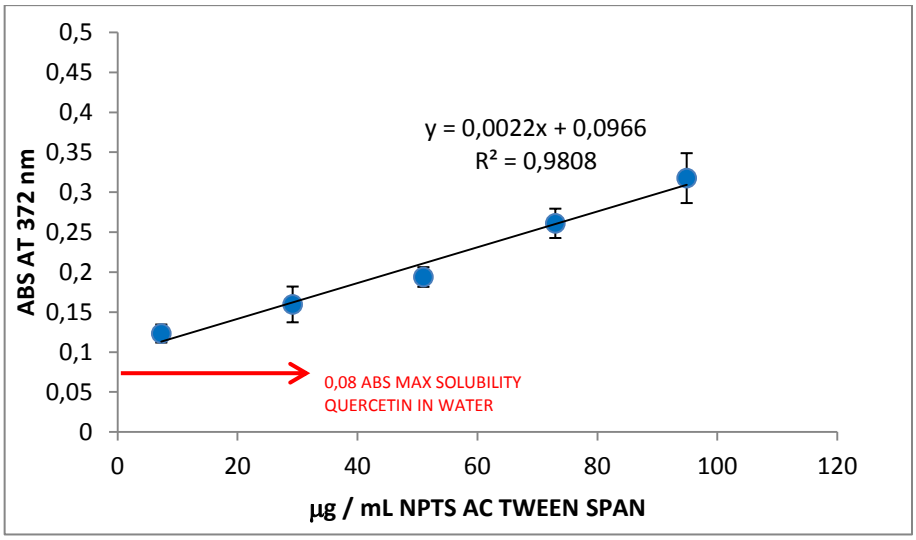


**Fig.3.56** Increasing concentration of quercetin at increasing concentration of alginate-chitosan nanoparticles.

The graph shows a linear trend between concentration of nanoparticles and solubilized quercetin for all the samples prepared with a good R value. Moreover all the concentrations of nanoparticles are able to dissolve quercetin over its solubility limit thus improving its water solubility.

### 3.6.5.3 Stability of quercetin in nanoparticles and protection from oxidation

The above samples were observed during time and a variation of the quercetin spectrum was observed. Indeed, the characteristic peak of quercetin decreases gradually until to disappear while a new peak appears at a maximum wavelength of 330 nm. As described before, the phenomenon is associated with the oxidative process of quercetin to quinone form (process and structures involved are reported in figure 3.32).

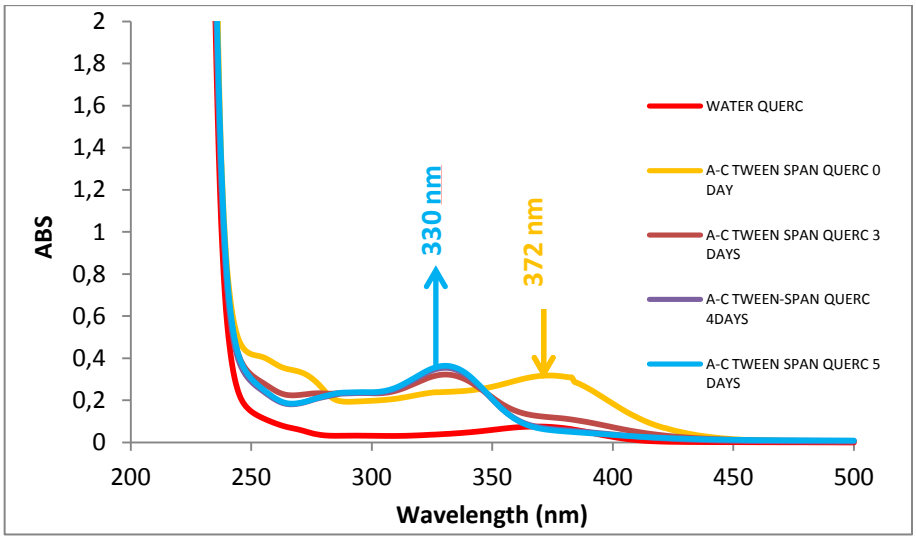


**Fig.3.57** Evolution of absorbance of the highest concentration (95 μg/ml) of alginate-chitosan nanoparticles during time.

Figure 3.57 shows the disappearing of the characteristic peak of a quercetin loaded sample (95 μg/ml of alginate-chitosan nanoparticles) at 372 nm (orange track) and the increment of intensity of the peak at 330 nm relative to an oxidized state of quercetin (blue track). The progress of the conversion of the reduced form into an oxidized state is reported in figure 3.58 showing the decay of the signal at 372 nm (left) and the increasing absorbance of the peak at 330 nm (right). As observed before, this oxidation process is not observed in quercetin stored in water ad ambient temperature (see figure 3.29).

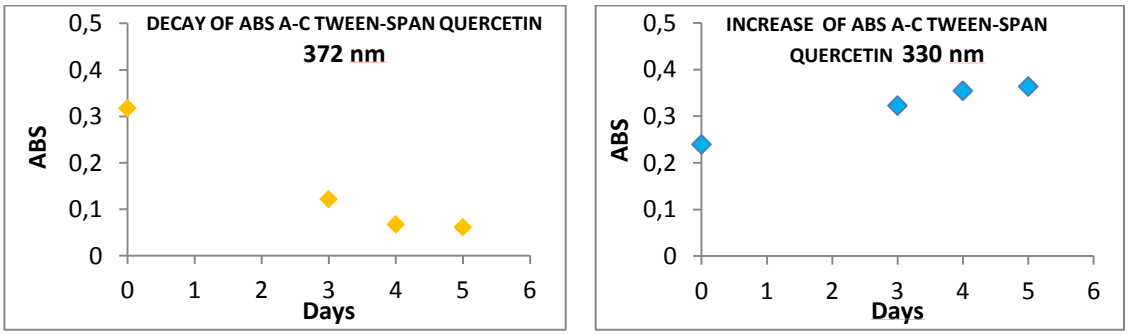


**Fig.3.58** Left: decay of absorbance peak at 372 nm during time of the highest concentrated sample (95 μg/ml). Right: increase of absorbance at 330 nm during time of the same sample.

Quercetin in the quinone form loses its antioxidant activity and therefore this process is unfavorable for a potential use of the nanoparticles as nutraceutical carriers. However, also in this case addition of ascorbic acid protects quercetin from the spontaneous oxidation as shown in figure3.59.

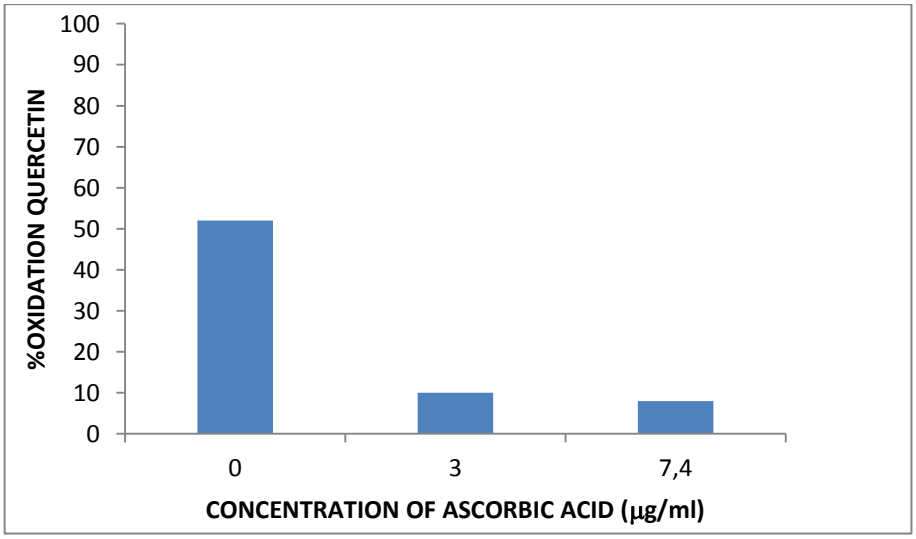


**Fig.3.59** Prevention of quercetin oxidation, adding different concentration of ascorbic acid.

Addition of ascorbic acid to alginate-chitosan nanoparticles (concentration 95 μg/ml) revealed a very useful approach to prevent the oxidation of the encapsulated quercetin. In fact as is possible to see from the graph, the percentage of oxidized quercetin decreases substantially in presence of ascorbic acid. The two concentrations of ascorbic acid explored (3 μg/ml and 7,4 μg/ml) show a similar capacity to prevent oxidation.

## 3.7 Alginate-chitosan nanoparticles: preparation without crosslinkers using Tween80-Span 80 as emulsifying agent for W/O nanoemulsion

Ionic alginate-chitosan nanoparticles were prepared also in emulsion with Tween 80-Span 80 following the protocol reported above but for the absence of the crosslinkers EDC/NHS. The procedure adopted for the preparation of the nanoemulsion (in

presence of Tween 80-Span 80) is identical both with and without crosslinkers. Briefly a W/O nanoemulsion was prepared adding drop by drop 2 ml of Tween 80-Span 80 mixed in proportion 6,5:3,5 to 8 ml of cyclohexane followed by 0,32 ml of a 0,5 % water solution of chitosan. In the meantime an identical emulsion was prepared using a 0,5 % aqueous solution of alginate. Finally the alginate emulsion was added to the chitosan emulsion. The resulting mixed emulsion was kept under stirring at ambient temperature for 48 h. The polymers were then precipitated by addition of a volume of acetone equal to the final volume of emulsion followed by centrifugation at 10000 rpm for 10 minutes. The pellet was resuspended in water and precipitated with 5 ml of acetone for further 4 times. After the last precipitation, the pellet was hydrated in water and sonicated for 15 minutes. The nanoparticles suspension was then washed with Amberlite AD2 for several times checking the complete removal of organic solvents and surfactant at the UV Vis. At the end of the washing procedure, the sample is ready to be analyzed.

### 3.7.1 Determination of particle size

Particle size was analyzed by NTA (see figure 3.60). The size distribution profile of the ionic alginate-chitosan nanoparticles is similar respect to that obtained for the sample prepared using the crosslinkers (see figure 3.47). Centrifugation of the sample at 10000 rpm has not a strong effect on the size distribution although there is a small increment in the number of larger particles (400-500 nm) compensated by an analogous increment of the particles with diameters within 100-200 nm. Therefore at difference to what observed in the case of Triton X-100 (see above) in this case the samples obtained with or without using EDC/NHS behaves very similarly suggesting that the nanoparticles formed by simple ionic interaction are relatively stable.

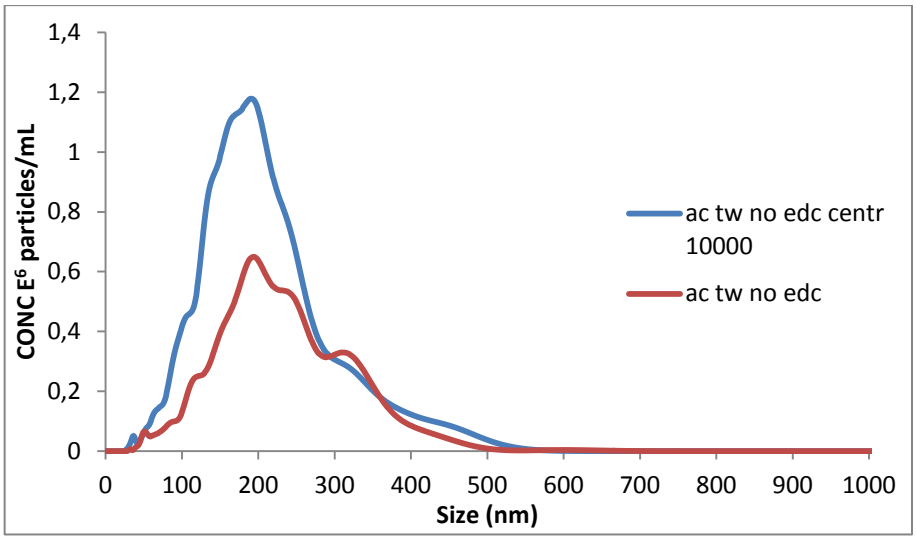


**Fig.3.60** Average size of nanoparticle measured using NTA before and after centrifugation.

## 3.7.2 Spectroscopic analysis (FT-IR)

Final composition of the ionic coacervate was spectrophotometrically studied with FT-IR to determine if both alginate and chitosan are still present after the several treatments to which the sample was subjected. The attribution and relative consideration about the characteristic peaks of pure polymers are reported in the previous paragraph. The spectrum obtained (see figure 3.61) is very broad. However, some typical resonances can be identified: the splitted vibrational band presenting two peaks at 1630 and 1610 $cm^{-1}$ is due to the characteristic bands of chitosan and alginate, and the same band is present in the spectrum of the covalently crosslinked alginate-chitosan system (see figure 3.49). Another splitted band includes the typical absorption band of asymmetric $COO^-$ of alginate at 1415 $cm^{-1}$. Peaks related to the skeleton of the rings at 1160-1020 $cm^{-1}$ are also present in the spectra. All together the spectrum is very similar to that studied for the alginate-chitosan covalent system.

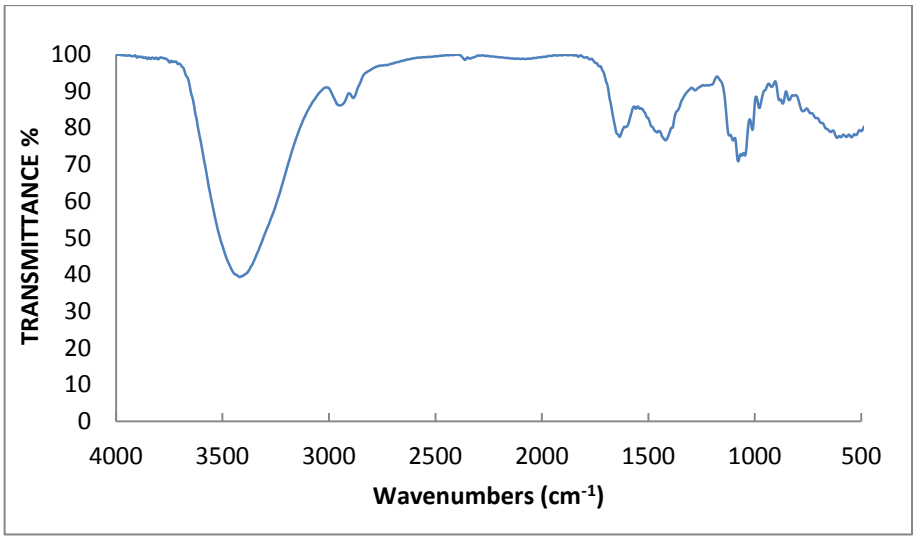


**Fig.3.61** FT-IR spectrum of alginate-chitosan ionic bonded matrix obtained in nanoemulsion in presence of tween80-span80 as emulsifying agent.

## 3.7.3 Determination of particle morphology

The morphology of the material obtained in the absence of EDC/NHS was analyzed by TEM after staining with uranyl acetate.

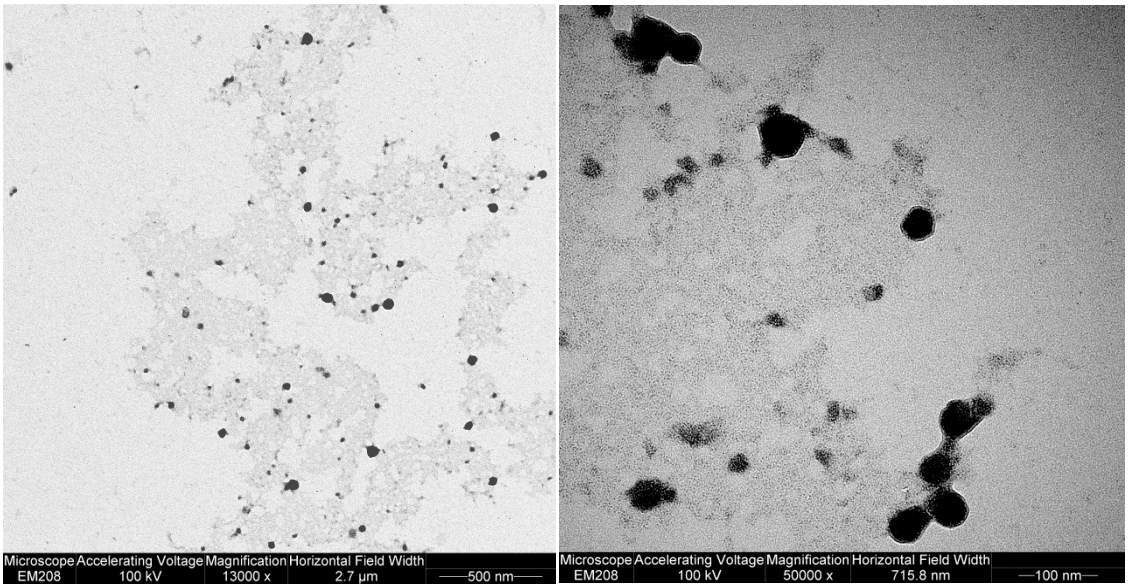


**Fig.3.62** Left: TEM images of alginate-chitosan ionic sample obtained using tween80-span80 as emulsifying agents. Right: sample at high magnification.

Figure 3.62 shows the presence of nanoparticles with an approximate diameter of 50-60 nm over a layer of non-structured material. Image at high magnification (right) confirms the presence of spherical partly fused nanoparticles. However, respect to the sample obtained using EDC/NHS (see figure 3.50), the number of nanoparticles is lower. In any case, the results obtained from TEM depict a different situation respect to the case of ionic coacervate obtained with Triton X-100. Indeed, with the Tween 80-Span 80 emulsion some nanoparticles are obtained while with the Triton X-100 emulsion only amorphous material was observed. This observation suggests that this type of nanoemulsion is able to stabilize the ionic interaction between alginate and chitosan respect to the nanoemulsion in which Triton X-100 was used. This result is in accordance with the data obtained from NTA and FT-IR underlying that covalent and ionic nanoparticles obtained using Tween 80-Span 80 emulsion show several similar properties.

### 3.7.4 Encapsulating properties of nanoparticles: loading of resveratrol

Ionic alginate-chitosan nanoparticles were investigated for their ability to encapsulate the hydrophobic nutraceutical resveratrol. The process of encapsulation followed the same procedure adopted for crosslinked alginate-chitosan nanoparticles. The samples were prepared in triplicates at five dilutions in a fixed volume of 1 ml of final sample. Resveratrol was added in a fixed concentration of 0,5 mg/ml and after precipitation of the excess of resveratrol, the samples were centrifuged. Taking in account the problems of the relative large sizes of the nanoparticles, the samples were subjected to a intermediate speed of rotation of 10000 rpm. Then the supernatant was collected and analyzed by UV–Vis measuring the characteristic absorbance peak of resveratrol at 307 nm. Also in this case, EDC/NHS crosslinked nanoparticles and ionic coacervates behave very similarly being able to entrap similar amounts of resveratrol and showing a similar dependence of the trapped efficiency from the concentration of polymers (data not shown). However, and in analogy with the case of Triton X-100 the ionic coacervate is less stable and resveratrol escapes more quickly from the nanoparticles

respect to the EDC/NHS crosslinked system which is stable for several days (see figure 3.63).

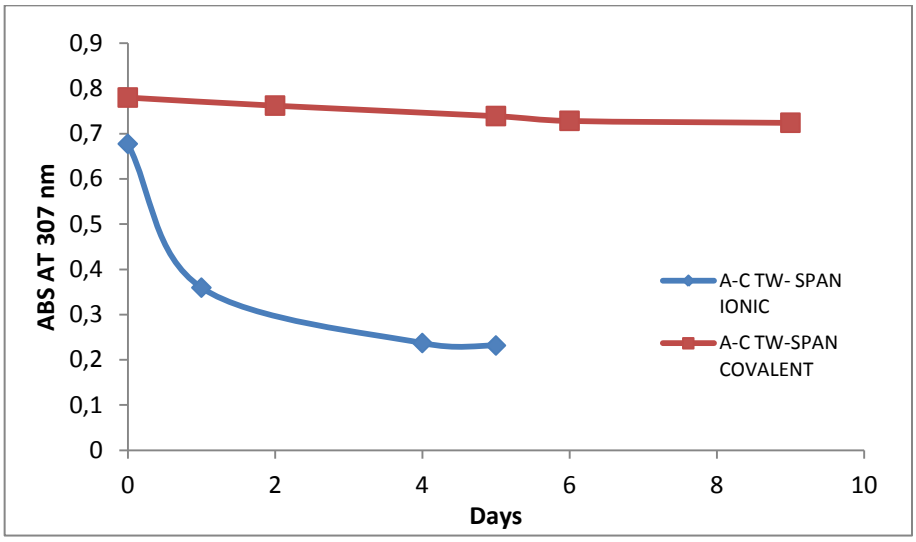


**Fig.3.63** Evolution of the absorbance at 307 nm for the highest concentrated sample (centrifuged at 10000 rpm) of covalent and ionic nanoparticles during the time.

## 3.7.5 Effect of salt concentration on the size of alginate-chitosan nanoparticles

Finally the effect of the ionic strength on the size of the two types of nanoparticles was examined by NTA (see figure 3.64). Increasing the concentration of NaCl the average diameter of the EDC/NHS crosslinked nanoparticles remains almost constant while that of the ionic coacervates suddenly increases at a 50 mM concentration of salt. Overall the behavior is very similar to that observed in the case of the preparation with Triton X-100 (see figure 3.41) and confirms that the ionic nanoparticles are less stable respect to the covalent ones.

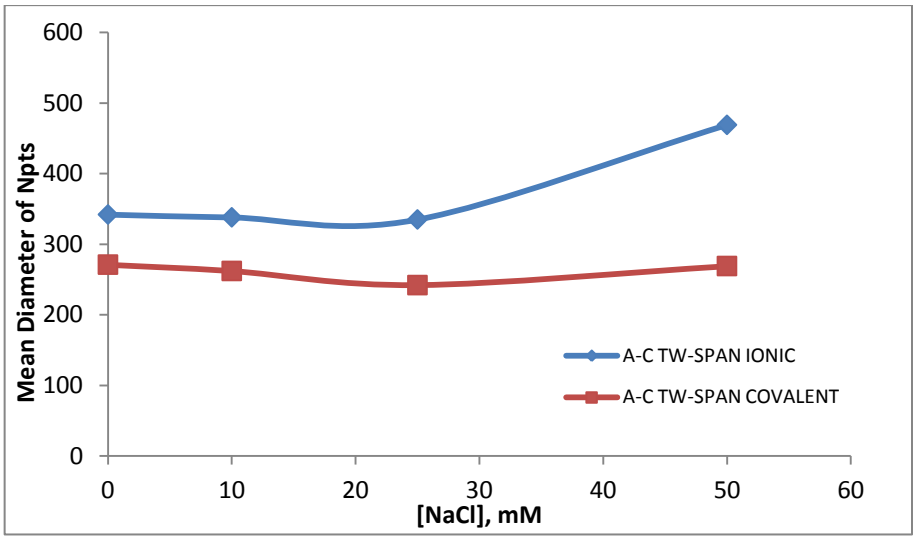


**Fig.3.64** Change in particle size after addition of NaCl on covalent and ionic alginate-chitosan nanoparticles. The sizes have been calculated considering as mean diameter the value referring to the 90% of the total particle population.

# Conclusions

# 4

# Conclusions

In this Thesis we have explored the possibility to form nanoparticles of alginate and chitosan covalently crosslinked thanks to the formation of amide bonds between the amino groups of alginate and the carboxyl groups of chitosan promoted by the zero-length EDC/NHS crosslinking reagents. The final aim was the development of suitable carriers for water insoluble nutraceuticals.

The results have shown that the reaction between alginate and chitosan in W/O emulsion leads to more stable systems compared to the reaction in water. The optimization of the emulsion represented a milestone for the aim of the project. Reactions in nanoemulsion, in particular, are an applicable strategy to obtain nanoparticles from carbohydrate polymers. In fact, the use of water nanodroplets as nanoreactors may prove to be a winner strategy for the stabilization of complex polymer matrices.

The FTIR analysis of the obtained nanoparticles, although does not give a definitive evidence about the formation of the covalent bonds between the polymers, demonstrates the presence of both alginate and chitosan polymers in the final composition of the nanoparticles. Moreover, a direct comparison between covalent and ionic nanoparticles reveal important structural differences thus supporting the effective formation of a covalently linked polymeric matrix.

NTA analysis shows that the nanoparticles are relatively small with an average size of 180 nm and are stable in time. The performed morphological investigation (TEM, SEM) also confirms the formation of spherical uniform nanoparticles. Preliminary toxicity studies performed on Caco-2 cells (MTT assay) exclude a toxic action of the nanoparticles.

Finally the capacity of the nanoparticles to entrap resveratrol and quercetin, molecules of high interest in food, was experimented. Results show a good ability of the systems to encapsulate those molecules. Aqueous solubility of bioactive molecules results improved when nanoparticles are present and nutraceuticals preserve their antioxidant activity after being loaded in the nanoparticles. In conclusion the

nanocarriers developed in this Thesis may represent an important alternative delivery system for uses both in food and pharmaceutical field.

## References:


1. *Diet, Nutrition and the Prevention of Chronic Disease Report of a Joint Who/FAO Expert Consultation*. (2003).
2. Sofi, F., Abbate, R., Gensini, G. F. & Casini, A. Accruing evidence on benefits of adherence to the Mediterranean diet on health : an updated systematic review and meta-analysis 1 , 2. *Am. J. Clin. Nutr.* **92,** 1189–1196 (2010).
3. de Lorgeril, M. & Salen, P. The Mediterranean-style diet for the prevention of cardiovascular diseases. *Public Health Nutr.* **9,** 118–123 (2006).
4. Yao, L. H. *et al.* Flavonoids in food and their health benefits. *Plant Foods Hum. Nutr.* **59,** 113–122 (2004).
5. Pandey, K. B. & Rizvi, S. I. Plant polyphenols as dietary antioxidants in human health and disease. *Oxid. Med. Cell. Longev.* **2,** 270–8 (2009).
6. Rothwell, J. A. *et al.* Systematic analysis of the polyphenol metabolome using the Phenol-Explorer database. *Mol. Nutr. Food Res.* 203–211 (2015). doi:10.1002/mnfr.201500435
7. Delmas, D., Lançon, A., Colin, D., Jannin, B. & Latruffe, N. Resveratrol as a chemopreventive agent: a promising molecule for fighting cancer. *Curr. Drug Targets* **7,** 423–442 (2006).
8. Manach, C. Polyphenols : food sources and bioavailability. *Am. J. Clin. Nutr.* **79,** 727–747 (2004).
9. Kasiotis, K. M., Pratsinis, H., Kletsas, D. & Haroutounian, S. A. Resveratrol and related stilbenes: Their anti-aging and anti-angiogenic properties. *Food Chem. Toxicol.* **61,** 112–120 (2013).
10. Delmas, D. *et al.* Transport, stability, and biological activity of resveratrol. *Ann. N. Y. Acad. Sci.* **1215,** 48–59 (2011).
11. Farkas, O., Jakus, J. & Héberger, K. Quantitative structure-antioxidant activity relationships of flavonoid compounds. *Molecules* **9,** 1079–1088 (2004).
12. Rathee, P. *et al.* Mechanism of action of flavonoids as anti-inflammatory agents: a review. *Inflamm. Allergy Drug Targets* **8,** 229–235 (2009).
13. Shashank Kumar and Abhay K. Pandey. Chemistry and Biological Activities of

Flavonoids: An Overview. *Hindawi Publ. Corp.* **2013,** 1–16 (2013).

14. Hanasaki, Y., Ogawa, S. & Fukui, S. The correlation between active oxygens scavenging and antioxidative effects of flavonoids. *Free Radic. Biol. Med.* **16,** 845–850 (1994).
15. Boots, A. W., Haenen, G. R. M. M. & Bast, A. Health effects of quercetin: from antioxidant to nutraceutical. *Eur. J. Pharmacol.* **585,** 325–37 (2008).
16. T. Shibamoto, K. Kanazawa, F. Shahidi, C. T. H. *Functional food and health*. (2008).
17. Stein, A. J. & Rodríguez-Cerezo, E. *Functional Food in the European Union*. (2008). doi:10.2791/21607
18. Gianfrilli, D. *et al.* Propionyl-L-carnitine, L-arginine and niacin in sexual medicine: A nutraceutical approach to erectile dysfunction. *Andrologia* **44,** 600–604 (2012).
19. Chen, L., Remondetto, G. E. & Subirade, M. Food protein-based materials as nutraceutical delivery systems. *Trends Food Sci. Technol.* **17,** 272–283 (2006).
20. Ting, Y., Jiang, Y., Ho, C. T. & Huang, Q. Common delivery systems for enhancing in vivo bioavailability and biological efficacy of nutraceuticals. *J. Funct. Foods* **7,** 112–128 (2014).
21. Bernal, J., Mendiola, J. a., Ibáñez, E. & Cifuentes, a. Advanced analysis of nutraceuticals. *J. Pharm. Biomed. Anal.* **55,** 758–774 (2011).
22. Pond, S. M. & Tozer, T. N. First-pass elimination. Basic concepts and clinical consequences. *Clin. Pharmacokinet.* **9,** 1–25 (1984).
23. Palombo, P. *et al.* Beneficial Long-Term Effects of Combined Oral/Topical Antioxidant Treatment with the Carotenoids Lutein and Zeaxanthin on Human Skin: A Double-Blind, Placebo-Controlled Study. *Skin Pharmacol. Physiol.* **20,** 199–210 (2007).
24. Nedovic, V., Kalusevic, A., Manojlovic, V., Levic, S. & Bugarski, B. An overview of encapsulation technologies for food applications. *Procedia Food Sci.* **1,** 1806–1815 (2011).
25. McClements, D. J. *Nanoparticle- and Microparticle-based Delivery Systems : Encapsulation, Protection and Release of Active Compounds*. (2014).
26. McClements, D. J., Decker, E. A., Park, Y. & Weiss, J. Structural Design Principles

forDelivery of Bioactive Components in Nutraceuticals an Functional Foods. *Crit. Rev. Food Sci. Nutr.* **49,** 577–606 (2009).

27. Hetal, T., Bindesh, P. & Sneha, T. A review on techniques for oral bioavailability enhancement of drugs. *Int. J. Pharm. Sci. Rev. Res.* **4,** 203–223 (2010).
28. Freitas, S., Merkle, H. P. & Gander, B. Microencapsulation by solvent extraction/evaporation: Reviewing the state of the art of microsphere preparation process technology. *J. Control. Release* **102,** 313–332 (2005).
29. Weiss, J., Takhistov, P. & McClements, D. J. Functional materials in food nanotechnology. *J. Food Sci.* **71,** 107–116 (2006).
30. H. B.Nair , B. Sung, V. R. Yadav, R. Kannappan, M. M. Chaturvedi, B. B. A. Delivery of antiinflammatory nutraceuticals by nanoparticles for the prevention and treatment of cancer. *Biochem. Pharmacol.* **80,** 1833–1843 (2010).
31. Acosta, E. Bioavailability of nanoparticles in nutrient and nutraceutical delivery. *Curr. Opin. Colloid Interface Sci.* **14,** 3–15 (2009).
32. Gupta, G. & Singh, A. A short review on stomach specific drug delivery system. *Int. J. PharmTech Res.* **4,** 1527–1545 (2012).
33. Desai, M. P., Labhasetwar, V., Walter, E., Levy, R. J. & Amidon, G. L. The mechanism of uptake of biodegradable microparticles in Caco-2 cells is size dependent. *Pharm. Res.* **14,** 1568–1573 (1997).
34. Panyam, J. & Labhasetwar, V. Biodegradable nanoparticles for drug and gene delivery to cells and tissue. *Adv. Drug Deliv. Rev.* **55,** 329–347 (2003).
35. Desai, M. P., Labhasetwar, V. & Amidon, G. L. Gastrointestinal uptake of biodegradable microparticles: effect of particle size. *Pharm. Res.* **13,** 1838–1845 (1996).
36. Tonneson, H. H., Smistad, G., Agren, T. & Karlsen, J. Studies on curcumin and curcuminoids. XXIII: Effects of curcumin on liposomal lipid peroxidation. *Int. J. Pharm.* **90,** 221–228 (1993).
37. Mignet, N., Seguin, J. & Chabot, G. Bioavailability of Polyphenol Liposomes: A Challenge Ahead. *Pharmaceutics* **5,** 457–471 (2013).
38. Trivedi, R. & Kompella, U. B. Nanomicellar formulations for sustained drug delivery: strategies and underlying principles. *Nanomedicine (Lond).* **5,** 485–505 (2010).

39. Taylor, M. J., Tanna, S. & Sahota, T. In vivo study of a polymeric glucose-sensitive insulin delivery system using a rat model. *J. Pharm. Sci.* **99,** 4215–4227 (2010).
40. Li, X. *et al.* Preparation of curcumin micelles and the in vitro and in vivo evaluation for cancer therapy. *J. Biomed. Nanotechnol.* **10,** 1458–68 (2014).
41. Zhou, B., Wu, L. M., Yang, L. & Liu, Z. L. Evidence for α-tocopherol regeneration reaction of green tea polyphenols in SDS micelles. *Free Radic. Biol. Med.* **38,** 78–84 (2005).
42. Tan, C., Wang, Y. & Fan, W. Exploring polymeric micelles for improved delivery of anticancer agents: Recent developments in preclinical studies. *Pharmaceutics* **5,** 201–219 (2013).
43. Gou, M. *et al.* Curcumin-loaded biodegradable polymeric micelles for colon cancer therapy in vitro and in vivo. *Nanoscale* **3,** 1558–1567 (2011).
44. Lucas-Abellán, C., Fortea, I., López-Nicolás, J. M. & Núñez-Delicado, E. Cyclodextrins as resveratrol carrier system. *Food Chem.* **104,** 39–44 (2007).
45. Mourtzinos, I., Salta, F., Yannakopoulou, K., Chiou, A. & Karathanos, V. T. Encapsulation of olive leaf extract in b-cyclodextrin. *J. Agric. Food Chem.* **55,** 8088–8094 (2007).
46. Kalogeropoulos, N., Yannakopoulou, K., Gioxari, A., Chiou, A. & Makris, D. P. Polyphenol characterization and encapsulation in b-cyclodextrin of a flavonoid-rich Hypericum perforatum (St John's wort) extract. *LWT - Food Sci. Technol.* **43,** 882–889 (2010).
47. Borghetti, G. S., Lula, I. S., Sinisterra, R. D. & Bassani, V. L. Quercetin/β-Cyclodextrin Solid Complexes Prepared in Aqueous Solution Followed by Spray-drying or by Physical Mixture. *AAPS Pharm. Sci.Tech.* **10,** 235–242 (2009).
48. Haiyun, D., Jianbin, C., Guomei, Z., Shaomin, S. & Jinhao, P. Preparation and spectral investigation on inclusion complex of b-cyclodextrin with rutin. *Spectrochim. Acta - Part A Mol. Biomol. Spectrosc.* **59,** 3421–3429 (2003).
49. Çelik, S. E., Özyürek, M., Tufan, A. N., Güçü, K. & Apak, R. Spectroscopic study and antioxidant properties of the inclusion complexes of rosmarinic acid with natural and derivative cyclodextrins. *Spectrochim. Acta - Part A Mol. Biomol. Spectrosc.* **78,** 1615–1624 (2011).
50. Mercader-Ros, M. T., Lucas-Abellán, C., Fortea, M. I., Gabaldón, J. a. & Núñez-

Delicado, E. Effect of HP-β-cyclodextrins complexation on the antioxidant activity of flavonols. *Food Chem.* **118,** 769–773 (2010).

51. Rudin Alfred, C. P. *The Elements of Polymer Science & Engineering*. (1998).
52. A.D. Jenkins. *Polymer Science: A Materials Science Handbook*. **2,** (1972).
53. Ahmed, E. M. Hydrogel: Preparation, characterization, and applications. *J. Adv. Res.* **6,** 105–121 (2013).
54. Lin, C.-C. & Metters, A. T. Hydrogels in controlled release formulations: Network design and mathematical modeling. *Adv. Drug Deliv. Rev.* **58,** 1379–1408 (2006).
55. Alvarenga, E. S. De. Characterization and Properties of Chitosan. *Biotechnol. Biopolym.* 91–108 (2011). doi:10.5772/17020
56. Ouwerx, C., Velings, N., Mestdagh, M. . & Axelos, M. a. . Physico-chemical properties and rheology of alginate gel beads formed with various divalent cations. *Polym. Gels Networks* **6,** 393–408 (1998).
57. Draget, K., Smidsrød, O. & Skjåk-Bræk, G. in *Alginates form algae. In : Steinbuchel A; Rhee SK; (eds) Polysaccharides and polyamides in the food iindustries: properties, production and patents. Wiley; Weinheim* 1–30 (2005). doi:10.1002/3527600035.bpol6008
58. Calvo, P. & Remunan-Lopez, C. Novel hydrophilic chitosan-polyethylene oxide nanoparticles as protein carriers. *J. Appl. Polym. Sci.* **63,** 125–132 (1997).
59. R. Bodmeier, H.G. Chen, O. P. A novel approach to the oral delivery of micro- or nanoparticles. *Pharm. Res* **6,** 413–417 (1989).
60. Liu, H. & Gao, C. Preparation and properties of ionically cross-linked chitosan nanoparticles. *Polym. Adv. Technol.* **20,** 613–619 (2009).
61. Fernández-Urrusuno, R., Calvo, P., Remuñán-López, C., Vila-Jato, J. L. & Alonso, M. J. Enhancement of nasal absorption of insulin using chitosan nanoparticles. *Pharmaceutical Research* **16,** 1576–1581 (1999).
62. Pan, Y. *et al.* Bioadhesive polysaccharide in protein delivery system: chitosan nanoparticles improve the intestinal absorption of insulin in vivo. *Int. J. Pharm.* **249,** 139–147 (2002).
63. Xu, Y. & Du, Y. Effect of molecular structure of chitosan on protein delivery properties of chitosan nanoparticles. *Int. J. Pharm.* **250,** 215–226 (2003).
64. Kawashima, Y. *et al.* Novel method for the preparation of controlled-release

theophylline granules coated with a polyelectrolyte complex of sodium polyphosphate-chitosan. *J. Pharm. Sci.* **74,** 264–268 (1985).

65. A. Sezer, J. A. Controlled release of piroxicam from chitosan beads. *Int. J. Pharm.* **121,** 113–116 (1995).
66. Sipoli, C. C., Radaic, A., Santana, N., Jesus, M. B. de & Torre, L. G. de la. Chitosan nanoparticles produced with the gradual temperature decrease technique for sustained gene delivery. *Biochem. Eng. J.* **103,** 114–121 (2015).
67. Nasti, A. *et al.* Chitosan/TPP and Chitosan/TPP-hyaluronic Acid Nanoparticles: Systematic Optimisation of the Preparative Process and Preliminary Biological Evaluation. *Res. Pharm. Sci.* **26,** 1918–1930 (2009).
68. Gan, Q., Wang, T., Cochrane, C. & McCarron, P. Modulation of surface charge, particle size and morphological properties of chitosan–TPP nanoparticles intended for gene delivery. *Colloids Surfaces B Biointerfaces* **44,** 65–73 (2005).
69. Stoica, R., Somoghi, R. & Ion, R. M. Preparation of chitosan – tripolyphosphate nanoparticles for the encapsulation of polyphenols extracted from rose hips. *Dig. J. Nanomater. Biostructures* **8,** 955–963 (2013).
70. Fabregas, A. *et al.* Impact of physical parameters on particle size and reaction yield when using the ionic gelation method to obtain cationic polymeric chitosan-tripolyphosphate nanoparticles. *Int. J. Pharm.* **446,** 199–204 (2013).
71. Berger, J. *et al.* Structure and interactions in covalently and ionically crosslinked chitosan hydrogels for biomedical applications. *Eur. J. Pharm. Biopharm.* **57,** 19–34 (2004).
72. Sarmento, B. *et al.* Alginate / Chitosan Nanoparticles are Effective for Oral Insulin Delivery. *Pharm. Res.* **24,** 2198–2206 (2007).
73. George, M. & Abraham, T. E. Polyionic hydrocolloids for the intestinal delivery of protein drugs : Alginate and chitosan — a review. *J. Control. Release* **114,** 1–14 (2006).
74. Rajaonarivony, M., Vauthier, C., Couarraze, G., Puisieux, F. & Couvreur, P. Development of a new drug carrier made from alginate. *J. Pharm. Sci.* **82,** 912–917 (1993).
75. Bystrický, S., Malovíková, A. & Sticzay, T. Interaction of alginates and pectins with cationic polypeptides. *Carbohydr. Polym.* **13,** 283–294 (1990).

76. Liang, J. *et al.* Synthesis, characterization and cytotoxicity studies of chitosan-coated tea polyphenols nanoparticles. *Colloids Surf. B. Biointerfaces* **82,** 297–301 (2011).
77. Harris, R., Lecumberri, E., Mateos-Aparicio, I., Mengíbar, M. & Heras, A. Chitosan nanoparticles and microspheres for the encapsulation of natural antioxidants extracted from Ilex paraguariensis. *Carbohydr. Polym.* **84,** 803–806 (2011).
78. Pavinatto, F. J., Caseli, L. & Oliveira, O. N. Chitosan in nanostructured thin films. *Biomacromolecules* **11,** 1897–908 (2010).
79. Sadek, R. F. H. Mutual interaction of polyelectrolytes. *Science (80-. ).* **110,** 552–554 (1949).
80. Chen, Y., Siddalingappa, B., Chan, P. H. H. & Benson, H. a E. Development of a chitosan-based nanoparticle formulation for delivery of a hydrophilic hexapeptide, dalargin. *Biopolym. - Pept. Sci. Sect.* **90,** 663–670 (2008).
81. Mao, H. Q. *et al.* Chitosan-DNA nanoparticles as gene carriers: Synthesis, characterization and transfection efficiency. *J. Control. Release* **70,** 399–421 (2001).
82. Duceppe, N. & Tabrizian, M. Factors influencing the transfection efficiency of ultra low molecular weight chitosan/hyaluronic acid nanoparticles. *Biomaterials* **30,** 2625–2631 (2009).
83. Deng, X. *et al.* Hyaluronic acid-chitosan nanoparticles for co-delivery of MiR-34a and doxorubicin in therapy against triple negative breast cancer. *Biomaterials* **35,** 4333–4344 (2014).
84. Oyarzun-Ampuero, F. A., Brea, J., Loza, M. I., Torres, D. & Alonso, M. J. Chitosan–hyaluronic acid nanoparticles loaded with heparin for the treatment of asthma. *Int. J. Pharm.* **381,** 122–129 (2009).
85. Aruffo, A., Stamenkovic, I., Melnick, M., Underhill, C. B. & Seed, B. CD44 is the principal cell surface receptor for hyaluronate. *Cell* **61,** 1303–1313 (1990).
86. Draganescu, D. A. N. *et al.* Entrapment of Flaxseed Extract into Xanthan-Chitosan Complex. *Cellul. Chem. Technol.* **47,** 231–238 (2013).
87. Sanna, V. *et al.* Polymeric Nanoparticles Encapsulating White Tea Extract for Nutraceutical Application. *J. Agric. Food Chem.* **63,** 2026–2032 (2015).
88. Kizilay, E., Kayitmazer, a. B. & Dubin, P. L. Complexation and coacervation of

polyelectrolytes with oppositely charged colloids. *Adv. Colloid Interface Sci.* **167,** 24–37 (2011).

89. Oliveira, A. L., von Staszewski, M., Pizones Ruiz-Henestrosa, V. M., Pintado, M. & Pilosof, A. M. R. Impact of pectin or chitosan on bulk, interfacial and antioxidant properties of (+)-catechin and β-lactoglobulin ternary mixtures. *Food Hydrocoll.* **55,** 119–127 (2016).
90. Kweon, D. & Lim, S. Preparation and Characteristics of a Water-Soluble Chitosan – Heparin Complex. *J. Appl. Polym. Sci.* **87,** 1784–1789 (2003).
91. Dhanasingh, S. & Nallaperumal, S. K. Chitosan / Casein Microparticles : Preparation , Characterization and Drug Release Studies. *Int. J. Biol. Biomol. Agric. Food Biotechnol. Eng.* **4,** 229–233 (2010).
92. Hosseini, S. M. H., Emam-Djomeh, Z., Sabatino, P. & Van der Meeren, P. Nanocomplexes arising from protein-polysaccharide electrostatic interaction as a promising carrier for nutraceutical compounds. *Food Hydrocoll.* **50,** 16–26 (2015).
93. López-León, T., Carvalho, E. L. S., Seijo, B., Ortega-Vinuesa, J. L. & Bastos-González, D. Physicochemical characterization of chitosan nanoparticles: Electrokinetic and stability behavior. *J. Colloid Interface Sci.* **283,** 344–351 (2005).
94. Rampino, A., Borgogna, M., Blasi, P., Bellich, B. & Cesàro, A. Chitosan nanoparticles: Preparation, size evolution and stability. *Int. J. Pharm.* **455,** 219–228 (2013).
95. Ebara, M. *et al. Smart Biomaterials*. (2014). doi:10.1007/978-4-431-54400-5
96. Bodmeier, R., Oh, K.-H. & Pramar, Y. Preparation and Evaluation Of Drug-Containing Chitosan Beads. *Drug Dev. Ind. Pharm.* **15,** 1475–1494 (1989).
97. Shu, X. Z. & Zhu, K. J. A novel approach to prepare tripolyphosphate/chitosan complex beads for controlled release drug delivery. *Int. J. Pharm.* **201,** 51–58 (2000).
98. Simsek-Ege, F. a., Bond, G. M. & Stringer, J. Polyelectrolye complex formation between alginate and Chitosan as a function of pH. *J. Appl. Polym. Sci.* **88,** 346–351 (2003).
99. Sarmento, B., Ribeiro, A. J., Veiga, F., Ferreira, D. C. & Neufeld, R. J. Insulin-

Loaded Nanoparticles are Prepared by Alginate Ionotropic Pre-Gelation Followed by Chitosan Polyelectrolyte Complexation. *J. Nanosci. Nanotechnol.* **7,** 2833–2841 (2007).

100. Takka, S. & Gürel, A. Evaluation of chitosan/alginate beads using experimental design: formulation and in vitro characterization. *AAPS PharmSciTech* **11,** 460–466 (2010).
101. Loquercio, A., Castell-Perez, E., Gomes, C. & Moreira, R. G. Preparation of Chitosan-Alginate Nanoparticles for *Trans* -cinnamaldehyde Entrapment. *J. Food Sci.* **80,** N2305–N2315 (2015).
102. Sarmento, B. *et al.* Development and Comparison of Different Nanoparticulate Polyelectrolyte Complexes as Insulin Carriers. *Int. J. Pept. Res. Ther.* **12,** 131–138 (2006).
103. Machluf, M. Alginate – Chitosan Complex Coacervation for Cell Encapsulation : Effect on Mechanical Properties and on Long-Term Viability. *Biopolymers* **82,** 570–579 (2006).
104. Vandenberg, G. W., Drolet, C., Scott, S. L. & Noue, J. De. Factors affecting protein release from alginate – chitosan coacervate microcapsules during production and gastric / intestinal simulation. *J. Control. Release* **77,** 297–307 (2001).
105. V. K. Malesu, D. S. and P. . L. . N. Chitosan – sodium alginate nanocomposites blended with cloisite 30b as a novel drug delivery system for anticancer drug curcumin. *Int. J. Appl. Biol. Pharm. Technol.* **2,** 402–411 (2011).
106. Belšćak-Cvitanović, A. *et al.* Encapsulation of polyphenolic antioxidants from medicinal plant extracts in alginate-chitosan system enhanced with ascorbic acid by electrostatic extrusion. *Food Res. Int.* **44,** 1094–1101 (2011).
107. Wang, A. N., Wu, L. G., Jia, L. L., Li, X. L. & Sun, Y. D. Alginate-Chitosan Microspheres for Controlled Release of Tea Polyphenol. *Adv. Mater. Res.* **152-153,** 1726–1729 (2010).
108. Rahaiee, S., Shojaosadati, S. A., Hashemi, M., Moini, S. & Razavi, S. H. Improvement of crocin stability by biodegradeble nanoparticles of chitosan-alginate. *Int. J. Biol. Macromol.* **79,** 423–432 (2015).
109. Kulkarni, V. H., Kulkarni, P. V. & Keshavayya, J. Glutaraldehyde-crosslinked

chitosan beads for controlled release of diclofenac sodium. *J. Appl. Polym. Sci.* **103,** 211–217 (2007).

110. Kathuria, N., Tripathi, A., Kar, K. K. & Kumar, A. Synthesis and characterization of elastic and macroporous chitosan-gelatin cryogels for tissue engineering. *Acta Biomater.* **5,** 406–418 (2009).
111. Rajalakshmi. Chitosan Nanoparticles - An Emerging Trend In Nanotechnology. *Int. J. Drug Deliv.* **6,** 204–229 (2014).
112. Muzzarelli, R. A. A. Genipin-crosslinked chitosan hydrogels as biomedical and pharmaceutical aids. *Carbohydr. Polym.* **77,** 1–9 (2009).
113. Moura, M. J., Figueiredo, M. M. & Gil, M. H. Rheological study of genipin cross-linked chitosan hydrogels. *Biomacromolecules* **8,** 3823–3829 (2007).
114. Karnchanajindanun, J., Srisa-ard, M. & Baimark, Y. Genipin-cross-linked chitosan microspheres prepared by a water-in-oil emulsion solvent diffusion method for protein delivery. *Carbohydr. Polym.* **85,** 674–680 (2011).
115. Arteche Pujana, M., Pérez-Álvarez, L., Cesteros Iturbe, L. C. & Katime, I. Biodegradable chitosan nanogels crosslinked with genipin. *Carbohydr. Polym.* **94,** 836–842 (2013).
116. Wang, Y.-S., Liu, L.-R., Jiang, Q. & Zhang, Q.-Q. Self-aggregated nanoparticles of cholesterol-modified chitosan conjugate as a novel carrier of epirubicin. *Eur. Polym. J.* **43,** 43–51 (2007).
117. Du, Y.-Z., Wang, L., Yuan, H., Wei, X.-H. & Hu, F.-Q. Preparation and characteristics of linoleic acid-grafted chitosan oligosaccharide micelles as a carrier for doxorubicin. *Colloids Surf. B. Biointerfaces* **69,** 257–63 (2009).
118. Galant, C., Kjoniksen, A. L., Nguyen, G. T. M., Knudsn, K. D.,&Nystrom, B. Altering Associations in Aqueous Solution of a Hydrophobically Modified Alginate in the Presence of Cyclodextrinmonomers. *J. Phys. Chem. B* **110,** 190–195 (2006).
119. Bernkop-Schnürch, A., Kast, C. E. & Richter, M. F. Improvement in the mucoadhesive properties of alginate by the covalent attachment of cysteine. *J. Control. Release* **71,** 277–285 (2001).
120. Y. Deng, D. Liu, G. Du, X. Li, J. C. Preparation and characterization of hyaluronan/chitosan scaffold crosslinked by 1-ethyl-3-(3 dimethylaminopropyl) carbodiimide. *Polym. Int.* **56,** 738–745 (2007).

121. Staroszczyk, H., Sztuka, K., Wolska, J., Wojtasz-Pająk, A. & Kołodziejska, I. Interactions of fish gelatin and chitosan in uncrosslinked and crosslinked with EDC films: FT-IR study. *Spectrochim. Acta Part A Mol. Biomol. Spectrosc.* **117,** 707–712 (2014).
122. Liu, Z. *et al.* Alginic acid-coated chitosan nanoparticles loaded with legumain DNA vaccine: effect against breast cancer in mice. *PLoS One* **8,** e60190 (2013).
123. Landfester, K. The generation of nanoparticles in miniemulsions. *Adv. Mater.* **13,** 765–768 (2001).
124. Tadros, T. F. *Emulsion Science and Technology*. *Emulsion Science and Technology* doi:10.1002/9783527626564
125. Davis, H. T. Factors determining emulsion type: Hydrophile—lipophile balance and beyond. *Colloids Surfaces A Physicochem. Eng. Asp.* **91,** 9–24 (1994).
126. J. Lyklema. *Fundamentals of Interface and Colloid Science: Liquid-Fluid Interfaces*.
127. M. J Rosen, J. . K. *Surfactant and Interfacial Phenomena*.
128. Opawale, F. & Burgess, D. Influence of Interfacial Properties of Lipophilic Surfactants on Water-in-Oil Emulsion Stability. *J. Colloid Interface Sci.* **197,** 142–50 (1998).
129. *Modern aspect of emulsion science*. (1998).
130. Griffin, W. Classification of surface active agent by 'HLB'. *J. cosmet sci* **1,** 311–326 (1949).
131. Taylor, P., Vaughan, C. D. & Rice, D. A. Predicting O / W Emulsion Stability By the ' Required Hlb Equation '. *J. Dispers. Sci. Technol.* **11,** 37–41 (2007).
132. *The HLB System a time-saving guide to emulsifier selection*. *ICI AMERICAS Inc.* **37,** (1980).
133. Robins, M. M. Emulsions - Creaming phenomena. *Curr. Opin. Colloid Interface Sci.* **5,** 265–272 (2000).
134. Barkat Ali Khan,. Basics of pharmaceutical emulsions: A review. *African J. Pharm. Pharmacol.* **5,** 2715–2725 (2011).
135. Jian Hua Yao, K. R. Elder, Hong Guo, M. G. Theory and Stimulation of Ostwald Rippening. *Physical Review* **47,** 14110–14125 (1993).
136. McClements, D. J. Nanoemulsions versus microemulsions: terminology,

differences, and similarities. *Soft Matter* **8,** 1719–1729 (2012).

137. Qian, C. & McClements, D. J. Formation of nanoemulsions stabilized by model food-grade emulsifiers using high-pressure homogenization: Factors affecting particle size. *Food Hydrocoll.* **25,** 1000–1008 (2011).
138. Chu, J. *et al.* Lecithin-linker formulations for self-emulsifying delivery of nutraceuticals. *Int. J. Pharm.* **471,** 92–102 (2014).
139. Knoth, A., Scherze, I. & Muschiolik, G. Effect of lipid type on water-in-oil-emulsions stabilized by phosphatidylcholine-depleted lecithin and polyglycerol polyricinoleate. *Eur. J. Lipid Sci. Technol.* **107,** 857–863 (2005).
140. Pinto Reis, C., Neufeld, R. J., Ribeiro, A. J. & Veiga, F. Nanoencapsulation I. Methods for preparation of drug-loaded polymeric nanoparticles. *Nanomedicine Nanotechnology, Biol. Med.* **2,** 8–21 (2006).
141. Desgouilles, S. *et al.* The Design of Nanoparticles Obtained by Solvent Evaporation: A Comprehensive Study. *Langmuir* **19,** 9504–9510 (2003).
142. Tanthapanichakoon W, Sowasod N, C. T. Development of Nanoencapsulated Curcumin in Chitosan for Cosmetic Use via Evaporation of O/W/O In*: Characterization and Control of Interfaces for High Quality advanced Materials II* (2011).
143. Pal, T. Polymethylmethacrylate Coated Alginate Matrix Microcapsules for Controlled Release of Diclofenac Sodium. *Pharmacol. Pharm.* **02,** 56–66 (2011).
144. Nagavarma, B. V. N., Yadav, H. K. S., Ayaz, A., Vasudha, L. S. & Shivakumar, H. G. Different techniques for preparation of polymeric nanoparticles - a review. *Asian J. Pharm. Clin. Res.* **5,** 16–23 (2012).
145. Beck-Broichsitter, M., Rytting, E., Lebhardt, T., Wang, X. & Kissel, T. Preparation of nanoparticles by solvent displacement for drug delivery: A shift in the ‘ ouzo region’ upon drug loading. *Eur. J. Pharm. Sci.* **41,** 244–253 (2010).
146. Microencapsulation: A promising technique for controlled drug delivery M.N. Singh, K.S.Y. Hemant,* M. Ram, and H.G. Shivakumar. *Res Pharm Sci* (2010).
147. Niwa, T., Takeuchi, H., Hino, T., Kunou, N. & Kawashima, Y. Preparations of biodegradable nanospheres of water-soluble and insoluble drugs with D , L-lactide I glycolide copolymer by a novel spontaneous emulsification solvent diffusion method, and the drug release behavior. *J. Control. Release* **25,** 89–98

(1993).

148. El-Shabouri, M. H. Positively charged nanoparticles for improving the oral bioavailability of cyclosporin-A. *Int. J. Pharm.* **249,** 101–108 (2002).
149. Mendoza-Munoz, N., Quintanar-Guerrero, D. & Allemann, E. The impact of the salting-out technique on the preparation of colloidal particulate systems for pharmaceutical applications. *Recent Pat. Drug Deliv. Formul.* **6,** 236–249 (2012).
150. Allouche, J. *Synthesis of Organic and Bioorganic Nanoparticles:An Overview of the Preparation Methods*. *Nanomaterials: A Danger or a Promise?* (2013). doi:10.1007/978-1-4471-4213-3
151. Ohya, Y., Shiratani, M., Kobayashi, H. & Ouchi, T. Release Behavior of 5-Fluorouracil from Chitosan-Gel Nanospheres Immobilizing 5-Fluorouracil Coated with Polysaccharides and Their Cell Specific Cytotoxicity. *J. Macromol. Sci. Part A* **31,** 629–642 (1994).
152. Songjiang, Z. & Lixiang, W. Amyloid-beta associated with chitosan nano-carrier has favorable immunogenicity and permeates the BBB. *AAPS PharmSciTech* **10,** 900–5 (2009).
153. Tokumitsu H, Ichiwawa H., Fukumori Y., B. L. H. Preparation of Gadopentetic Acid-Loaded Chitosan Microparticles for Gadolidium Neutron- Capture Therapy of Cancer by a Novel Emulsion-Droplet Coalescence Technique. *Chem.Pharm Bull.* **47,** 838–842 (1999).
154. A. Gamini, S Paoletti, F. Z. *Chain rigidity of polyuronate: Static Light Scattering of aqueous solutions of Hyaluronate and Alginate*. *Laser Light Scattering in Biochemistry, pg 294, S.E. Harding, D.B. Sattelle, V.A.Bloomfield Eds,* (1992).
155. H. Grasdalen. High-field, 1H-n.m.r. spectroscopy of alginate: sequential structure and linkage conformations. *Carbohydr. Res.* 255–260 (1983).
156. Kasaai M.R., Arul J., C. G. Intrinsic Viscosity–Molecular Weight Relationship for Chitosan. *J. Polym. Sci. Part B Polym. Phys.* **38,** 2591–2598 (2000).
157. Roberts, G. A. F. & Domszy, J. G. Determination of the viscometric constants for chitosan. *Int. J. Biol. Macromol.* **4,** 374–377 (1982).
158. Berth, G. & Dautzenberg, H. The degree of acetylation of chitosans and its effect on the chain conformation in aqueous solution. *Carbohydr. Polym.* **47,** 39–51 (2002).

159. Filipe, V., Hawe, A. & Jiskoot, W. Critical evaluation of nanoparticle tracking analysis (NTA) by NanoSight for the measurement of nanoparticles and protein aggregates. *Pharm. Res.* **27,** 796–810 (2010).
160. Hashida, M., Egawa, M., Muranishi, S. & Sezaki, H. Role of intramuscular administration of water-in-oil emulsions as a method for increasing the delivery of anticancer to regional lymphatics. *J. Pharmacokinet. Biopharm.* **5,** 225–239 (1977).
161. Lupi, F. R., Gabriele, D., De Cindio, B., S??nchez, M. C. & Gallegos, C. A rheological analysis of structured water-in-olive oil emulsions. *J. Food Eng.* **107,** 296–303 (2011).
162. Wilson, R., Van Schie, B. J. & Howes, D. Overview of the preparation, use and biological studies on polyglycerol polyricinoleate (PGPR). *Food Chem. Toxicol.* **36,** 711–718 (1998).
163. Van Nieuwenhuyzen, W. Lecithin production and properties. *J. Am. Oil Chem. Soc.* **53,** 425–427 (1976).
164. van Nieuwenhuyzen, W. & Szuhaj, B. F. Effects of lecithins and proteins on the stability of emulsions. *Fett-Lipid.* **100,** 282–291 (1998).
165. Ferreira, B. M. S., Ramalho, J. B. V. S. & Lucas, E. F. Demulsification of Water-in-Crude Oil Emulsions by Microwave Radiation: Effect of Aging, Demulsifier Addition, and Selective Heating. *Energy & Fuels* **27,** 615–621 (2013).
166. Chen, G. & He, G. Separation of water and oil from water-in-oil emulsion by freeze/thaw method. *Sep. Purif. Technol.* **31,** 83–89 (2003).
167. Kocherginsky, N. M., Tan, C. L. & Lu, W. F. Demulsification of water-in-oil emulsions via filtration through a hydrophilic polymer membrane. *J. Memb. Sci.* **220,** 117–128 (2003).
168. Sonvico, F. *et al.* Formation of self-organized nanoparticles by lecithin/chitosan ionic interaction. *Int. J. Pharm.* **324,** 67–73 (2006).
169. Hafner, A., Lovrić, J., Voinovich, D. & Filipović-Grčić, J. Melatonin-loaded lecithin/chitosan nanoparticles: Physicochemical characterisation and permeability through Caco-2 cell monolayers. *Int. J. Pharm.* **381,** 205–213 (2009).
170. Schofield, C. R. Composition of soybean lecithin. *J. Am. Oil Chem. Soc.* **58,** 889–

892 (1981).

171. Aveyard, R., Binks, B. P. & Clint, J. H. Emulsions Stabilized Solely by Colloidal Particles. *Adv. Colloid Interface Sci.* **100-102,** 503–546 (2003).

172. Zielinska-Jurek, A., Reszczynska, J., Grabowska, E. & Zaleska, A. Nanoparticles Preparation Using Microemulsion Systems. *Microemulsions - An Introd. to Prop. Appl.* 229–250 (2012). doi:0.5772/2300

173. Zhi, J., Wang, Y., Lu, Y., Ma, J. & Luo, G. In situ preparation of magnetic chitosan/Fe3O4 composite nanoparticles in tiny pools of water-in-oil microemulsion. *React. Funct. Polym.* **66,** 1552–1558 (2006).

174. Zhi, J., Wang, Y. & Luo, G. Adsorption of diuretic furosemide onto chitosan nanoparticles prepared with a water-in-oil nanoemulsion system. *React. Funct. Polym.* **65,** 249–257 (2005).

175. Guibal, E. Heterogeneous catalysis on chitosan-based materials: A review. *Prog. Polym. Sci.* **30,** 71–109 (2005).

176. Xu, J. *et al.* Design and characterization of antitumor drug paclitaxel-loaded chitosan nanoparticles by W/O emulsions. *Int. J. Biol. Macromol.* **50,** 438–443 (2012).

177. Silva, S. M. L. *et al.* Application of Infrared Spectroscopy to Analysis of Chitosan/Clay Nanocomposites. *Infrared Spectrosc. - Mater. Sci. Eng. Technol.* 43–62 (2012). doi:10.5772/35522

178. Namanga, J., Foba, J., Ndinteh, D. T., Yufanyi, D. M. & Krause, R. W. M. Synthesis and magnetic properties of a superparamagnetic nanocomposite 'pectin-magnetite nanocomposite'. *J. Nanomater.* **2013,** 1–8 (2013).

179. Omar Zaki, S. S., Ibrahim, M. N. & Katas, H. Particle size affects concentration-dependent cytotoxicity of chitosan nanoparticles towards mouse hematopoietic stem cells. *J. Nanotechnol.* **2015,** 1–5 (2015).

180. Zhang, Y., Wei, W., Lv, P., Wang, L. & Ma, G. European Journal of Pharmaceutics and Biopharmaceutics Preparation and evaluation of alginate – chitosan microspheres for oral delivery of insulin. *Eur. J. Pharm. Biopharm.* **77,** 11–19 (2011).

181. Zarate, J. *et al.* Design and characterization of calcium alginate microparticles coated with polycations as protein delivery system. *J. Microencapsul.* **28,** 614–20

(2011).

182. Bekale, L., Agudelo, D. & Tajmir-Riahi, H. A. Effect of polymer molecular weight on chitosan-protein interaction. *Colloids Surfaces B Biointerfaces* **125,** 309–317 (2015).

183. Schatz, C., Viton, C., Delair, T., Pichot, C. and Domard, a. Typical physicochemical behaviours of chitosan in aqueous solution. *Biomacromolecules* **4,** 641–648 (2003).

184. Istenic, K. *et al.* Encapsulation of resveratrol into Ca-alginate submicron particles. *J. Food Eng.* **167,** 196–203 (2015).

185. Zheng, S.-Y., Li, Y., Jiang, D., Zhao, J. & Ge, J.-F. Anticancer effect and apoptosis induction by quercetin in the human lung cancer cell line A-549. *Mol. Med. Rep.* **5,** 822–6 (2012).

186. Wybranowski, T. & Kruszewski, S. Optical Spectroscopy Study of the Interaction Between Quercetin and Human Serum Albumin. *Acta Phys. Pol. A* **125,** A–57–A–60 (2014).

187. Luchoomun J., Sinibaldi D., C. xi-L. *Antioxidant Therapy for Chronic Inflammatory diseases. In: Leading Edge Antioxidants Research*. (2007).

188. Boots, A. W., Kubben, N., Haenen, G. R. M. M. & Bast, A. Oxidized quercetin reacts with thiols rather than with ascorbate: Implication for quercetin supplementation. *Biochem. Biophys. Res. Commun.* **308,** 560–565 (2003).

189. Deladino, L., Anbinder, P. S., Navarro, A. S. & Martino, M. N. Encapsulation of natural antioxidants extracted from Ilex paraguariensis. *Carbohydr. Polym.* **71,** 126–134 (2008).

190. Bartkowiak, A. & Hunkeler, D. Alginate−Oligochitosan Microcapsules: A Mechanistic Study Relating Membrane and Capsule Properties to Reaction Conditions. *Chem. Mater.* **11,** 2486–2492 (1999).

191. Hwang, S. W. *et al.* Poly(L-lactic acid) with added a-tocopherol and resveratrol: Optical, physical, thermal and mechanical properties. *Polym. Int.* **61,** 418–425 (2012).

192. Gåserød, O., Smidsrød, O. & Skjåk-Bræk, G. Microcapsules of alginate-chitosan - I. A quantitative study of the interaction between alginate and chitosan. *Biomaterials* **19,** 1815–1825 (1998).

193. Mahdi, E. S. *et al.* Effect of surfactant and surfactant blends on pseudoternary phase diagram behavior of newly synthesized palm kernel oil esters. *Drug Des. Devel. Ther.* **5,** 311–323 (2011).

194. Shafiq-un-Nabi, S. *et al.* Formulation development and optimization using nanoemulsion technique: a technical note. *AAPS PharmSciTech* **8,** Article 28 (2007).

195. Friedman, A. J. *et al.* Antimicrobial and anti-inflammatory activity of chitosan-alginate noparticles : a Targeted Therapy for Cutaneous Pathogens. *J Invest Dermat* **133,** 1231–1239 (2013).